FEW-BODY PROBLEM IN ULTRA-COLD ATOMS

Ludovic PRICOUPENKO

LABORATOIRE DE PHYSIQUE THÉORIQUE DE LA MATIÈRE CONDENSÉE

UNIVERSITÉ PIERRE ET MARIE CURIE - Paris

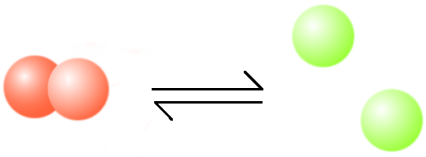

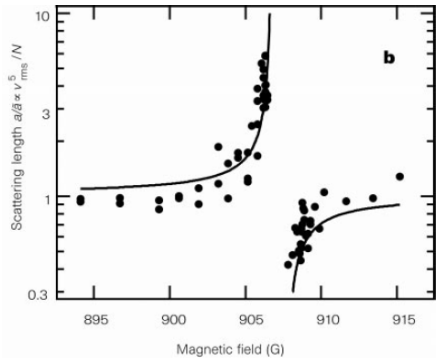

Contents

Introduction

Historically, the few-body problem has been first explored in the context of nuclear physics. The pioneering works on resonant few-body systems have been developed by the Russian school in reference to the tritium or to the deuteron-nucleon scattering problem. All these contributions are based on the remarkable fact that a large class of non trivial low energy properties can be expressed only by using elementary solutions of the free Schrödinger equation, while the short range interaction is taken into account by setting proper asymptotic conditions on the wave function. This explains why the concepts introduced in these key references may apply in other domains of quantum mechanics and are thus of broad interest. Paradoxically, the quest for Efimov states predicted in 1970 has never found clear evidence in nuclear experiments but in cold gases in 2006 by using the Feshbach resonance technique (a concept again borrowed from nuclear physics!) which allows to fully explore the resonant regime. The experimental breakthrough of 2006 has stimulated new theoretical studies on the few-body problem and this explain why this set of lectures focuses on the Efimov effect.

The aim of this course is to introduce young physicists to this fascinating domain. In the first lecture the universal collisional properties of the interaction near a resonance are recalled and the Wigner Bethe Peierls is introduced in a general form which allows to find easily the integral equations in few-body systems. The specific character of the atomic interactions near a magnetic Feshbach resonance is also introduced by using a separable two-channel. This model is useful for obtaining deviations from universal laws. In the second lecture, the Efimov effect is presented by following the historical progression from the work of Skorniakov and Ter-Martirosian to the breakthrough of Efimov. The data of the first experimental evidences of Efimov states are compared with the results given by the separable two-channel model. After the observation of the three-body Efimov states, the resonant four-body problem opens exciting prospects with the existence of universal four bosons resonances tightly linked to the Efimov trimers or the prediction of pure Efimov tetramers composed of three fermions interacting with one impurity. Currently, the four-body problem is a hot topic and the third lecture provides an introduction to this issue.

Chapter 1

Cold collisions and effective interactions

Contents

Preamble

The microscopic description of interaction between two atoms is rather sophisticated and solving the few-body problem by using the actual interaction potentials should be a very technical task. Hopefully a large class of low energy properties which have an important role in cold atoms can be studied accurately with effective interactions involving a small number of parameters. Using effective approach has not only a technical advantage but also it allows to put forward general properties and to obtain analytical results which have an 'universal' character in the sense that they are not specific to the details of the interparticle interaction. This explains why this first lecture focuses on the modeling of the interactions in cold atoms and on some essentials aspects of quantum scattering. For a general introduction to the quantum scattering theory the interested reader is encouraged to work on the classical textbooks in Refs. [Bla52, Mes61, Mot65, Lan67, Tay72]. There are also several very good reviews which are specialized on cold atomic collisions [Dal98, Wei99, Koh06, Chi10] or also the lectures of Claude Cohen Tannoudji which can be downloaded on the web [CCT].

1.1 Cold atomic collisions

1.1.1 The multi-channel reality

In usual experiments using ultracold gases, trapped atoms are neutral and in a S state. Quite generally, there exists a magnetic field $\mathbf{B}$ which imposes a preferred direction (usually one consider $\mathbf{B} = \mathcal{B}\hat{\mathbf{e}}_z$ and atoms are

prepared in given Zeeman states of energy E_{f,m_f} (which is a function of $\mathcal{B}$ labeled by the hyperfine quantum numbers (f, m_f). Two colliding atoms (labeled by $i = 1, 2$) are asymptotically in the states $|f_i, m_{f_i}\rangle$ and the system is thus defined by the quantum numbers $\alpha = \{f_1, m_{f_1}, f_2, m_{f_2}, l, m_l\}$ where l, m_l are the azimuthal quantum numbers of the relative angular momentum and α is the index of a scattering channel. If the total energy of the two-body system E is smaller than $E_{f_1,m_{f_1}} + E_{f_1,m_{f_2}}$ the channel is said to be 'closed' while in the other case it is an open channel: the interatomic distances can be arbitrarily large (the total wave function is not $\mathcal{L}^2$). For alkali atoms, electrons in the inner shells contribute essentially to the hard core repulsion and for intermediate distances one can only take into account the electron in the last shell through an exchange potential

$$U^{\text{exch}}(\mathbf{r}) = U_0(\mathbf{r})P_0 + U_1(\mathbf{r})P_1 \tag{1.1}$$

where P_S is the projection operator on the singlet ($S = 0$) or triplet ($S = 1$) states of the total electronic spin $\mathbf{S} = \mathbf{S}_1^{\text{e}} + \mathbf{S}_2^{\text{e}}$ and the potentials U_0 and U_1 are computed in the Born Oppenheimer approximation by considering the electronic coordinates as the fast variables. This interaction is not diagonal in the basis of the scattering channels and gives rise to a coupling between the channels *via* the hyperfine interaction terms. Their also exists magnetic dipole-dipole interactions between atoms but it is usually neglected. This also gives rise to an inter-channel coupling. The most important contribution among these interacting terms is the electronic one:

$$U^{\text{dipolar}}(\mathbf{r}) = \frac{\mu_0}{4\pi r^3}\left[\boldsymbol{\mu}_1^{\text{e}} \cdot \boldsymbol{\mu}_2^{\text{e}} - 3(\boldsymbol{\mu}_1^{\text{e}} \cdot \mathbf{r})(\boldsymbol{\mu}_2^{\text{e}} \cdot \mathbf{r})\right], \tag{1.2}$$

where $\boldsymbol{\mu}_i^{\text{e}}$ is the electronic magnetic moment. The projection of the total momentum over $\hat{\mathbf{e}}_z$ commutes with the total Hamiltonian, so that the coupling exists only between channels having the same value of $m_{f_1} + m_{f_2} + m_l$). Finally, the microscopic description of the interatomic forces involves a multi-channel theory and is rather involved. These lectures deal only with properties resulting from two-body elastic collisions thus the incoming and outcoming states are in the same Zeeman states (the open-channel). In what follows it is assumed that there is only one open channel and thus only the effect of the coupling with closed channels is considered.

For large relative distances r, $U_0(\mathbf{r}) \simeq U_1(\mathbf{r})$ and if one neglects the magnetic dipole-dipole interaction in Eq. (1.2), the interaction between two atoms can be approximated by a constant plus a van der Waals potential $V_{\text{vdW}}(r)$ resulting from the induced electric dipole-dipole force:

$$V_{\text{vdW}}(r) = -\frac{C_6}{r^6}, \tag{1.3}$$

where C_6 is the London's constant which does not depend on the hyperfine state of the two colliding atoms. Dimensional analysis provides a characteristic length scale for this behavior of the binary interaction at large distances [Gri93, Mar94, Dal98, Gao98]:

$$R_{\text{vdW}} = \frac{1}{2}\left(\frac{2\mu C_6}{\hbar^2}\right)^{\frac{1}{4}}, \tag{1.4}$$

In what follows it is denoted as the van der Waals range. The order of magnitude of this length is about few nanometers (for example $R_{\text{vdW}} = 1.7$ nm for two colliding lithium atoms and $R_{\text{vdW}} = 5.3$ nm for two colliding Cesium atoms). At shorter distances *i.e.* for subnanometric scales, the electronic clouds of the two atoms interpenetrate which lead to a violent repulsive force: this is the hard core part of the interacting potential.

1.1.2 Orders of magnitude of the collisional energy

The van der Waals range provides the characteristic 'high energy' scale in scattering processes:

$$E_{\text{vdW}} = \frac{\hbar^2}{2\mu R_{\text{vdW}}^2}. \tag{1.5}$$

The order of magnitude of this energy is about few hundreds of micro Kelvins. Ultra-cold atomic gases are extremely dilute with a typical atomic density ranging from 10^{13} to 10^{15} atoms per cm^3[1]. Thus the typical interatomic distance is of the order of few hundred of nanometers: several orders of magnitude larger than R_{vdW}. At such interatomic distances, the interacting potential has a very small value with respect to E_{vdW} (for example, for two cesium atoms, one finds $V_{\text{vdW}}(r) = 5\,10^{-2}$ nK for $r = 100$ nm) which can be neglected. The

[1] This density is several order of magnitude smaller than the one in the air ($2,7\,10^{19}$ molecules per cm^3) for standard conditions of pressure and temperature.

density in the gas is also sufficiently small that in general, configurations where three or more atoms are within a volume of the order of $R_{\rm vdW}^3$ are not relevant. Hence, for the typical densities in the cloud, atomic collisions are essentially binary. The typical temperature in the cloud ranges from the micro to the nano Kelvin, the de Broglie wavelength $\lambda_T = \left(\frac{2\pi\hbar^2}{\mu k_B T}\right)^{1/2}$ is greater than few hundred of nanometers and is thus very large with respect to $R_{\rm vdW}$.

As a conclusion, the typical colliding energy are very small with respect to the characteristic energy of the van der Waals interaction ($E_{\rm vdW}$). Furthermore, the typical range of the interaction potential ($R_{\rm vdW}$) is several order of magnitude smaller than the other atomic length scales in the cloud. For few-body configurations with interatomic distances smaller or of the order of $R_{\rm vdW}$, in addition to the couplings among all the possible channels one has to take into account three-body (or more) interacting potentials. Hopefully, the scale decoupling between 'high' and 'low' energy processes allows to avoid such detailed microscopic description of the potentials. Thus for a large class of phenomenon, two-body interactions can be modeled by using effective short range potentials with the constraint that they reproduce accurately the low energy scattering properties of the actual pairwise potentials.

1.2 Scattering in the low energy regime

This section reviews basic notions on two-body scattering for short range potentials. They are especially useful for the formulation of zero-range effective interactions. The two particles of reduced mass μ, are described in their center of mass frame by the relative coordinates $\mathbf{r}$ the wave vector $\mathbf{k}$ and the momentum $\mathbf{p} = \hbar\mathbf{k}$. They are supposed to interact through a short range and isotropic potential V of compact support b which is of the order of the van der Waals range in Eq. (1.4). Even if the actual interaction potential has a van der Waals tail the results of this section are important for understanding scattering properties in the s- and p-wave channel which are essential in ultracold atoms.

1.2.1 Predominance of s wave scattering

For an incoming state of wavevector $\mathbf{k}_0$ and collisional energy $E = \hbar^2 k_0^2/2\mu$ (measured from the continuum threshold), the scattering state $|\Psi_{\mathbf{k}_0}\rangle$ in the center of mass frame is formally given by the Lippmann-Schwinger equation:

$$\langle \mathbf{r}|\Psi_{\mathbf{k}_0}\rangle = \langle \mathbf{r}|\mathbf{k}_0\rangle + \int d^3r' \langle \mathbf{r}|G^0(E+i0^+)|\mathbf{r}'\rangle\langle \mathbf{r}'|V|\Psi_{\mathbf{k}_0}\rangle. \tag{1.6}$$

where $G^0(z)$ is the resolvent for the free Hamiltonian:

$$G^0(z) = \frac{1}{z - H_0} \quad \text{with} \quad H_0 = \frac{\mathbf{p}^2}{2\mu} \tag{1.7}$$

and the choice of the prescription $i0^+$ selects an outgoing wave. In Eq. (1.6) the convention $\langle \mathbf{r}|\mathbf{k}_0\rangle = \exp(i\mathbf{k}_0\cdot\mathbf{r})$ is used and more generally throughout these lectures, this convention is also used in the $\mathbf{k}$ representation: $\langle \mathbf{k}|\Psi\rangle = \int d^3r \langle \mathbf{r}|\Psi\rangle \exp(-i\mathbf{k}\cdot\mathbf{r})$. In this representation the scattering states in Eq. (1.6) can be written as a function of the half on-shell transition matrix (or t-matrix) defined by $\langle \mathbf{k}|T(E+i0^+)|\mathbf{k}_0\rangle = \langle \mathbf{k}|V|\Psi_{\mathbf{k}_0}\rangle$ with[2]

$$\langle \mathbf{k}|\Psi_{\mathbf{k}_0}\rangle = (2\pi)^3\delta(\mathbf{k}-\mathbf{k}_0) + \frac{\langle \mathbf{k}|T(E+i0^+)|\mathbf{k}_0\rangle}{E+i0^+ - \frac{\hbar^2k^2}{2\mu}}. \tag{1.8}$$

Another important object of the scattering theory is the scattering amplitude $f(\mathbf{k},\mathbf{k}_0)$ which is proportional to the on-shell transition matrix ($k = k_0$):

$$f_{k_0}(\hat{\mathbf{e}}_{\mathbf{k}}, \hat{\mathbf{e}}_{\mathbf{k}_0}) = -\frac{\mu}{2\pi\hbar^2}\langle \mathbf{k}|T(E+i0^+)|\mathbf{k}_0\rangle\Big|_{|\mathbf{k}|=|\mathbf{k}_0|}. \tag{1.9}$$

Taking the inverse Fourier transform of Eq. (1.8) one finds

$$\langle \mathbf{r}|\Psi_{\mathbf{k}_0}\rangle = \exp(i\mathbf{k}_0\cdot\mathbf{r}) + f_{k_0}(\hat{\mathbf{e}}_{\mathbf{r}}, \hat{\mathbf{e}}_{\mathbf{k}_0})\frac{\exp(ik_0r)}{r}, \tag{1.10}$$

[2] In its general definition, the t-matrix is a function of the complex variable z with $T(z) = V + V\frac{1}{z-H_0-V}V$ [Tay72].

showing that the scattering amplitude characterizes the large distance behavior of the scattering states. For an isotropic interaction potential the kernel in the Lippmann-Schwinger equation is also isotropic implying that it can be solved independently in each subspace of definite value of the angular momentum. The incoming plane wave fixes the natural quantization axis along $\hat{\mathbf{e}}_{\mathbf{k}_0} = \mathbf{k}_0/k_0$ and the scattering state can be decomposed over all the partial waves as:

$$\langle \mathbf{r}|\Psi_{\mathbf{k}_0}\rangle = \sum_{l=0}^{\infty} P_l(\hat{\mathbf{e}}_{\mathbf{k}_0}\cdot\hat{\mathbf{e}}_{\mathbf{r}})R_l(r). \tag{1.11}$$

where P_l is the Legendre polynomial of degree l and $R_l(r)$ is the radial wave function. The radial equation

$$\left[-\frac{1}{r}\frac{d^2}{dr^2}r\cdot - k_0^2 + \frac{l(l+1)}{r^2} + \frac{2\mu}{\hbar^2}V(r)\right]R_l(r) = 0 \tag{1.12}$$

is characterized by a kinetic barrier for non vanishing angular momentum $l > 0$. For the actual interatomic potentials with a van der Waals tail, the height of the barrier is of the order of $E_{\rm vdW} = \frac{\hbar^2}{2\mu R_{\rm vdW}^2}$. In absence of interaction, the radial wavefunction satisfying the correct asymptotic condition at large distance can be obtained from the expansion of the plane wave over the partial waves:

$$\langle \mathbf{r}|\mathbf{k}_0\rangle = \sum_{l=0}^{\infty}(i)^l(2l+1)P_l(\hat{\mathbf{e}}_{\mathbf{k}_0}\cdot\hat{\mathbf{e}}_{\mathbf{r}})j_l(k_0r). \tag{1.13}$$

In Eq. (1.13), $j_l(z) = z^l\left(-\frac{1}{z}\frac{d}{dz}\right)^l\frac{\sin z}{z}$ is the spherical Bessel function which is regular at the origin. At large distance

$$j_l(k_0r) \underset{k_0r\to\infty}{\sim} \frac{1}{k_0r}\sin\left[k_0r - \frac{\pi l}{2}\right]. \tag{1.14}$$

This last expression, can be interpreted as the superposition of an outgoing and of an ingoing spherical waves as:

$$\frac{\sin\left(k_0r - \frac{\pi l}{2}\right)}{r} = \frac{1}{2ir}\left[e^{i(k_0r-\frac{\pi l}{2})} - e^{-i(k_0r-\frac{\pi l}{2})}\right]. \tag{1.15}$$

In presence of the interacting potential $V(r)$, as we consider only elastic collisions there is a conservation of the ingoing and outgoing flux of particles. Thus, the action of the interaction can be traduced by a phase shift in the outgoing wave with respect to the free outgoing wave l which is defined through the substitution:

$$\left[e^{i(k_0r-\frac{\pi l}{2})} - e^{-i(k_0r-\frac{\pi l}{2})}\right] \to \left[e^{i(k_0r-\frac{\pi l}{2}+2\delta_l(k_0))} - e^{-i(k_0r-\frac{\pi l}{2})}\right]. \tag{1.16}$$

In Eq. (1.16), $\delta_l(k_0)$ is called the scattering phase shift. Often in place of the phase shift, for an isotropic potential as is supposed here the scattering process is characterized in each partial wave by a scattering amplitude denoted by f_l which are obtained from the expansion of the full scattering amplitude $f_{k_0}(\hat{\mathbf{e}}_{\mathbf{r}}, \hat{\mathbf{e}}_{\mathbf{k}_0})$ over the Legendre polynomials. The partial scattering amplitudes are thus defined from the behavior of the wave function at large distance ($k_0r \gg 1$):

$$\langle \mathbf{r}|\Psi_{\mathbf{k}_0}\rangle = \exp(i\mathbf{k}_0\cdot\mathbf{r}) + \sum_{l=0}^{\infty}(2l+1)P_l(\hat{\mathbf{e}}_{\mathbf{k}_0}\cdot\hat{\mathbf{e}}_{\mathbf{r}})f_l(k_0)\frac{\exp(ik_0r)}{r}.. \tag{1.17}$$

Using the identity

$$\exp(2i\delta_l) = 1 + 2i\exp(i\delta_l)\sin\delta_l \tag{1.18}$$

and from Eq. (1.13), Eq. (1.15) and Eq. (1.16), the partial scattering amplitudes can be expressed in terms of the phase shift δ_l as

$$f_l(k_0) = \frac{1}{k_0\cot\delta_l(k_0) - ik_0}. \tag{1.19}$$

The cross section can be also expressed in terms of the partial scattering amplitudes as

$$\sigma = \int d\Omega_{\mathbf{r}}\,|f_{k_0}(\hat{\mathbf{e}}_{\mathbf{r}}, \hat{\mathbf{e}}_{\mathbf{k}_0})|^2 = \sum_{l=0}^{\infty}\sigma_l \quad \text{where} \quad \sigma_l = 4\pi(2l+1)|f_l|^2. \tag{1.20}$$

All the topics addressed in these lectures concern properties involving low-energy binary processes. This means that the characteristic wavelength of the relative particle is very large with respect to the potential range *i.e.*

$k_0 b \ll 1$ and that the collisional energy is very much smaller than the characteristic energy scale of the pairwise potential. In this regime and for $r < b$, one can neglect the energy in the radial equation but not the pairwise potential while for $b < r \ll 1/k_0$ the energy and the potential can be both neglected in the radial equation. In this last regime of short distances the radial wave function has an universal behavior *i.e.* a behavior independent of the collisional energy[3]:

$$R_l(r) \sim c_{(+)} r^l - c_{(-)} r^{-l-1}. \tag{1.21}$$

In Eq. (1.21) the ratio $c_{(-)}/c_{(+)}$ depends on the shape of the pairwise potential and on the azimuthal quantum number l, it is in principle determined by solving the radial equation for all values of the radius. The behavior of the radial function at small distance in Eq. (1.21) can be also expressed in terms of the phase shift. For this purpose, we first deduce the large distance behavior of $R_l(r)$ from the definition of the scattering phase shift in Eq. (1.16):

$$R_l(r) \underset{r \gg b}{\propto} \frac{1}{r} \sin\left[k_0 r - \frac{\pi l}{2} + \delta_l(k_0)\right] \tag{1.22}$$

Then for $r > b$, the solution of Eq. (1.12) satisfying Eq. (1.22) can be expressed as a linear combination ion of the two spherical Bessel functions $j_l(z)$ and $y_l(z) = -z^l \left(-\frac{1}{z}\frac{d}{dz}\right)^l \frac{\cos z}{z}$ and using the fact that

$$y_l(k_0 r) \underset{k_0 r \to \infty}{\sim} \frac{-1}{k_0 r} \cos\left[k_0 r - \frac{\pi l}{2}\right], \tag{1.23}$$

one finally obtains from Eqs. (1.14,1.22,1.23)

$$R_l(r) = \mathcal{N}_l(k_0)\left[j_l(k_0 r) - y_l(k_0 r)\tan\delta_l(k_0)\right] \tag{1.24}$$

where $\mathcal{N}_l(k_0)$ is a normalization factor. For small values of z, $j_l(z) = z^l/(2l+1)!! + \ldots$ and $y_l(z) = -(2l-1)!!/z^{l+1} + \ldots$ which allows to have the relation between the scattering phase shift and the behavior of the radial function at small distance:

$$\tan\delta_l(k_0) \underset{k_0 b \ll 1}{=} -\frac{c_-}{c_+} \times \frac{k_0^{2l+1}}{(2l-1)!!(2l+1)!!}. \tag{1.25}$$

Equation (1.25) provides the behavior of the partial scattering amplitude in the low energy limit with $f_l(k_0) \propto k_0^{2l}$. Thus in the low energy regime where $k_0 b \ll 1$ (and as a consequence of the kinetic barrier) two-body scattering is essentially isotropic unless the particles are identical fermions in which case the Pauli principle imposes that the p-wave scattering is the dominant process.

1.2.2 s wave and p wave scattering amplitudes in the low energy limit

In the low energy limit, the s wave phase-shift is often approximated at the first order in k and the scattering amplitude is written as

$$f_0(k) \simeq -\frac{1}{\frac{1}{a} + ik - \frac{r_e k^2}{2}} \tag{1.26}$$

where a is the scattering length:

$$a = -\lim_{k\to 0} \frac{\tan\delta_0(k)}{k}. \tag{1.27}$$

and r_e is the effective range. For a potential with a van der Waals tail, the dimensional analysis provides the typical value taken by $|a|$ and $|r_e|$ with the van der Waals range $R_{\rm vdW}$. This analysis is confirmed by the exact solution given in Ref. [Gao98] and also justifies the choice $b = \mathcal{O}(R_{\rm vdW})$. For sufficiently small energies $|E| \ll E_{\rm vdW}$, the effective range can be neglected so that the scattering amplitude is approximated by

$$f_W(k_0) = \frac{-1}{\frac{1}{a} + ik_0}. \tag{1.28}$$

[3] For $l \geq 1$ this property follows directly from the presence of the kinetic barrier which implies that E can be neglected in the radial equation. For $l = 0$ this property can be shown from the form of the radial solution as follows. From Eq. (1.6), for $E = 0$ the wave function tends to unity for large interparticle distances so that for $r > b$ the radial wave function is $R_0(r) = \frac{1}{k_0 r} \times \sin\left[k_0 r + \delta_0(k_0)\right]$ and the phase shift is a linear function of k_0. In the limit of vanishing energy, $k_0 \to 0$ and one obtains Eq. (1.21) where $c_{(+)} = 1$ and $c_{(-)}$ does not depend on k_0.

Taking the Fourier transform of Eq. (1.17) and using the expressions of the scattering amplitudes in Eq. (1.28) one obtains the expression of the half on-shell transition matrix in the regime of small energy $|E| \ll \hbar^2/(\mu b^2)$ and small momentum $|\mathbf{k}|b \ll 1$. It appears that in this limit, it only depends on the collisional energy E (not on the momentum $\mathbf{k}$) and thus it coincides with the low energy on-shell t-matrix denoted $t(E+i0^+)$:

$$\langle \mathbf{k}|T(E+i0^+)|\mathbf{k}_0\rangle \sim t(E+i0^+) \equiv \frac{2\pi\hbar^2}{\mu} \times \frac{1}{\frac{1}{a}+ik_0}. \tag{1.29}$$

The transition matrices in Eq. (1.29) and the scattering amplitudes in Eq. (1.28) are the basic objects for describing low energy collisional processes which occurs in few- and many-body systems.

In the p wave channel, the effective range approximation of the scattering amplitude amounts to keep the two first terms of the series of $k_0 \cot \delta_l(k_0)$ as $k_0 \to 0$ it can be thus written as:

$$f_1(k) = \frac{-1}{\frac{1}{\mathcal{V}_s k^2} + \alpha + ik} \tag{1.30}$$

where $\mathcal{V}_s$ is the scattering volume and α is the effective range parameter.

1.3 Zero-range models

1.3.1 Wigner-Bethe-Peierls model

The short range details and even the characteristic range of the interaction do not appear explicitly in the expression of the transition matrix in Eq. (1.29) or equivalently of the scattering amplitude in Eq. (1.28) for a low energy process

$$|E| \ll \frac{\hbar^2}{\mu b^2} \qquad \text{and} \qquad |E| \ll \frac{\hbar^2}{\mu r_e^2}. \tag{1.31}$$

That is why it appears natural to model the interaction by using a formal zero-range potential. The fact that the force is zero-range means that the wave function $\Psi(\mathbf{r})$ of the relative particle solves the free Schrödinger equation everywhere excepted at the origin $r = 0$. It is useful to write the action of the zero-range interaction on the wave function as a δ source term in the Schrödinger equation with

$$\left(-\frac{\hbar^2}{2\mu}\Delta_{\mathbf{r}} - E\right)\Psi(r) = -S_\Psi \delta(\mathbf{r}). \tag{1.32}$$

where S_Ψ is the source amplitude. The source term in the right hand side of Eq. (1.32) can be seen as the formal substitution:

$$V(\mathbf{r})\Psi(\mathbf{r}) \longrightarrow S_\Psi \delta(\mathbf{r}) \tag{1.33}$$

in the actual Schrödinger equation. Moreover, as shown by the Lippmann-Schwinger equation (1.6) using a δ-regularized interaction leads to a purely isotropic scattering process. Thus Eq. (1.32) leads to a purely s wave scattering. Eq. (1.32) is not closed: a relation between S_Ψ and Ψ is missing: this is the so-called contact condition introduced by Wigner-Bethe-Peierls [Wig33, Bet35]. The Wigner-Bethe-Peierls (WBP) model is constructed is such a way that the two-body scattering amplitude coincides *exactly* with the low energy approximation in Eq. (1.28)[4]. For this purpose one can notice that the scattering length a corresponds to the ratio $c_{(-)}/c_{(+)}$ in Eq. (1.21) with $l = 0$. The WBP model amounts to continuing this equation for arbitrarily small values of the interparticle distance which corresponds to imposing the following contact condition on the wave function as the relative distance r tends to zero:

$$\langle \mathbf{r}|\Psi\rangle \underset{r\to 0}{=} A_\Psi \left(\frac{1}{a} - \frac{1}{r}\right) + \mathcal{O}(r). \tag{1.34}$$

[4]When Wigner Bethe and Peierls have introduced this method for the description of the deuteron very little was known about the nuclear interaction. At this stage, the zero-range model was somehow a minimal model for the description of the interaction between a proton and a neutron in a non perturbative regime. The features of the deuteron are now very well known: the two nucleons are in a triplet state with a binding energy of the order of 2.22 Mev. In this spin state, the scattering length is equal to 5.4 fermis while the effective range is equal to 2.7 fermis *i.e.* of the same order of magnitude than the deuteron radius of approximately 2 fermis. The WBP model provides thus just a qualitative description of the deuteron. Nevertheless, in the singlet spin state, the scattering length between two nucleons is large and negative: for instance for two neutrons it is $a_s \sim -18.7$ fermis [Gon99]. Hence, in this spin configuration $b/|a_s| \sim 0.1$. In this case the WBP model is relevant and well justified for colliding wave number of the order of $1/a_s$.

From the identity $\Delta\left(\frac{1}{r}\right) = -4\pi\delta(\mathbf{r})$, one can deduce that A_Ψ is proportional to the source amplitude with

$$S_\Psi = \frac{2\pi\hbar^2}{\mu} A_\Psi. \tag{1.35}$$

As an exercise, it is formative to derive the scattering states in Eq. (1.28) from Eq. (1.32) and Eq. (1.34). For the scattering state at energy $E = \frac{\hbar^2 k_0^2}{2\mu} > 0$, Eq. (1.6) reads

$$|\Psi_{\mathbf{k_0}}\rangle = |\mathbf{k}_0\rangle + S_\Psi G^0(E + i0^+)|0_\mathbf{r}\rangle \tag{1.36}$$

where $|0_\mathbf{r}\rangle$ is the ket associated with the contact of the two particles: $\langle\mathbf{r}|0_\mathbf{r}\rangle = \delta(\mathbf{r})$. Equation (1.36) shows that for the scattering states one has $S_\Psi = t(E_0)$ and $f_W(k_0) = -\frac{\mu S_\Psi}{2\pi\hbar^2}$. In the configuration space the outgoing Green's function is

$$\langle\mathbf{r}|G^0(E + i0^+)|\mathbf{r}'\rangle = -\frac{\mu}{2\pi\hbar^2}\frac{\exp(ik_0|\mathbf{r} - \mathbf{r}'|)}{|\mathbf{r} - \mathbf{r}'|}, \tag{1.37}$$

and as expected Eq. (1.36) can be written as

$$\langle\mathbf{r}|\Psi_{\mathbf{k_0}}\rangle = \exp(i\mathbf{k}_0 \cdot \mathbf{r}) + f_W(k_0)\frac{\exp(ik_0 r)}{r}. \tag{1.38}$$

For vanishing values of the inter-particle distance,

$$\langle\mathbf{r}|\Psi_{\mathbf{k_0}}\rangle \underset{r\to 0}{=} [1 + ik_0 f_W(k_0)] + \frac{f_W(k_0)}{r} + \mathcal{O}(r). \tag{1.39}$$

Imposing the contact condition in Eq. (1.34) gives:

$$\frac{f_W(k_0)}{a} = -1 - ik_0 f_W(k_0) \tag{1.40}$$

which provides the desired result. In more general situations, for instance in presence of an external potential or in the few-body problem, the limit in Eq. (1.34) is taken for a fixed value of the center of mass of the interacting pair and S_Ψ is a function of the colliding energy and of all the degrees of freedom excepted the relative coordinates $\mathbf{r}$ [5].

As a conclusion of this section, the δ distribution in the right hand side of Eq. (1.32) imposes a $1/r$ singularity for the eigenstates at $r = 0$. The WBP contact condition in Eq. (1.34) amounts to select among the singular solutions the ones which for $r > b$ are good approximation of the eigenstates of the actual pairwise potential in the low energy regime (1.31). The WBP model can thus be seen as a filtering method allowing to extract the relevant singular solution of the free Schrödinger equation.

1.3.2 A handy formulation of the Wigner Bethe Peierls model

In practical calculations the contact condition in Eq. (1.34) is not always easy or straightforward to handle. For instance in the dimensional reduction issue where one is interested on the colliding properties in quasi-1D or -2D geometries one is tempted to expand the wave functions over the basis of eigenfunctions of the free Hamiltonian in presence of the anisotropic trapping potential. However the basis is composed of regular functions at the contact. Thus the limit $r \to 0$ in Eq. (1.34) does not commute with the infinite summation over the basis [6]. Another example is the few-body problem without external potential which is more naturally expressed in the momentum representation as a consequence of translational invariance while Eq. (1.34) applies in the configuration space. The method presented in this section is taken from Ref. [Pri11a] and applies also in low dimensions [Pri10a]. A similar method was also used in the dimensional reduction issue in Ref. [Pri08]. In the subsequent lines, the contact condition is expressed in arbitrary representation. Furthermore problems of uniform convergence are avoided while preserving the structure of the WBP model. For this purpose, the δ-distribution is replaced by a function $\langle\mathbf{r}|\delta_\epsilon\rangle$ which converges toward $\delta(\mathbf{r})$ in the limit where ϵ tends to zero.

[5] Using a zero range approach in a presence of an external potential say $U(\mathbf{R})$ means that the spatial variation of U can be neglected at the scale of the actual range of the pairwise potential b.

[6] The function $F(r) = r\langle\mathbf{r}|\Psi\rangle$ has a finite limit at $r = 0$. However, if one expands $\langle\mathbf{r}|\Psi\rangle$ over regular basis functions, each term of the series associated with $F(r)$ tends to zero at $r = 0$: there is no uniform convergence. This feature is discussed in details by Claude Cohen Tannoudji in the lecture 4 of the year 1998-1999 at Collège de France [CCT]

Intermediary calculations are achieved for a finite value of ϵ and the limit $\epsilon \to 0$ is taken *in fine*. A convenient choice is to choose a Gaussian function:

$$\langle \mathbf{r}|\delta_\epsilon\rangle = \frac{1}{(2\pi\epsilon^2)^{3/2}} \exp\left(-\frac{r^2}{\epsilon^2}\right), \tag{1.41}$$

so that $\delta(\mathbf{r}) = \lim_{\epsilon\to 0}\langle \mathbf{r}|\delta_\epsilon\rangle$. With this particular choice, in the momentum space, the representation of the delta term is:

$$\langle \mathbf{k}|\delta_\epsilon\rangle = \chi_\epsilon(k) = \exp\left(-\frac{k^2\epsilon^2}{4}\right). \tag{1.42}$$

Matrix elements and states without index ϵ are considered in their zero-range limit which corresponds in this formalism to the limit $\epsilon \to 0$:

$$\lim_{\epsilon\to 0}|\Psi_\epsilon\rangle = |\Psi\rangle. \tag{1.43}$$

It is also useful to introduce the 'reference state' denoted by $|\phi_\epsilon^\Lambda\rangle$ which results from the action of the 2-body Green's function $G^0(E_\Lambda)$ in free space on $|\delta_\epsilon\rangle$ at the negative energy $E_\Lambda = -\frac{\hbar^2\Lambda^2}{2\mu}$ where Λ is chosen positive ($\Lambda \in \mathbb{R}^+$) according to the usual prescription in scattering theory:

$$|\phi_\epsilon^\Lambda\rangle = G^0(E_\Lambda)|\delta_\epsilon\rangle \quad \Longrightarrow \quad \langle \mathbf{k}|\phi_\epsilon^\Lambda\rangle = -\frac{2\mu}{\hbar^2} \times \frac{\chi_\epsilon(k)}{k^2+\Lambda^2}. \tag{1.44}$$

In the zero-range limit where $\epsilon = 0$, $\langle \mathbf{r}|\phi_\epsilon^\Lambda\rangle$ has an $1/r$ singularity for $r \to 0$:

$$\langle \mathbf{r}|\phi^\Lambda\rangle \underset{r\to 0}{=} \frac{\mu}{2\pi\hbar^2}\left(-\frac{1}{r}+\Lambda\right) + \mathcal{O}(r) \tag{1.45}$$

Without specific representation, the source amplitude is a ket associated with all the degree of freedom of the system excepted the relative coordinates and is denoted by $|S_\Psi\rangle$. The contact condition in Eq. (1.34) can then be written in terms of the reference state as:

$$\lim_{r\to 0}\lim_{\epsilon\to 0}\langle \mathbf{r}|\Psi_\epsilon - \mathrm{S}_\Psi\phi_\epsilon^\Lambda\rangle = \frac{|\mathrm{S}_\Psi\rangle}{t(E_\Lambda)}, \tag{1.46}$$

where $t(E_\Lambda)$ defined in (1.29) is the on-shell t-matrix at energy E_Λ associated with the scattering amplitude (1.28) where $k = i\Lambda$ and thus

$$t(E_\Lambda) = \frac{2\pi\hbar^2}{\mu}\frac{a}{1-\Lambda a}. \tag{1.47}$$

In the configuration space, the state $|\Psi_\epsilon - \mathrm{S}_\Psi\phi_\epsilon^\Lambda\rangle$ is a smooth function for (r,ϵ) close to $(0,0)$. It is thus possible to commute the $r \to 0$ and $\epsilon \to 0$ limits in Eq. (1.46):

$$\lim_{r\to 0}\lim_{\epsilon\to 0}\langle \mathbf{r}|\Psi_\epsilon - \mathrm{S}_\Psi\phi_\epsilon^\Lambda\rangle = \lim_{\epsilon\to 0}\lim_{r\to 0}\langle \mathbf{r}|\Psi_\epsilon - \mathrm{S}_\Psi\phi_\epsilon^\Lambda\rangle. \tag{1.48}$$

Finally, the WBP contact condition can be written without specifying any representation as:

$$\lim_{\epsilon\to 0}\langle 0_\mathbf{r}|\Psi_\epsilon - \mathrm{S}_\Psi\phi_\epsilon^\Lambda\rangle = \frac{|\mathrm{S}_\Psi\rangle}{t(E_\Lambda)}. \tag{1.49}$$

Eq. (1.49) is by construction, invariant in a change of $\Lambda \in \mathbb{R}^+$: one recovers the Λ freedom which allows to improve approximate schemes in the many-body problem [Ols01, Pri04b, Pri11b]. Moreover, the $\epsilon \to 0$ limit can be taken equivalently as follows:

$$\lim_{\epsilon\to 0}\langle \delta_\epsilon|\Psi_\epsilon - \mathrm{S}_\Psi\phi_\epsilon^\Lambda\rangle = \frac{|\mathrm{S}_\Psi\rangle}{t(E_\Lambda)}, \tag{1.50}$$

The contact condition in Eq. (1.50) can be expressed in any desired representation by inserting a closure relation in the scalar product concerning the relative particle. For example in the momentum representation, one can insert at the right of the bra $\langle\delta_\epsilon|$ in Eq. (1.50) the closure relation:

$$\int \frac{d^3k}{(2\pi)^3}|\mathbf{k}\rangle\langle\mathbf{k}| = \mathbb{1}, \tag{1.51}$$

which provides the WBP contact condition in the momentum representation:

$$\lim_{\epsilon\to 0}\left(\int \frac{d^3k}{(2\pi)^3}\chi_\epsilon(k)\langle \mathbf{k}|\Psi_\epsilon - \mathrm{S}_\Psi\phi_\epsilon^\Lambda\rangle\right) = \frac{|\mathrm{S}_\Psi\rangle}{t(E_\Lambda)}. \tag{1.52}$$

Eq. (1.49) allows to obtain in a simple way the standard integral equations of few-body problems in the zero range limit and also to compute the induced scattering resonances and related scattering problems in presence of an harmonic transverse confinement [Pri11a]. As for $|S_\Psi\rangle$, the amplitude of the diverging part in Eq. (1.34) is in general a ket $|A_\Psi\rangle$ associated with all the degrees of freedom excepted the relative coordinates of the interacting pair $\mathbf{r}$. Using Eq. (1.35), the contact condition in Eq. (1.52) can be also written in terms of this amplitude as

$$\lim_{\epsilon\to 0}\left[\int \frac{d^3k}{(2\pi)^3}\left(\chi_\epsilon(k)\langle \mathbf{k}|\Psi_\epsilon\rangle + \frac{4\pi\chi_\epsilon^2(k)}{k^2+\Lambda^2}|A_\Psi\rangle\right)\right] = -\frac{|\mathrm{A}_\Psi\rangle}{f_W(i\Lambda)}. \tag{1.53}$$

1.3.3 The radius-range inequality for the p-wave interaction

It is possible to construct a zero range model for a pure p wave interaction [Pri06a, Pri06b] associated with the scattering amplitude in Eq. (1.30) but its explicit form is not useful in what follows. The model provides the scattering states

$$\Psi_{\mathbf{k}_0}(\mathbf{r}) = \exp(i\mathbf{k}_0\cdot\mathbf{r}) - 3i(\hat{\mathbf{e}}_{\mathbf{k}_0}\cdot\hat{\mathbf{e}}_{\mathbf{r}})f_1(k_0)\partial_r\left[\frac{\exp(ik_0r)}{k_0r}\right]. \tag{1.54}$$

We focus here on the fact that the scattering states in Eq. (1.54) are not orthogonal with each others, furthermore the scalar product between two different eigenstates diverge ! the physical meaning of this strange property lies in the fact that for $r < b$ *i.e.* in the interior domain of the pairwise potential, the wave function in Eq. (1.54) has nothing to do with the actual wave function in this region. More precisely, the divergence in the scalar product is due to the unphysical $1/r^2$ behavior of the scattering states in the interior domain. Interestingly, it is possible to restore the hermiticity of the zero-range model by introducing a modified scalar product which takes into account implicitly the contribution of the eigenstates in the interior domain. For two states (say $|\Psi\rangle, |\Psi'\rangle$) which are linear combinations of the eigenstates of the zero-range model associated with the scattering amplitude in Eq. (1.30), it can be written as

$$(\Psi|\Psi')_0 = \int d^3\mathbf{r}\, g(r)\Psi^*(\mathbf{r})\Psi'(\mathbf{r}) \tag{1.55}$$

where $g(r)$ is the following metrics:

$$g(r) = 1 + \delta(r)\left[(\alpha r^2 - r)\,.\right]. \tag{1.56}$$

For positive values of the scattering volume, the zero-range model supports a bounds state of binding wave number

$$q_\mathrm{B} = \frac{1}{\sqrt{\alpha\mathcal{V}_\mathrm{s}}} \tag{1.57}$$

which can be also deduced from the imaginary pole of the scattering amplitude in Eq. (1.30). The radial part of the bound state normalized with respect to the modified scalar product in Eq.(1.55) is:

$$R(r) = \frac{1}{\sqrt{\alpha - 3q_\mathrm{B}/2}}\,\partial_r\left[\frac{\exp(-q_\mathrm{B}r)}{r}\right]. \tag{1.58}$$

The normalization factor in Eq. (1.58) can be also deduced from the residue of the scattering amplitude (1.30) at the energy $\epsilon_B = -\hbar^2q_\mathrm{B}^2/m$ as shown by using an argumentation based on analyticity properties (see [Lan67] section 128). The bound state of the zero-range model is physically relevant in the limit of small binding energy *i.e.* for a large value of the scattering volume with respect to b^3. In this regime, the probability of finding the dimer outside the range of the actual potential of compact support b is $\int_b^\infty dr\, r^2R^2(r) = 1/\alpha b$. Thus $\alpha > 0$ and

$$b\alpha > 1 \tag{1.59}$$

which is the radius-range inequality. One can check that this inequality is verified for example in ^{40}K for the resonance at $B_0 \simeq 198.5$ G with $\alpha b \simeq 2.8$ [Tic04] (even if the actual interatomic potential has not a compact support).

1.4 Scattering resonances and unitary limit

1.4.1 Resonance condition and shallow bound state

The contribution σ_l of a partial wave l in the cross section (1.20) is maximum whenever $k_0 \cot\delta_l(k_0)$ reaches a minimum. This corresponds to a scattering resonance, meaning that the probability of scattering for two colliding particles is large. The maximum value that can be achieved is $\sigma_l = 4\pi/k_0^2$ and this regime is called the 'unitary limit' in the partial wave l [7]. In the s wave, it is achieved for an infinite scattering length ($|a| = \infty$) and for a large interval of momentum such that the low energy condition in Eq. (1.31) is satisfied. For a large scattering length ($|a| \gg b$) the maximum is at $k_0 = 0$ with $\sigma_0 = 4\pi a^2$ which is very large compared to the classical value $\sigma_0 = 4\pi b^2$ of the hard sphere potential of radius b. In the s wave resonant regime, the pairwise short range potential affects the form of the wave function at interparticle distances which are large with respect to the potential radius b. More precisely, the scattering states in Eq. (1.8) can be decomposed in an incoming part $|\phi_{\rm inc}\rangle = |\mathbf{k}_0\rangle$ and a scattered part $|\phi_{\rm scatt}\rangle$. At large distance and in the resonant regime:

$$\left|\frac{\langle \mathbf{r}|\phi_{\rm scatt}\rangle}{\langle \mathbf{r}|\phi_{\rm inc}\rangle}\right| \underset{r\gg b}{=} \frac{|a|}{r} \tag{1.60}$$

this ratio is greater than or of the order of unity for $b \ll r < |a|$, where $|a|$ is arbitrarily large. The zero-range potential approach is a formalism which allows to evaluate accurately the wave function in configurations where particles are outside the potential radius while configuration where two or more particles are inside the potential radius are not reliably described. Consequently, the WBP approach is very well suited for studying systems in the resonant regime where the wave function is modified by the interaction at interparticle distances which are large compared to the potential radius. For a positive scattering length, the scattering amplitude in Eq. (1.28) has a real pole at negative energy $E = -E_{\rm dim}$ with a wave number $k_0 = iq_{\rm dim}$:

$$E_{\rm dim} = \frac{\hbar^2}{2\mu a^2} \qquad ; \qquad q_{\rm dim} = \frac{1}{a} \tag{1.61}$$

In the resonant regime, this pole is associated with the existence of a shallow dimer of binding energy $E_{\rm dim}$, which is thus very well described in the zero-range approach (the probability that the relative pair has a radius greater than the potential radius b is $\exp(-2b/a) \sim 1$). The eigenstate of the dimer $|\phi_s\rangle$ coincides exactly in the zero-range limit with the reference state at $\Lambda = \frac{1}{a}$ in Eq. (1.45). In the configuration space the normalized dimer state is

$$\phi_s(\mathbf{r}) = \frac{1}{r\sqrt{2\pi a}} \exp(-\frac{r}{a}). \tag{1.62}$$

In the p wave channel, the unitary limit is reached for a negative and large value of the scattering volume and a wave number [8] $k_{\rm QB} = \frac{1}{\sqrt{-\mathcal{V}_s\alpha}}$. The scattering resonance corresponds to the presence of a quasi bound state at the positive energy $\hbar^2 k_{\rm QB}^2/(2\mu)$ which has a finite lifetime due to the existence of the kinetic barrier. In the vicinity of the unitary limit, the collisional energy is of the order of the quasi bound state: $k_0 = k_{\rm QB} + \delta k_0$ with $k_{\rm QB} = \frac{1}{\sqrt{-\alpha\mathcal{V}_s}}$ and the scattering amplitude is of the form

$$f_1(k_0) \sim -\frac{1}{ik_0 - 2\alpha\frac{\delta k_0}{k_{\rm QB}}}. \tag{1.63}$$

The resonance width in the scattering cross section is thus of the order of $k_{\rm QB}/\alpha$ which is necessarily narrow as a consequence of the radius-range inequality in Eq. (1.59). For an infinite scattering volume, ($|\mathcal{V}_{\rm s}| = \infty$), $f_1(k_0) = 1/(\alpha + ik_0)$, but unlike what happens in the s wave and as a consequence of the radius-range inequality in Eq. (1.59), the effective range term α can never be neglected with respect to the unitary term ik_0.

As a conclusion of this section, there are three issues characterizing the resonant scattering regime which are important for these lectures:

- the resonance in a partial wave occurs when the two-body system is near the threshold of appearance of a bound (or quasi-bound) shallow state in this partial wave;

[7] The origin of this appellation lies in the fact that the ik_0 term in the partial scattering amplitude f_l is a consequence of the conservation of the number of particles in the scattering process.

[8] If the scattering volume is not large with respect to b^3, $k_{\rm QB}\cot\delta_1(k_{\rm QB})$ cannot be neglected with respect to $k_{\rm QB}$ and the unitary limit is not reached.

- this shallow state can be described by a zero-range model;
- the s wave unitary limit occurs in a large interval of values of the momentum ($k < \min(1/b, 1/r_e)$) which is in sharp contrast with the p wave (or higher partial wave) unitary limit which occurs unavoidably in a narrow interval of the momentum.

1.4.2 Feshbach and shape resonances

If one neglects the inter-channel coupling, each channel of the interatomic interaction supports a large number of discrete states which are nothing but diatomic molecules. Away from shape resonances (this concept is defined below) the extension of all these molecules is of the order of the van der Waals range $R_{\rm vdW}$ or smaller. The Feshbach resonance corresponds to a coherent population of such a molecular state by the colliding pair of the open channel. The Feshbach mechanism is thus a consequence of the inter-channel coupling. The simplest way to describe the Feshbach resonance mechanism is given by a two-channel model where the typical potentials are displayed in Fig. (1.1).

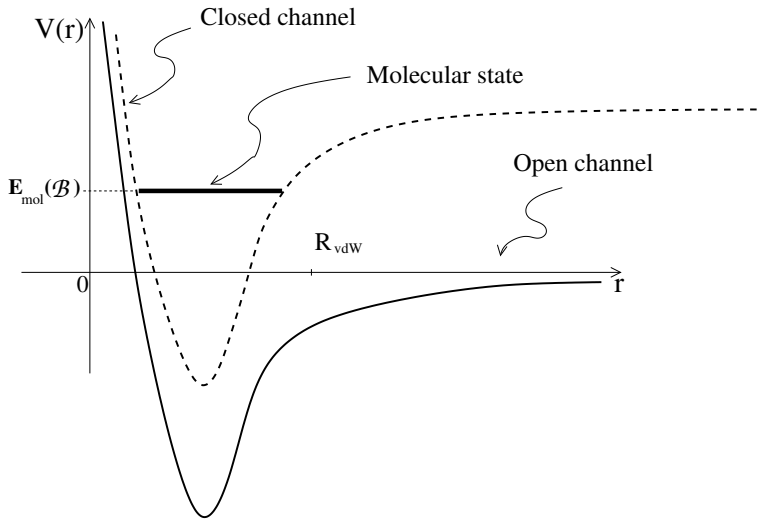

Figure 1.1: *Schematic view of the interatomic potentials in an open channel and a closed channel. The Feshbach resonance mechanism consists in the coherent coupling between a bound state in the closed channel and the colliding pair in the open channel. The resonance can be tuned by using the fact that the molecular energy $E_{\rm mol}(\mathcal{B})$ is a function of the external magnetic field $\mathbf{B} = \mathcal{B}\hat{\mathbf{e}}_z$.*

As a consequence of the Zeeman effect, the molecular energy $E_{\rm mol}$ measured with respect to the continuum threshold of the open channel is a function of the external magnetic field $\mathcal{B}$ with a law which can be considered as affine in the vicinity of the resonance:

$$E_{\rm mol} = \delta\mu(\mathcal{B} - \mathcal{B}_0^{\rm cl}). \tag{1.64}$$

In Eq.(1.64), $\mathcal{B}_0^{\rm cl}$ is the magnetic field at which the molecular state energy crosses the threshold of the open channel continuum and $\delta\mu$ denotes the difference between the magnetic moments for an atomic pair in the open channel and the molecular state in the closed channel. Thus, by a fine tuning of the magnetic field it is possible to reach the resonant regime where the coupling between the molecular state and the colliding pair is maximum. The first predictions of Feshbach resonances in alkali have been achieved by using a two-channel model [Moe95]. In the s wave, using this magnetic Feshbach resonance technique, it is possible in principle to tune the scattering length to any possible value from $-\infty$ to $+\infty$. However in current experiments the fluctuations of the external magnetic field limit the maximum absolute value that can be reached for the scattering length with an order of magnitude of 10^4 nm. The Feshbach resonance technique has played a central role in the observation of Efimov states which are studied in the other lectures.

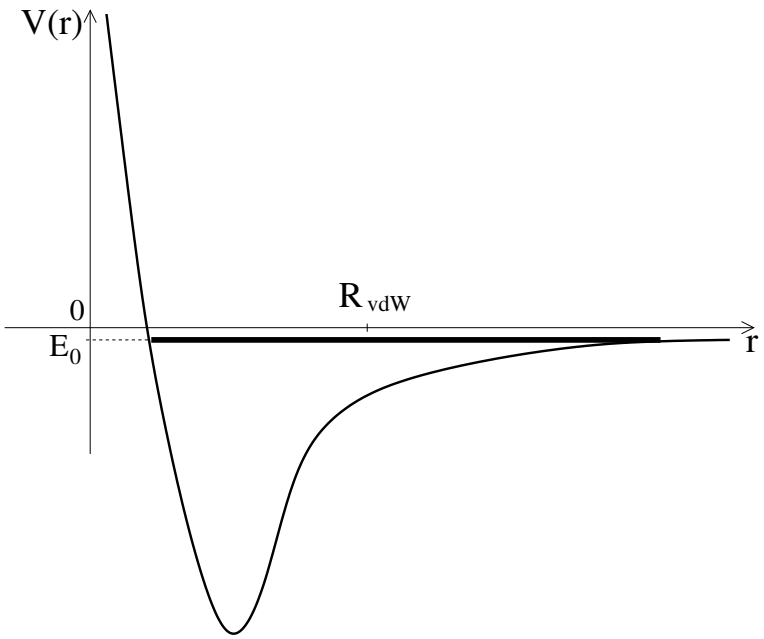

Figure 1.2: *In the case of a shape resonance, the potential in the open channel has a shallow bound (or quasi-bound) state,* i.e. *its energy E_0 is in the vicinity of the continuum threshold of the open channel.*

The shape (or potential) resonance is another type of scattering resonance in cold atoms. This resonance is linked to the shape of the pairwise potential in the open channel which support a shallow bound (or quasi-bound) state Fig. (1.2). A s wave shape resonance corresponds to a large absolute value of the scattering length away from a Feshbach resonance *i.e.* when the coupling between the atomic pair in the open channel and the molecular states is negligible. In what follows the scattering length in absence of Feshbach resonance is denoted by $a_{\rm bg}$ and is called the background scattering length. Thus, for a shape resonance $|a_{\rm bg}| \gg b$.

1.5 Separable two-channel model for the resonant regime

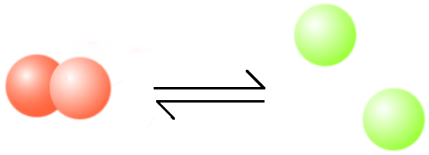

1.5.1 Motivation

Near a s wave scattering resonance, in the low momentum regime the scattering length is the only characteristic parameter for the interaction. This provides an universal character of the resonance which can be thus described by using a one channel model as for instance the WBP zero range model. However scattering resonances in cold atoms have their own specificity which can be relevant in order to have quantitative laws in intermediary regimes near a resonance. For instance, for a magnetic Feshbach resonance the scattering length can be parameterized as a function of the external magnetic field $\mathcal{B}$ by the law [Moe95]:

$$a = a_{\rm bg}\left(1 - \frac{\Delta\mathcal{B}}{\mathcal{B} - \mathcal{B}_0}\right) \tag{1.65}$$

where $\mathcal{B}_0$ is the magnetic field at which the resonance occurs[9] and $\Delta\mathcal{B}$ is the width of the resonance. A characteristic length denoted hereafter as the 'width radius' can be associated with this width [Pet04b]:

$$R^\star = \frac{\hbar^2}{m a_{\rm bg}\delta\mu\Delta\mathcal{B}}. \tag{1.66}$$

[9] $\mathcal{B}_0$ is different from $\mathcal{B}_0^{\rm cl}$ in Eq. (1.64). For example, the separable two-channel model gives an explicit expression for this magnetic shift in Eq. (1.85)

The characteristic parameters of some known resonance achieved experimentally are shown in the table (1.1) and the table (1.2) gives their characteristic energies $E_{\rm vdW}$ of Eq. (1.5), $\delta\mu\Delta\mathcal{B}$ and $E_{\rm bg} = \frac{\hbar^2}{m a_{\rm bg}^2}$. These data have been taken from Ref. [Chi10].

Species	B_0 [G]	$\Delta\mathcal{B}$ [G]	$\delta\mu$ [μ_B]	$a_{\rm bg}[a_0]$	$R_{\rm vdW}[a_0]$	$R^\star[a_0]$
^{133}Cs	-11.8	28	2.3	1704	101	0.13
^{85}Rb	155	10.7	-2.32	-443	82.2	2.7
^{39}K	402	-52	1.5	-29	64.6	29
^{39}K	752	-0.4	3.9	-35	64.6	1.2×10^3
^{23}Na	907	1	4	56.7	44.5	5×10^2

Table 1.1: *Parameters of few magnetic Feshbach resonances in cold atoms from Ref. [Chi10]. $R_{\rm vdW}$ is the van der Waals range in Eq. (1.4).*

In the vicinity of a shape resonance $|a_{\rm bg}| \gg R_{\rm vdW}$ so that $E_{\rm bg} \ll E_{\rm vdW}$ (this is the case of the resonance at -11.8 Gauss for the cesium and at 155 G for the rubidium). The case of the cesium is particularly interesting because the background scattering length is large and positive showing that there exists a shallow dimer in the open channel in absence of a Feshbach resonance. The resonance at 752 G for the potassium is an example of narrow resonance: $R^\star \gg R_{\rm vdW}$ or also $|\delta\mu\Delta\mathcal{B}| \ll E_{\rm vdW}$.

Species	$\mathcal{B}_0[G]$	$\delta\mu\Delta\mathcal{B}/h$ [MHz]	$E_{\rm bg}/h$ [MHz]	$\lvert\delta\mu\Delta\mathcal{B}\rvert/E_{\rm bg}$	$E_{\rm bg}/E_{\rm vdW}$
^{133}Cs	-11.8	1.2×10^2	9.3×10^{-3}	1.2×10^4	3.5×10^{-3}
^{85}Rb	155	-35	0.21	1.6×10^2	3.4×10^{-2}
^{39}K	402	-1.1×10^2	1.1×10^2	1	5
^{39}K	752	-2.2	75	2.9×10^{-2}	3.4
^{23}Na	907	5.6	48	.11	0.6

Table 1.2: *Characteristic energies for the resonances of the table (1.1).*

The WBP model gives no information about the resonance width which is a crucial issue for experiments. One can wonder what are the respective roles of the three lengths $b, a_{\rm bg}$ and $R^\star$ in few-body properties: what happens if a Feshbach resonance occurs near a shape resonance ($|a_{\rm bg}| \gg b$) ? or also what is the effect of the finite range b of the interatomic potential ? For all these reasons, it is interesting to have a quantitative finite range model which encapsulates the Feshbach or the shape resonance mechanism and which is sufficiently simple to be used in the study of few-body systems.

In the p wave and s wave such models have been used in the context of few-body systems in Refs. [Jon08, Jon10, Mor11a] and for the two-spin component Fermi gas in Ref. [Wer09]. They are parameterized by two-body properties and for the few-body problem, they lead to integral equations having the same degree of complexity than the ones obtained with the WBP model.

1.5.2 Purely s wave interactions

The simplest way to introduce the separable two-channel model is to use the second quantized formalism and to choose the momentum representation. The model introduced below is a simplification of the one of Refs. [Koh06, Lee07]. The atoms in the open-channel are neutral and spinless bosons of mass m. The model supports also a discrete and structureless bosonic molecular state of mass $2m$. The description of the closed-channel is reduced to this molecular state. In the two channel model, the molecule in the closed channel is thus distinct from the dimers which are the bound states of the full Hamiltonian. The Feshbach resonance mechanism is encapsulated by a coherent coupling between atomic pairs of the open channel and the molecular state. The model contains a direct interaction term between atoms in the open channel which allows to take into account the background *i.e.* off-resonance scattering length ($a_{\rm bg}$). The Hamiltonian is expressed in terms of the operators of creation and annihilation ($a^\dagger_{\mathbf{k}}, a_{\mathbf{k}}$) of one atomic boson of wave vector $\mathbf{k}$ and of the operators of creation and annihilation ($b^\dagger_{\mathbf{k}}, b_{\mathbf{k}}$) of one molecule of wave vector $\mathbf{k}$. By definition, the operators $a_{\mathbf{k}}$ and $b_{\mathbf{k}}$

obey standard bosonic commutation rules:

$$[a_{\mathbf{k}}, a^\dagger_{\mathbf{k}'}] = (2\pi)^3\delta(\mathbf{k}-\mathbf{k}') \ , \ [b_{\mathbf{k}}, b^\dagger_{\mathbf{k}'}] = (2\pi)^3\delta(\mathbf{k}-\mathbf{k}'). \tag{1.67}$$

and any other commutator vanishes. The Hamiltonian of the model can be written as the sum of three terms:

$$H = H_{\rm at} + H_{\rm mol} + V_{\rm at-mol}, \tag{1.68}$$

The three terms in Eq. (1.68) are defined as follows:

- $H_{\rm at}$ is the atomic Hamiltonian and is thus linked to the open-channel:

$$H_{\rm at} = \int \frac{d^3k}{(2\pi)^3}\frac{\hbar^2k^2}{2m}a^\dagger_{\mathbf{k}}a_{\mathbf{k}} + \frac{g_0}{2}\int \frac{d^3Kd^3kd^3k'}{(2\pi)^9}\chi_b(k)\chi_b(k')a^\dagger_{\frac{\mathbf{K}}{2}-\mathbf{k}'}a^\dagger_{\frac{\mathbf{K}}{2}+\mathbf{k}'}a_{\frac{\mathbf{K}}{2}+\mathbf{k}}a_{\frac{\mathbf{K}}{2}-\mathbf{k}}. \tag{1.69}$$

  the interaction between atoms is separable: it is characterized by a coupling constant g_0 and the normalized Gaussian weight $\chi_b(k)$ of Eq. (1.42)[10] with $\epsilon = b$. The cut-off length b mimics the existence of the finite range of the actual pairwise interatomic potential and is thus of the order of the van der Waals range $R_{\rm vdW}$. The particular choice for the shape of the function $\chi_b(k)$ is not essential: it is only a convenient choice for analytical calculations and it is aimed to give a qualitative description of the short range physics. In Eq. (1.69) the threshold for the continuum of delocalized two-body states is chosen at zero energy.

- $H_{\rm mol}$ is the molecular Hamiltonian and is thus associated with the closed-channel:

$$H_{\rm mol} = \int \frac{d^3K}{(2\pi^3)}\left(\frac{\hbar^2K^2}{4m} + E_{\rm mol}\right)b^\dagger_{\mathbf{K}}b_{\mathbf{K}}, \tag{1.70}$$

  where the molecular energy $E_{\rm mol}$ is given by Eq. (1.64).

- $V_{\rm at-mol}$ couples the two channels:

$$H_{\rm at-mol} = \Lambda\int \frac{d^3Kd^3k}{(2\pi)^6}\,\chi_b(k)\,b^\dagger_{\mathbf{K}}a_{\frac{\mathbf{K}}{2}-\mathbf{k}}a_{\frac{\mathbf{K}}{2}+\mathbf{k}} + \text{h.c.} \tag{1.71}$$

  and thus models the Feshbach resonance mechanism. The inter-channel coupling in Eq. (1.71) is characterized by a constant Λ (chosen here to be real) and for convenience the same cut-off function $\chi_b(k)$ as in Eq. (1.69) is used. This choice is motivated by the fact that the actual size of the molecular state is of the order of the van der Waals range and thus fixes the spatial scale where the coherent coupling occurs. Interestingly, when applied in the context of the few-body problem, this particular choice permits one to obtain single closed equations for the three- and four-body problems [Jon08, Mor11a] similar to the ones obtained in the zero-range model [Pri11a].

Scattering amplitude

The general ansatz for the two-body problem in the center of mass frame is a coherent superposition of two atoms in the open channel and of one molecule at rest in the closed channel:

$$|\Psi\rangle = \int \frac{d^3k}{(2\pi)^3}A_{\mathbf{k}}a^\dagger_{\mathbf{k}}a^\dagger_{-\mathbf{k}}|0\rangle + \beta b^\dagger_{\mathbf{0}}|0\rangle. \tag{1.72}$$

In Eq. (1.72) $A(\mathbf{k})$ is the wave function in the momentum representation for the atomic pair. The equations verified by the amplitudes $A(\mathbf{k})$ and β in Eq. (1.72) are obtained from the projection onto the atomic and molecular subspaces of the stationary Schrödinger's equation at energy E: $(E-H)|\Psi\rangle = 0$ gives

$$\left(E - \frac{\hbar^2k^2}{m}\right)A_{\mathbf{k}} = \Lambda\chi_b(k)\beta + g_0\chi_b(k)\gamma \tag{1.73}$$

$$(E - E_{\rm mol})\beta = 2\Lambda\gamma \tag{1.74}$$

[10] In these lectures, in order to show the similarity between the separable two-channel model and the formulation of the zero-range approach of section (1.3.2), the definition of the cut-off function slightly differs from the one of Refs. [Jon08, Wer09, Jon10, Pri11b] which can be recovered by the substitution $b \to b\sqrt{2}$.

where $\gamma = \int \frac{d^3k'}{(2\pi)^3}\chi_b(k')A_{\mathbf{k}'}$. From Eqs. (1.73,1.74) one obtain an equation for the atomic wave function $A_{\mathbf{k}}$:

$$\left(\frac{\hbar^2k^2}{m} - E\right)A_{\mathbf{k}} = -\frac{g_0\chi_b(k)}{2\Lambda}\left(E - E_{\rm mol} + \frac{2\Lambda^2}{g_0}\right)\beta. \tag{1.75}$$

Interestingly, Eq. (1.75) is similar to the Schrödinger equation of the zero-range model in Eq. (1.32) where modulo an energy dependent multiplicative factor, β plays the role of the source amplitude S_A with [11]

$$S_A = \Lambda\beta^{\rm eff} \quad \text{and} \quad \beta^{\rm eff}(E) = \beta \times \frac{g_0}{2\Lambda^2}\left(E - E_{\rm mol} + \frac{2\Lambda^2}{g_0}\right). \tag{1.76}$$

For a scattering process, the atomic wave function is characterized by an incoming plane wave of momentum $\mathbf{k}_0$ and an outgoing spherical wave. Hence the expression of $A_{\mathbf{k}}$ obtained from Eq. (1.75) is

$$A_{\mathbf{k}} = (2\pi)^3\delta(\mathbf{k} - \mathbf{k}_0) + \frac{\Lambda\beta^{\rm eff}(E)\chi_b(k)}{E - \frac{\hbar^2k^2}{m} + i0^+}. \tag{1.77}$$

By identification of Eq. (1.77) and Eq. (1.8), the half on-shell transition matrix is thus:

$$\langle\mathbf{k}|T(E + i0^+)|\mathbf{k}_0\rangle = \Lambda\beta^{\rm eff}(E)\chi_b(k). \tag{1.78}$$

From Eqs. (1.73,1.74) one finds a closed equation for β and Eqs. (1.9,1.78) provide the scattering amplitude of the two-channel model denoted by $f_s(k_0)$:

$$\frac{m|\chi_b(k_0)|^2}{4\pi\hbar^2 f_s(k_0)} = \int \frac{d^3k}{(2\pi)^3}\frac{|\chi_b(k)|^2}{E - 2\epsilon_{\mathbf{k}} + i0^+} - \frac{E - E_{\rm mol}}{2\Lambda^2 + g_0(E - E_{\rm mol})}. \tag{1.79}$$

This scattering amplitude is fully isotropic showing that in this model, scattering occurs only in the s-wave. In the absence of inter-channel coupling ($\Lambda = 0$), the scattering amplitude at zero energy is by definition equals to the opposite of the background scattering length $a_{\rm bg}$ and from Eq. (1.79), one finds:

$$a_{\rm bg} = \sqrt{\frac{\pi}{2}}\frac{bg_0}{g_0 - g_0^{\rm c}} \quad \text{with} \quad g_0^{\rm c} = -\frac{(2\pi)^{3/2}\hbar^2 b}{m}. \tag{1.80}$$

The model is thus able to describe the neighborhood of a shape resonance ($|a_{\rm bg}| \gg b$) with $g_0 \sim g_0^{\rm c}$. Away from a shape resonance, $|a_{\rm bg}|$ is of the order of the potential range b. For convenience the full calculation of the scattering amplitude in Eq. (1.79) for $\Lambda \neq 0$ is performed at negative energy where $k_0 = iq$ and $q > 0$. Using again the definition of the scattering length $f_s(0) = -a$ and Eqs. (1.64,1.65,1.80) it is possible to express the scattering amplitude as a function of the parameters of the Feshbach resonance:

$$\frac{1}{f_s(iq)} = q\,\mathrm{erfc}\left(\frac{qb}{\sqrt{2}}\right) - \frac{e^{-\frac{q^2b^2}{2}}}{a_{\rm bg}}\left[1 - \frac{\delta\mu\Delta\mathcal{B}}{E - \delta\mu(\mathcal{B} - \mathcal{B}_0 - \Delta\mathcal{B})}\right], \tag{1.81}$$

where erfc() is the complementary error function which equals unity at zero, the resonance width is

$$\Delta\mathcal{B} = \frac{8\pi\hbar^2\Lambda^2 a_{\rm bg}}{mg_0^2\delta\mu}, \tag{1.82}$$

and the magnetic detuning is

$$\mathcal{B} - \mathcal{B}_0 = \frac{E_{\rm mol}}{\delta\mu} - \frac{2\Lambda^2}{g_0\delta\mu} + \Delta\mathcal{B}. \tag{1.83}$$

Expanding $1/f_s(E)$ at the first order in E, one finds the expression of the effective range of the model defined in Eq. (1.26):

$$r_{\rm e} = \frac{4b}{\sqrt{2\pi}} - \frac{b^2}{a} - 2R^\star\left(1 - \frac{a_{\rm bg}}{a}\right)^2. \tag{1.84}$$

[11] Forgetting the energy dependence of the source amplitude, the two models differ in the way that the zero-range limit is taken. For the two-channel model, in order to keep fixed a given low energy scattering behavior, the interaction parameters in the Hamiltonian Eq. (1.68) vary as a function of b as ($b \to 0$). In contrast, in the "δ_ϵ" formulation of the WBP model of sec. (1.3.2), the scattering length is not a function of ϵ.

Away from the Feshbach resonance, $a \sim a_{\rm bg}$ and $r_{\rm e} \sim \frac{4b}{\sqrt{2\pi}} - \frac{b^2}{a_{\rm bg}}$ and this justifies the choice made for the cut-off parameter $b \equiv \mathcal{O}(R_{\rm vdW})$.

It is remarkable that the parameters of the model can be adjusted in such a way that the scattering length a coincides exactly with the phenomenological law in Eq. (1.65). Equation (1.82) shows that the width radius is always positive. The model provides also the magnetic shift for the position of the resonance obtained from Eqs. (1.64,1.83):

$$\mathcal{B}_0^{\rm cl} - \mathcal{B}_0 = \frac{\Delta\mathcal{B}}{1 - b\sqrt{\pi}/(a_{\rm bg}\sqrt{2})}. \tag{1.85}$$

Dimers

The binding energy of the dimers of the model $E_{\rm dim} = \frac{\hbar^2 q_{\rm dim}^2}{m} > 0$ are found by searching the poles of the scattering amplitude $f_s(k_0)$ for $E = \frac{\hbar^2 k_0^2}{2m}$ and $k_0 = iq$, $q > 0$ (see [Lan67] section 128). In the limit where E and $\delta\mu(\mathcal{B} - \mathcal{B}_0)$ have both large and negative values, the leading term in the expansion of the left hand side gives the solution $E = E_{\rm mol} = -E_{\rm dim}$: *i.e.*, far from resonance the dimer coincides with the molecular state and is essentially in the closed channel. At finite detuning there are essentially two types of situations:

(i) For $a_{\rm bg} < b\sqrt{\pi/2}$, the dimer exists for a negative energy detuning $\delta\mu(\mathcal{B} - \mathcal{B}_0)$. The dimer results from the coupling between the atomic pair in the open channel and the molecular state. It is called in what follows the Feshbach dimer.

(ii) For $a_{\rm bg} > b\sqrt{\pi/2}$, away from the Feshbach resonance and for positive energy detunings $[\delta\mu(\mathcal{B} - \mathcal{B}_0) \to +\infty]$, a dimer exists in the open-channel it is called the background dimer. For negative energy detunings $[\delta\mu(\mathcal{B} - \mathcal{B}_0) < 0]$ there is another dimer. At threshold [*i.e.* for $\delta\mu(\mathcal{B} - \mathcal{B}_0) = 0^-$], the second dimer corresponds to the Feshbach dimer and for decreasing values of the energy detuning there is an avoided crossing between the Feshbach and the background dimers.

The two situations are displayed Fig. (1.3) where $q_{\rm dim} a_{\rm bg}$ is plotted as a function of the energy detuning $\delta\mu(\mathcal{B} - \mathcal{B}_0)$ in the case where $q_{\rm dim} b \ll 1$ and $|a_{\rm bg}|$ is large with respect to b [12] for a given value of the ratio $|a_{\rm bg}|/R^\star$. For a negative background scattering length ($a_{\rm bg} \ll -b$) only the Feshbach dimers exists and the corresponding branch is plotted in the negative region of the product $q_{\rm dim} a_{\rm bg}$ and of the energy detuning. For a positive background scattering length ($a_{\rm bg} \gg b$), $q_{\rm dim} a_{\rm bg}$ is positive and there are two branches.

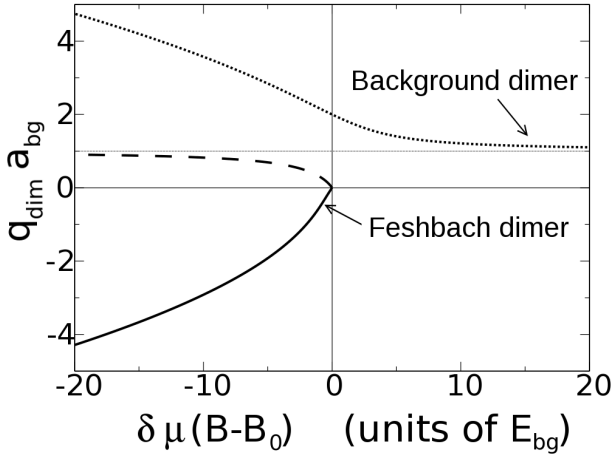

Figure 1.3: *Dimer for $q_{\rm dim} b \ll 1$ and the ratio $|a_{\rm bg}|/R^\star = 2$. The product $q_{\rm dim} a_{\rm bg}$ is plotted as a function of the energy detuning $\delta\mu(\mathcal{B} - \mathcal{B}_0)$. In the regime of negative background scattering length ($a_{\rm bg} < 0$) only one shallow dimer exists (solid line). For positive scattering length ($a_{\rm bg} > 0$) there exists an avoided crossing between the Feshbach dimer and the background dimer respectively (dashed and dotted lines respectively).*

[12] These inequalities enables to formally set $b = 0$ in Eq. (1.81).

For shallow dimers, the model allows to find an approximation for the binding wave number of the dimer beyond the 'universal' expression of Eq. (1.61) given by the WBP model [Pri11c]:

$$q_{\rm dim} \simeq \frac{-a+\sqrt{a^2+4R^\star(a-a_{\rm bg})-\frac{8ba}{\sqrt{2\pi}}+2b^2}}{2R^\star(a-a_{\rm bg})-\frac{4ba}{\sqrt{2\pi}}+b^2}. \tag{1.86}$$

Broad and narrow resonances

As noticed before, the Feshbach resonance can be qualified as broad or narrow resonance depending on the value of the width radius with respect to the van der Waals range. For a broad resonance, $R^\star$ is of the same order of magnitude or smaller than b, meaning that the correction to the universal law in Eq. (1.61) depends on the details of the true interatomic potential. Interestingly, if at finite detuning these corrections are known either experimentally or from microscopic computations, this can be a way to adjust the value of the parameter b. This is illustrated on Fig. (1.4) on the resonance at 402 G for potassium where microscopic computations are available [Der07].

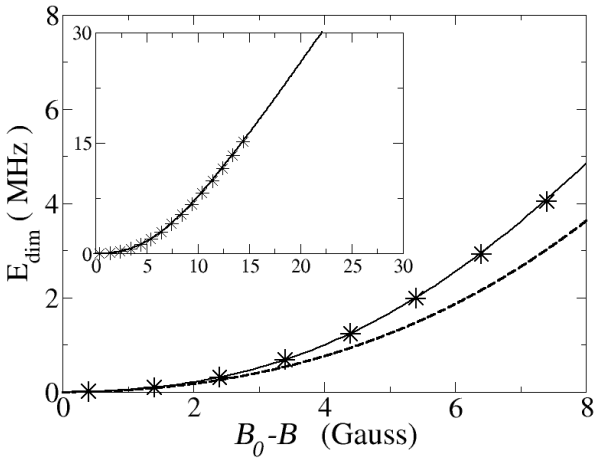

Figure 1.4: *Spectrum of the Feshbach dimer for the resonance at 402 G in ^{39}K. Stars: microscopic computations [Der07]; continuous line: two-channel model used in this paper where $b = 1.7\ R_{\rm vdW}$; dashed line: universal law $E_{\rm dim} = \hbar^2/(ma^2)$. Inset: for large detunings, the binding energy tends to $-E_{\rm mol}$.*

In the case of a narrow resonance the parameter $R^\star$ is large and positive and thus the effective range in Eq. (1.84) is large and negative. This explains why the effective range model based on the approximation of the scattering amplitude in Eq. (1.26) is relevant in this regime and has been successfully used in Ref. [Pet04b]. However, the separable two-channel contains more information than what is contained in the two parameters $r_{\rm e}$ and a. More precisely for $R^\star \gg b\left|\frac{\mathcal{B}-\mathcal{B}_0}{\Delta\mathcal{B}}\right|$, the short range parameter b can be neglected in Eq. (1.86) giving:

$$q_{\rm dim} \sim \frac{-a+\sqrt{a^2+4R^\star(a-a_{\rm bg})}}{2R^\star(a-a_{\rm bg})}. \tag{1.87}$$

One can notice that the expression in Eq. (1.86) is different from the one obtained in the effective range approach where the expression of $r_{\rm e}$ is taken from Eq. (1.84). In Fig. (1.5) the dimer spectrum obtained from the two-channel model is plotted for the narrow resonance of ^{39}K near 752 G and compared with the approximate law in Eq. (1.87) and also with the prediction of the effective range approximation.

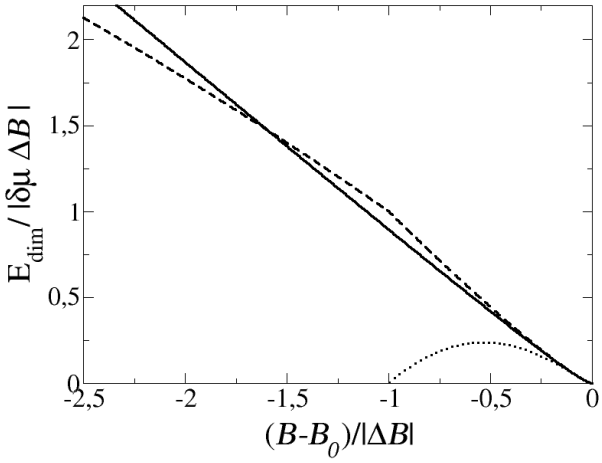

Figure 1.5: *Spectrum of the shallow dimer for the narrow resonance of ^{39}K at 752 G ($a_{\rm bg} = -35\ a_0$, $\Delta\mathcal{B} = -0.4$ G, $\delta\mu = 1.5\ \mu_B$, $R_{\rm vdW} = 64.6\ a_0$). Solid line: binding energy $E_{\rm dim}$ obtained from the two-channel model in units of $|\delta\mu\Delta\mathcal{B}|$ as a function of the relative detuning $(\mathcal{B} - \mathcal{B}_0)/|\Delta\mathcal{B}|$; dashed line: approximate law for narrow resonances from Eq.(1.87); dotted line: binding energy in the effective range approximation.*

Neighborhood of a shape resonance Trapped cesium atoms are in the vicinity of shape resonance with an anomalously large and positive background scattering length. Thus there exists a shallow background dimer away from a Feshbach resonance. The spectrum of the dimers in the vicinity of the resonance at -12 G is displayed in Fig. (1.6). The binding energies are plotted in logarithmic coordinates in order to show the large level repulsion (which is a consequence of the large value of the ratio $|\delta\mu\Delta\mathcal{B}|/E_{\rm bg}$).

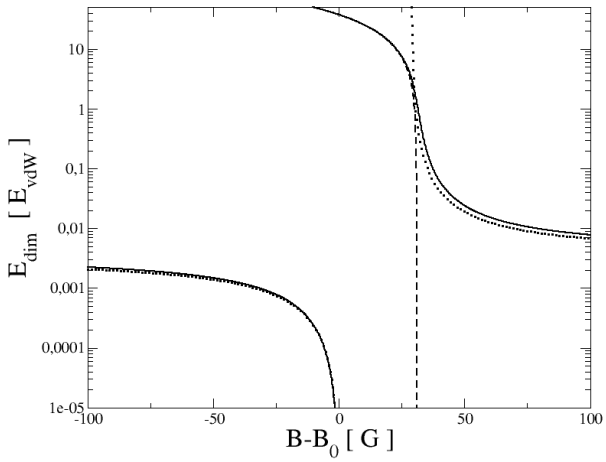

Figure 1.6: *Spectrum for cesium dimers in the vicinity of the Feshbach resonance located at a magnetic field near -12 G. This figure illustrates a level repulsion between the Feshbach dimer and the background dimer. Solid line: spectrum derived from the two-channel model with $b = R_{\rm vdW}$; dotted line: spectrum from Eq. (1.31); dashed line: molecular energy. For the lowest branch the exact calculation and the approximate law obtained from Eq. (1.31) almost coincide.*

The first observation of Efimov has been achieved in the vicinity of this resonance. Hence it is important to test the reliability of the separable two-channel model for the description of the dimers. In Ref. [Jon08], it has been shown that the experimental data for the dimer spectroscopy of Ref. [Mar07] are well reproduced by the separable two-channel model (even in the region of the repulsion where the scattering length cross zero) with a value of the short range parameter approximately equals to the van der Waals range ($b = R_{\rm vdW}$). This feature is displayed in Fig. (1.7).

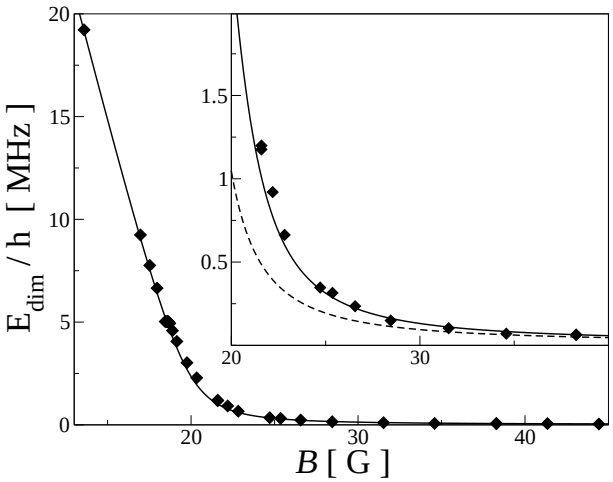

Figure 1.7: *Dimer spectrum for the resonance at -12 G for cesium atoms in the region studied experimentally by the group of Innsbruck. The data are taken from Ref. [Mar07]. Diamonds: experimental data; solid line: result of the separable two-channel model (1.68) where $b = R_{\rm vdW}$; dashed line: universal law of the WBP model (1.61).*

1.5.3 Identical fermions in the vicinity of a p wave Feshbach resonance

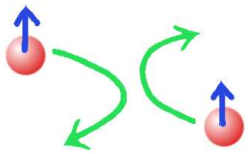

As noticed before, taking into account the p wave interaction in cold collisions is relevant in the case where one considers fully polarized (*i.e.* identical) fermions. In particular, in the light of the properties observed for atomic systems in the vicinity of a s wave resonance, it is interesting to have a separable two-channel model of the Feshbach resonance for fermions. Microscopically the p wave Feshbach resonance is achieved by the coherent coupling between a molecular state with an internal angular momentum $l = 1$ and atomic pairs. In experiments, the resonance is tuned by using an external magnetic field which introduces a preferred direction in the system say $\hat{\mathbf{e}}_z$, if the magnetic field is $\mathcal{B}\hat{\mathbf{e}}_z$. As a result, the two molecular states in the orbitals $\hat{\mathbf{e}}_x \pm i\hat{\mathbf{e}}_y$ [13] are degenerate [Tic04] while there is a lifting of degeneracy with the orbital $\hat{\mathbf{e}}_x$. This phenomenon is neglected in order to simplify the discussion.

In this approximation, the two-channel model is very similar to the one introduced for bosons. Its ingredients are the following:

(i) three structureless bosonic molecular states in the closed channel expressed in the vectorial basis $(\hat{\mathbf{e}}_x, \hat{\mathbf{e}}_y, \hat{\mathbf{e}}_z)$;

(ii) A cut-off function for the coupling between an atomic pair and the molecular state. The choice of a vectorial basis for the molecular states imposes also that the cut-off function has a vectorial character $[\boldsymbol{\chi}_b(\mathbf{k}) = \mathbf{k}\chi_b(k)]$.

The Hamiltonian is given in Eqs. (15,121) in Ref. [Jon08]. In this model, the scattering is purely in the p wave and the parameters can adjusted in order to find an law for the scattering volume $\mathcal{V}_{\rm s}$ analogous to Eq. (1.65):

$$\mathcal{V}_{\rm s} = \mathcal{V}_{\rm bg}\left(1 - \frac{\Delta\mathcal{B}}{\mathcal{B} - \mathcal{B}_0}\right). \tag{1.88}$$

Furthermore, the p wave scattering amplitude (Eq. (125) in Ref. [Jon08]) can be written in a form analogous to

[13] We use the vectorial representation of the orbitals p defined from the relations: $Y_{10}(\Omega) = i\sqrt{3/(4\pi)}\hat{\mathbf{e}}_z \cdot \mathbf{n}$ and $Y_{1\pm1}(\Omega) = \mp\sqrt{3/(8\pi)}(\hat{\mathbf{e}}_x \pm \hat{\mathbf{e}}_y) \cdot \mathbf{n}$ where $\mathbf{n}$ is the unitary vector defined by the angles Ω (see [Lan67] section 57).

Eq. (1.81):

$$\frac{1}{f_p(iq)} = q\,\mathrm{erfc}\left(\frac{qb}{\sqrt{2}}\right) + \frac{\exp(-q^2b^2/2)}{\mathcal{V}_{\rm bg}q^2}\left[1 - \frac{\delta\mu\Delta\mathcal{B}}{E - \delta\mu(\mathcal{B}-\mathcal{B}_0-\Delta\mathcal{B})} + \frac{q^2\mathcal{V}_{\rm bg}\sqrt{2}}{b\sqrt{\pi}}\right], \tag{1.89}$$

where the usual analytical continuation $k_0 = iq$ with $q > 0$ has been used. At resonance, the effective range parameter in Eq. (1.30) is

$$\alpha = \alpha^\star + \frac{\sqrt{2}}{b\sqrt{\pi}} \quad \text{where} \quad \alpha^\star = \frac{\hbar^2}{m\mathcal{V}_{\rm bg}\delta\mu\Delta\mathcal{B}} > 0. \tag{1.90}$$

Similarly to the s wave resonance, the resonance is narrow for $\alpha^\star \gg 1/R_{\rm vdW}$. Eq. (1.90) is an illustration of the radius-range inequality of Eq. (1.59). The minimal value for the parameter α is obtained in the limit of the broadest p wave Feshbach resonances [14].

[14] In this limit $\alpha = \frac{\sqrt{2}}{b\sqrt{\pi}}$ and the multiplicative factor close to unity not present in Eq. (1.59) is a consequence of the fact that the interaction potential in the open-channel has not a compact support.

Chapter 2

Three bosons in the resonant regime

Contents

2.1 Preamble

This lecture follows the historical progression which has led to the discovery of the Efimov states in the 70's and their observation in 2006. Simple exact solutions provide deep insight in the nature of physical phenomenon and I hope that this exciting issue will be inspiring for young physicists.

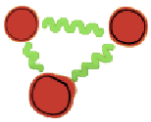

2.2 WBP model for few body systems

In the study of s wave resonant systems, the Wigner Bethe Peierls model is at first sight a natural formalism to use as it describes only the low energy scale linked to the resonance $[|E| \sim \hbar^2/(ma^2)]$ and thus it encapsulates directly the scale separation with 'high energy' processes $[|E| \sim \hbar^2/(mR_{\rm vdW}^2)]$. In using this model where the short range details of the interaction are ignored, one expects to obtain 'universal' laws on few-body observables depending only on one parameter for the interaction: the scattering length.

The generalization of the WBP model introduced in the first lecture for few- or many-body systems can be done as follows. For a N-body system, the particles are labeled by the number $i = 1 \dots N$. Each interacting term in the Schrödinger equation is replaced by a source term. For a state $|\Psi\rangle$ the source amplitude for an interacting pair (ij) is denoted by the ket $|S_\Psi^{i=j}\rangle$ which is associated with a function of all the degree of freedom excepted the relative coordinates of the pair (ij). The ket associated with the function $\delta_\epsilon(\mathbf{r}_{ij})$ where $\mathbf{r}_{ij}$ are the

relative coordinates of the pair (ij) is denoted by $|(ij):\delta_\epsilon\rangle$. Using these notations the stationary Schrödinger equation for the state $|\Psi\rangle$ of energy E can be written as

$$(H_0 - E)|\Psi_\epsilon\rangle = -\sum_{(i<j)_{\rm int}} |S_\Psi^{i\leftrightharpoons j}\rangle \otimes |(ij):\delta_\epsilon\rangle. \tag{2.1}$$

In Eq. (2.1) H_0 is the free Hamiltonian *i.e.* the Hamiltonian without the pairwise potentials of the interacting pair and $(i<j)_{\rm int}$ means that the summation is restricted to the interacting pairs (ij). Finally, the source amplitudes $|S_\Psi^{i\leftrightharpoons j}\rangle$ are obtained by imposing the contact condition given by Eq. (1.50) for each interacting pair:

$$\lim_{\epsilon\to 0}\langle(ij):\delta_\epsilon|\left[|\Psi_\epsilon\rangle - |{\rm S}_\Psi^{i\leftrightharpoons j}\rangle \otimes |(ij):\phi_\epsilon^\Lambda\rangle\right] = \frac{|{\rm S}_\Psi^{i\leftrightharpoons j}\rangle}{t(E_\Lambda)}, \tag{2.2}$$

where $|(ij):\phi_\epsilon^\Lambda\rangle$ is the ket associated with the function $\langle \mathbf{r}_{ij}|\phi_\epsilon^\Lambda\rangle$ obtained from Eq. (1.44).

2.3 Puzzling findings obtained from the zero-range approach

2.3.1 Skorniakov Ter-Martirosian equation

In this section a closed equation for the source amplitudes of the WBP model is derived in the case of three spinless identical bosons. The particles have a mass m and are considered in their center of mass frame without external potential.

The translation invariance of the system suggests to use Eqs. (2.1,2.2) in the momentum representation. We thus introduce the momentum $\mathbf{k}_i$ for each particle $i = 1\dots 3$. The relative and total momentum of a given pair of particles (ij) are denoted by

$$\boldsymbol{k}_{ij} = \frac{\mathbf{k}_i - \mathbf{k}_j}{2} \quad \text{and} \quad \boldsymbol{K}_{ij} = \mathbf{k}_i + \mathbf{k}_j. \tag{2.3}$$

As a consequence of the bosonic symmetry, the source amplitudes $|S^{1\leftrightharpoons 3}\rangle$ and $|S^{2\leftrightharpoons 3}\rangle$ are deduced from $|S^{1\leftrightharpoons 2}\rangle$ by exchange of the particles:

$$|S^{1\leftrightharpoons 2}\rangle = |S^{1\leftrightharpoons 3}\rangle = |S^{2\leftrightharpoons 3}\rangle. \tag{2.4}$$

Using the translational invariance, without loss of generality the total momentum can be set to zero. The stationary states $|\Psi\rangle$ and the source amplitudes can then be factorized as:

$$\langle \mathbf{k}_1,\mathbf{k}_2,\mathbf{k}_3|\Psi\rangle = \delta(\mathbf{k}_1+\mathbf{k}_2+\mathbf{k}_3)\langle \mathbf{k}_1,\mathbf{k}_2,\mathbf{k}_3|\psi\rangle \quad \text{and} \quad \langle \mathbf{K}_{12},\mathbf{k}_3|S^{1\leftrightharpoons 2}\rangle = \frac{4\pi\hbar^2}{m}\delta(\mathbf{k}_1+\mathbf{k}_2+\mathbf{k}_3)\langle \mathbf{k}_3|A_\psi\rangle \tag{2.5}$$

and the stationary Schrödinger equation reads

$$\left[\frac{\hbar^2}{2m}\left(k_1^2+k_2^2+k_3^2\right) - E\right]\langle \mathbf{k}_1,\mathbf{k}_2,\mathbf{k}_3|\psi\rangle = -\frac{4\pi\hbar^2}{m}\sum_{1\le i<j\le 3}\langle \mathbf{k}_{ij}|\delta_\epsilon\rangle\langle \mathbf{k}_i|A_\psi\rangle, \tag{2.6}$$

where $\mathbf{k}_1+\mathbf{k}_2+\mathbf{k}_3 = 0$. A three-body scattering process in the center of mass frame is characterized by an incoming state $|\psi^{(0)}\rangle$ (a regular solution of the free Schrödinger equation) at positive energy ($E>0$). From Eq. (2.6) one obtains:

$$\langle \mathbf{k}_1,\mathbf{k}_2,\mathbf{k}_3|\psi\rangle = \langle \mathbf{k}_1,\mathbf{k}_2,\mathbf{k}_3|\psi^{(0)}\rangle + \frac{4\pi\hbar^2}{m}\frac{\sum_{1\le i<j\le 3}\langle \mathbf{k}_{ij}|\delta_\epsilon\rangle\langle \mathbf{k}_i|A_\psi\rangle}{E+i0^+ - \frac{\hbar^2}{2m}\left(k_1^2+k_2^2+k_3^2\right)} \tag{2.7}$$

where the usual prescription $E\to E+i0^+$ selects an outgoing wave. In the zero range limit ($\epsilon\to 0$), the WBP contact condition in Eq. (1.52) written for the pair (12) is:

$$\int \frac{d^3k_{12}}{(2\pi)^3}\left[\langle \mathbf{k}_1,\mathbf{k}_2,\mathbf{k}_3|\psi\rangle + \frac{4\pi\langle \mathbf{k}_3|A_\psi\rangle}{k_{12}^2+\Lambda^2}\right] = -\frac{\langle \mathbf{k}_3|A_\psi\rangle}{f_W(i\Lambda)}. \tag{2.8}$$

Equation (2.8) is invariant in a change of the free parameter Λ (where $\Lambda\in\mathbb{R}^+$). For a negative eigenenergy ($E<0$) and for the choice

$$\Lambda = \sqrt{-\frac{mE}{\hbar^2}+\frac{3}{4}k_3^2}, \tag{2.9}$$

the two terms involving $\langle \mathbf{k}_3|A_\psi\rangle$ in the integral at the left hand side of Eq. (2.8) simplify with each others. This choice has a physical meaning which can be understood by performing the simple decomposition which would be exact if the total energy was purely kinetic:

$$E = \frac{\hbar^2 k_3^2}{2m} + \frac{\hbar^2 K_{12}^2}{4m} + \frac{\hbar^2 k_{12}^2}{m} \Longrightarrow \frac{\hbar^2 k_{12}^2}{m} = E - \frac{3\hbar^2 k_3^2}{4m}. \tag{2.10}$$

where the identity $\mathbf{K}_{12} = -\mathbf{k}_3$ has been used. Thus $E_\Lambda = -\hbar^2\Lambda^2/m$ where Λ is given by Eq. (2.9) corresponds somehow to the available energy of the two colliding particles in their own center of mass frame. This energy is often called the colliding (or relative) energy for the pair (12) and is denoted by $E_{\rm col}$. Using this definition, the left hand side of Eq. (2.6) can be rewritten as:

$$\frac{\hbar^2}{2m}\left(k_1^2 + k_2^2 + k_3^2\right) - E = \frac{\hbar^2 k_{12}^2}{m} - E_{\rm col}. \tag{2.11}$$

In the case where the eigenenergy E is positive, the integral equation for $\langle \mathbf{k}|A_\psi\rangle$ is recovered by analytical continuation. In what follows, the substitution $\mathbf{k}_3 \to \mathbf{K}$ is performed and $k_{\rm col}$ denotes the wave number associated with this colliding energy:

$$k_{\rm col} = \begin{cases} i\sqrt{-mE/\hbar^2 + 3K^2/4} & \text{if} \quad K^2 > mE/\hbar^2 \\ \\ \sqrt{mE/\hbar^2 - 3K^2/4} & \text{otherwise.} \end{cases} \tag{2.12}$$

The two other terms in the integral of Eq. (2.8) associated with $\mathrm{D}(\mathbf{k}_1)$ and $\mathrm{D}(\mathbf{k}_2)$ give the same contribution. Eventually, using the fact that the integration is done for a fixed value of $\mathbf{K}_{12}$, one can perform the change of variable $d^3k_{12} = d^3k_1$ which provides the Skorniakov Ter-Martirosian (STM) equation [Sko57]

$$\int \frac{d^3k}{\pi^2} \frac{\langle \mathbf{k}|A_\psi\rangle}{k^2 + K^2 + \mathbf{K}\cdot\mathbf{k} - \frac{m}{\hbar^2}E - i0^+} = \frac{\langle \mathbf{K}|A_\psi\rangle}{f_W(k_{\rm col})} + \int \frac{d^3k}{(2\pi)^3} \langle \mathbf{k} - \frac{\mathbf{K}}{2}, -\mathbf{k} - \frac{\mathbf{K}}{2}, \mathbf{K}|\psi^{(0)}\rangle. \tag{2.13}$$

2.3.2 The pathologies of the zero-range model for three interacting bosons

In Ref. [Dan61] Danilov shows that as it stands Eq. (2.13) is ill defined: the Hamiltonian in the WBP model for three interacting bosons is not self-adjoint because the isotropic eigenstates are not orthogonal with each others. He solves this problem by introducing a three-body contact condition for the wave function. Nevertheless, Minlos and Fadeev realized after this work that even with this method, the zero-range model leads to a spectrum which is not bounded from below [Min62]. This section gathers these essential findings of the Russian school.

All the pathologies of the STM equation correspond to the unphysical short range behavior of the three-body wave function. This issue can thus be studied in the high momentum limit of $\langle \mathbf{k}|A_\psi\rangle$ where the inverse scattering length $1/a$ is negligible in Eq. (2.13). Consequently, in this section the discussion is focused on the properties of isotropic and negative energy solutions of the STM equation in the unitary regime (this corresponds to $|a| = \infty$ in the WBP model and the s wave component of $\langle \mathbf{k}|A_\Psi\rangle$ is denoted by

$$D(k) = \int \frac{d\Omega}{4\pi} \langle \mathbf{k}|A_\psi\rangle. \tag{2.14}$$

Furthermore, it is also more simple to consider only the case of negative energy solution which implies that $\psi_0 = 0$ in Eq. (2.13). In the unitary regime there isn't any two-body bound state in the WBP model. Thus if a negative energy solution of the STM equation exists, this is a three-body bound state (trimer) in absence of shallow dimer. This type of bound state is called 'Borromean': a small wink to the coat of arms of the Borromeo family representing three rings bound together but which are all free if only one ring is left out. In what follows we use the binding wave number $q > 0$ for the trimers defined by:

$$E = -\frac{\hbar^2 q^2}{m}. \tag{2.15}$$

The kernel of the integral in the STM equation (2.13) is rotationally invariant so that the eigenfunctions can thus be studied separately in each momentum sector. In the unitary limit $D(k)$ verifies the integral equation

$$D(k)\sqrt{q^2 + \frac{3k^2}{4}} = \frac{2}{\pi}\int_0^\infty du\, D(u)\mathcal{K}_q(k,u), \tag{2.16}$$

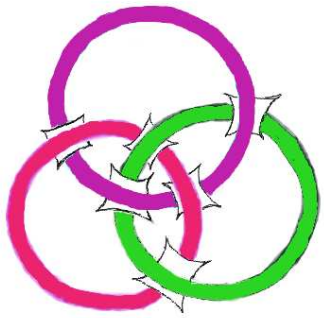

Figure 2.1: *Borromean rings*

where the s wave kernel of the STM equation is given by

$$\mathcal{K}_q(k,u) = \frac{u}{k}\ln\left(\frac{u^2+k^2+q^2+ku}{u^2+k^2+q^2-ku}\right). \tag{2.17}$$

Equation (2.16) can be solved by using the method introduced in Ref. [Gog08]. For this purpose, the integration is extended to the full real axis and $D(k)$ is continued to the domain of negative momentum with the even parity $D(k) = D(-k)$. Hence in the right hand side of Eq. (2.16) the limits of the integral are from $-\infty$ to $+\infty$ and the factor $2/\pi$ is replaced by a factor $1/\pi$. Furthermore, performing the change of variables

$$u = \frac{2q}{\sqrt{3}}\sinh\xi \quad , \quad k = \frac{2q}{\sqrt{3}}\sinh\xi' \tag{2.18}$$

and introducing the function ϕ_0 defined by

$$\frac{\phi_0(\xi)}{\cosh\xi} = uD(u), \tag{2.19}$$

the integral equation transforms into

$$\frac{4}{\pi\sqrt{3}}\int_{-\infty}^{\infty} d\xi'\,\phi_0(\xi')\ln\left(\frac{e^{2\xi}+e^{\xi+\xi'}+e^{2\xi'}}{e^{2\xi}-e^{\xi+\xi'}+e^{2\xi'}}\right) = \phi_0(\xi). \tag{2.20}$$

Finally performing the change of variable $z = e^{\xi}$ and introducing the function $g(z) = \phi_0(\xi)$ one obtains:

$$\frac{4}{\pi\sqrt{3}}\int_{0}^{\infty} \frac{dz'}{z'}\,g(z')\ln\left(\frac{z'^2+zz'+z^2}{z'^2-zz'+z^2}\right) = g(z). \tag{2.21}$$

This equation is scale invariant in the transform $z \to \lambda z$ which suggests that the solutions can be searched as power laws: $g(z) = z^s$. Injecting this ansatz into Eq. (2.21) gives an eigenvalue equation for the exponent s:

$$\frac{4}{\pi\sqrt{3}}\int_{0}^{\infty} dx\,x^{s-1}\ln\left(\frac{x^2+x+1}{x^2-x+1}\right) = 1 \tag{2.22}$$

which is well defined only for $-1 < \Re(s) < 1$. The integral in Eq. (2.22) can be performed in the complex plane and one finally finds the equation satisfied by s:

$$s = \frac{8}{\sqrt{3}}\frac{\sin\left(\frac{s\pi}{6}\right)}{\cos\left(\frac{s\pi}{2}\right)}. \tag{2.23}$$

Equation (2.23) is invariant in the change $s \to -s$ and is solved graphically in Fig. (2.2). There exists only two conjugate imaginary solutions $s = \pm i s_0$ where $s_0 = 1.00624\ldots$ and the lowest real and positive solution lies in the vicinity of $s = 2$.

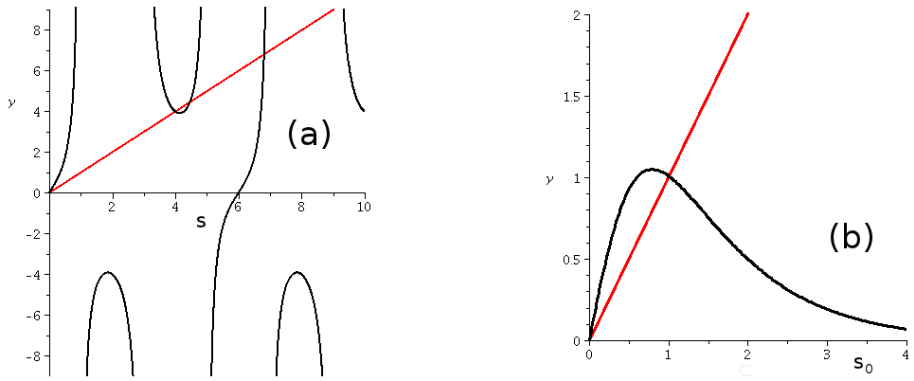

Figure 2.2: Graphical solution of the eigenequation $s = \frac{8}{\sqrt{3}} \frac{\sin\left(\frac{s\pi}{6}\right)}{\cos\left(\frac{s\pi}{2}\right)}$: (a) real solutions for the exponent s: (b) imaginary solution for $s = is_0$.

The isotropic solutions of the STM equation at unitarity are thus of the form

$$g(z) = c_{(+)} z^{is_0} + c_{(-)} z^{-is_0}. \tag{2.24}$$

Using the natural assumption that $D(k)$ is a regular function in the low momentum limit implies that $\phi_0(0) = 0$ and $g(1) = 0$. Hence $c_{(+)} = -c_{(-)}$ and the analytical expression for the source amplitude is given by:

$$D(k) = \frac{1}{k\sqrt{q^2 + \frac{3k^2}{4}}} \sin\left[s_0 \operatorname{arcsinh}\left(\frac{k\sqrt{3}}{2q}\right)\right]. \tag{2.25}$$

This result first obtained in Ref. [Min62] is striking: all the real positive values for the binding wave number q are allowed meaning that it is not quantized and that there exists a continuum of negative energy solution. Moreover the spectrum is not bounded from below ! This is the so-called Thomas collapse which is a characteristic of numbers of systems composed of particles interacting through a pairwise zero-range potential [Tho35]. In Ref. [Dan61] Danilov shows that the scalar product between two eigenstates does not vanish so that the existence of this continuum of negative energy solutions implies that the WBP is not self-adjoint for three bosons. The reason of this inconsistency has a physical meaning and can be understood by considering the high momentum behavior of $D(k)$ obtained from Eq. (2.25):

$$D(k) \underset{k\to\infty}{\propto} \frac{1}{k^2} \sin\left[s_0 \ln\left(\frac{k\sqrt{3}}{q}\right)\right]. \tag{2.26}$$

In Eq. (2.26) the binding wave number appears explicitly in the short range behavior of the three-body wave function which is a physical nonsense because one expects that for low energy states (*i.e.* for energies $|E|$ much less than the characteristic energy of the true pairwise interaction potential between particles) this asymptotic behavior is independent of the eigenenergy. On this physical basis Danilov introduced a filtering procedure (somehow a three-body contact condition) by imposing an unique high momentum behavior for all the eigenstates. This condition can be written in terms of a three-body parameter $\kappa^\star$ as:

$$D(k) \underset{k\to\infty}{\propto} \frac{1}{k^2} \sin\left[s_0 \ln\left(\frac{k\sqrt{3}}{\kappa^\star}\right)\right]. \tag{2.27}$$

One can notice that by construction the three-body parameter is not unique [Eq. (2.26) is invariant in a change $\kappa^\star \to \kappa^\star \exp(\pi/s_0)$] and more interestingly the zero-range model of Danilov supports a discrete scaling symmetry as Eqs. (2.25,2.26) are invariant in the change:

$$k \to \lambda_0 \times k \qquad q \to \lambda_0 \times q \quad \text{and} \quad D \to \frac{D}{\lambda_0^2} \tag{2.28}$$

where

$$\lambda_0 = \exp\left(\frac{\pi}{s_0}\right) = 22.694\ldots \quad \text{and} \quad \lambda_0^2 = 515.02\ldots \tag{2.29}$$

Hence, all the binding wave numbers q_n can be deduced from the reference $q = \kappa^\star$ by an integer power of the scaling factor λ_0 [Min62]:

$$q_n = \kappa^\star \exp\left(\frac{-n\pi}{s_0}\right) \quad (n \in \mathbb{Z}). \tag{2.30}$$

Unfortunately even if the self-adjointness is restored, the model of Danilov does not cure the Thomas collapse[1].

In this section only the unitary case was considered. However the model of Danilov (introduced for solving the neutron-deuteron scattering problem) is more general as the filtering condition in Eq. (2.27) can be applied for finite values of the scattering length [2]. Thus, the zero-range model of Danilov is defined by two parameters: a and $\kappa^\star$. In the unitary regime the model of Danilov even though it is a zero-range model introduces a momentum scale (the three-body parameter $\kappa^\star$) which breaks the continuous scaling symmetry of the WBP model [Cas04]. Nevertheless the continuous scaling symmetry is replaced by the discrete symmetry of Eq. (2.29).

2.4 The breakthrough of Efimov

In Ref. [Efi70] Efimov gives the physical meaning of the zero-range formulation in the three-body problem. This analysis provides a physical interpretation of the results obtained by Danilov Minlos and Fadeev. For this purpose he uses the configuration space representation which allows to have a more intuitive understanding of the system. The three important results of this work are the following:

- the Thomas collapse can be mapped onto the problem of the fall of a fictitious particle in the center of an attractive $1/r^2$ potential in a two-dimensional space;
- the spectrum of Minlos and Fadeev in Eq. (2.30) has a physical meaning in the low energy limit *i.e.* for $|E| \ll \hbar^2/(mb^2)$. Consequently, the spectrum for three resonant bosons interacting through a pairwise short range potential at resonance ($|a| = \infty$) has an accumulation point at zero energy;
- the spectrum in the regime where the scattering length is large in absolute value compared to the potential radius is composed of branches which can be deduced with each others by a homothety.

This section closely follows the reasoning of Efimov in Ref. [Efi71]. Without loss of generality, the three bosons are studied in their center of mass frame and the center of mass is denoted by $\mathbf{C} = \frac{\mathbf{r}_1+\mathbf{r}_2+\mathbf{r}_3}{3}$. Equations have a simple form in terms of the Jacobi coordinates:

$$\mathbf{r}_{ij} = \mathbf{r}_i - \mathbf{r}_j \quad ; \quad \boldsymbol{\rho}_k = \frac{2}{\sqrt{3}}\left(\mathbf{r}_k - \frac{\mathbf{r}_i + \mathbf{r}_j}{2}\right). \tag{2.31}$$

and of the hyper radius

$$R = \sqrt{r_{ij}^2 + \rho_k^2} = \sqrt{2\sum_{i=1}^{3}(\mathbf{r}_i - \mathbf{C})^2}. \tag{2.32}$$

In Eq. (2.31) the triplet (i, j, k) is deduced by permutations from the triplet $(1, 2, 3)$. Following the general method of Fadeev [Fad61] and in order to privilege the interacting pairs, the wave function is written as a sum of three terms:

$$\langle \mathbf{r}_1, \mathbf{r}_2, \mathbf{r}_3 | \psi \rangle = \chi(\mathbf{r}_{12}, \boldsymbol{\rho}_3) + \chi(\mathbf{r}_{13}, \boldsymbol{\rho}_2) + \chi(\mathbf{r}_{32}, \boldsymbol{\rho}_1) = (1 + Q)\chi(\mathbf{r}_{12}, \boldsymbol{\rho}_3) \tag{2.33}$$

where $Q = P_{13} + P_{23}$ and P_{ij} exchanges particle i with particle j. For convenience we use the notation $\mathbf{r} = \mathbf{r}_{12}$ and $\boldsymbol{\rho} = \boldsymbol{\rho}_3$. In the center of mass frame the kinetic operator for the system is:

$$T = -\frac{\hbar^2}{2m}\left(\Delta_{\mathbf{r}_1} + \Delta_{\mathbf{r}_2} + \Delta_{\mathbf{r}_3}\right) = -\frac{\hbar^2}{m}\left(\Delta_{\mathbf{r}} + \Delta_{\boldsymbol{\rho}}\right). \tag{2.34}$$

The three bosons interact through a pairwise potential V in vicinity of a s wave resonance and each term in the Fadeev decomposition of Eq. (2.33) verifies the equation

$$(T - E)\,\chi(\mathbf{r}, \boldsymbol{\rho}) = -V(\mathbf{r})(1 + Q)\chi(\mathbf{r}, \boldsymbol{\rho}). \tag{2.35}$$

[1] Minlos and Fadeev noticed in Ref. [Min62] that the unitary spectrum in Eq. (2.30) coincides with the spectrum of a particle falling in an attractive $1/r^2$ potential.

[2] One has to keep in mind that the model is relevant only in the vicinity of a s wave scattering resonance.

As we search for the bound states of the model, the energy in Eq. (2.35) is negative with $E = -\frac{\hbar^2 q^2}{m}$ where $q > 0$. Summation of the equations deduced from Eq. (2.35) for each Fadeev component provides the stationary Schrödinger equation at energy E verified by the three-body wave function ψ.

For coordinates $\boldsymbol{\rho}$ kept fixed (and $\rho \gg b$) while the interparticle distance r takes values of the order of b, the three-body wave function verifies:

$$(T - E)\,\langle \mathbf{r}_1, \mathbf{r}_2, \mathbf{r}_3 | \psi \rangle = -V(\mathbf{r}) \langle \mathbf{r}_1, \mathbf{r}_2, \mathbf{r}_3 | \psi \rangle = -V(\mathbf{r}) \chi(\mathbf{r}, \boldsymbol{\rho}). \tag{2.36}$$

For $\rho \gg b$ and $r > b$, ψ solves the free Schrödinger equation. In this configuration, the term $\chi(\mathbf{r}_{12}, \boldsymbol{\rho}_3)$ gives the dominant contribution in the Fadeev decomposition of Eq. (2.33). This justifies the use of the WBP model where the pairwise interaction potential V is replaced by the contact condition in Eq. (1.34) *i.e.* r can take arbitrarily small values and

$$\langle \mathbf{r}_1, \mathbf{r}_2, \mathbf{r}_3 | \psi \rangle \underset{r \to 0}{=} \langle \boldsymbol{\rho} | A_\psi \rangle \left(\frac{1}{a} - \frac{1}{r} \right). \tag{2.37}$$

In Eq. (2.37) the limit is taken at a fixed value of $\boldsymbol{\rho}$. This approximation amounts to neglecting the contribution of $Q\chi(\mathbf{r}, \boldsymbol{\rho})$ on the wave function ψ for an interparticle distance r larger than (but of the order of) b. This assumption is justified for $\rho \gg b$. In the limit of vanishing interparticle distances $r \to 0$ the diverging part in the Fadeev decomposition is thus given by $\chi(\mathbf{r}, \boldsymbol{\rho})$ and one has:

$$\langle \boldsymbol{\rho} | A_\psi \rangle = -\lim_{r \to 0} [r \chi(\mathbf{r}, \boldsymbol{\rho})]. \tag{2.38}$$

Hence, inspired by the result of Danilov one might guess that near a s wave scattering resonance, the asymptotic behavior of $\chi(\mathbf{r}, \boldsymbol{\rho})$ for $\rho \gg b$ has an universal character. This is indeed the case as is shown in the following lines.

The regular part of $\psi(\mathbf{r}, \boldsymbol{\rho})$ in Eq. (2.37) is provided by the relation:

$$\frac{\langle \boldsymbol{\rho} | A_\psi \rangle}{a} = \lim_{r \to 0} \partial_r \left[r \langle \mathbf{r}_1, \mathbf{r}_2, \mathbf{r}_3 | \psi \rangle \right]. \tag{2.39}$$

In the limit $\mathbf{r} \to 0$, one obtains $\boldsymbol{\rho}_1 = \boldsymbol{\rho}_2 = \frac{\mathbf{r}_{13}}{\sqrt{3}} = \frac{\mathbf{r}_{23}}{\sqrt{3}}$ and $\boldsymbol{\rho}_3 = -2\boldsymbol{\rho}_1$ so that:

$$\langle \mathbf{r}_1, \mathbf{r}_2, \mathbf{r}_3 | \psi \rangle \underset{r \to 0}{=} \chi(\mathbf{r}, \boldsymbol{\rho}) + 2\chi(-\sqrt{3}\boldsymbol{\rho}/2, -\boldsymbol{\rho}/2) \tag{2.40}$$

and the regular part of ψ is thus

$$\frac{\langle \boldsymbol{\rho} | A_\psi \rangle}{a} = \lim_{r \to 0} \partial_r [r \chi(\mathbf{r}, \boldsymbol{\rho})] + 2\chi(-\sqrt{3}\boldsymbol{\rho}/2, -\boldsymbol{\rho}/2). \tag{2.41}$$

Using Eqs. (2.38,2.41), the WBP contact condition in Eq. (2.37) associated with the interacting pair (12) gives:

$$\lim_{r \to 0} -\frac{r}{a} \chi(\mathbf{r}, \boldsymbol{\rho}) = \lim_{r \to 0} \partial_r [r \chi(\mathbf{r}, \boldsymbol{\rho})] + 2\chi(-\sqrt{3}\boldsymbol{\rho}/2, -\boldsymbol{\rho}/2). \tag{2.42}$$

The interaction acts only in the s wave channel of the relative particle so that the general ansatz for the non-trivial Fadeev components can be expanded over the Legendre polynomials as:

$$\chi(\mathbf{r}, \boldsymbol{\rho}) = \sum_{l=0}^{\infty} P_l(\hat{\mathbf{e}}_{\boldsymbol{\rho}} \cdot \hat{\mathbf{e}}_z) \frac{\chi_l(r, \rho)}{r\rho} \tag{2.43}$$

where by construction the functions χ_l verify at finite interparticle distance r the boundary condition

$$\chi_l(r, \rho = 0) = 0. \tag{2.44}$$

In what follows, we consider only the s wave ansatz ($l = 0$). In this particular case, at negative energy $E = -\frac{\hbar^2 q^2}{m}$ where $q > 0$, the wave equation and the contact equation can be written as:

$$\left(\partial_r^2 + \partial_\rho^2 - q^2 \right) \chi_0 = 0 \tag{2.45}$$

$$\partial_r \chi_0(r, \rho) \Big|_{r=0} + \frac{8}{R\sqrt{3}} \chi_0(\sqrt{3}R/2, R/2) = -\frac{\chi_0(0, R)}{a}.. \tag{2.46}$$

As this clearly appears in the subsequent lines, it is useful to write Eqs. (2.45,2.46) in terms of the hyper angle $\alpha \in [0, \frac{\pi}{2}]$ and of the hyper radius R defined by ($\rho = R\cos\alpha, r = R\sin\alpha$). Using the fact that as $r \to 0$ one obtains $\partial_r = \frac{1}{R}\partial_\alpha$ and making the formal substitution $\chi_0(r,\rho) \to \chi_0(R,\alpha)$, Eqs.(2.45,2.46) transform into:

$$\left(\partial_R^2 + \frac{1}{R}\partial_R + \frac{1}{R^2}\partial_\alpha^2 - q^2\right)\chi_0(R,\alpha) = 0 \tag{2.47}$$

$$\partial_\alpha \chi_0(R,\alpha)\Big|_{\alpha=0} + \frac{8}{\sqrt{3}}\chi_0(R,\pi/3) = -\frac{R}{a}\chi_0(R,0). \tag{2.48}$$

A crucial point is to realize that in the unitary limit (meaning that $|a| = \infty$ *and* the zero range limit is performed), the problem is *exactly* separable in the variables R and α [a consequence of the scale invariance of the contact condition in Eq. (2.37)]. We thus introduce the ansatz

$$\chi_0(R,\alpha) = F(R)\phi(\alpha). \tag{2.49}$$

One can notice *en passant* that the hyper radial function $F(R)/R$ is nothing but the Fourier transform of the isotropic solution $D(k)$ of the STM equation (modulo a multiplicative constant). This can be seen from the identity (2.38) and the equations (2.43) and (2.49):

$$\langle \boldsymbol{\rho}|A_\psi\rangle = -\lim_{r\to 0}\frac{\chi_0(r,\rho)}{\rho} = -\phi(0)\frac{F(\rho)}{\rho}. \tag{2.50}$$

Let us consider the two momentum $\mathbf{k} = (k_1 - k_2)/2$ and $\mathbf{K} = (2k_3 - k_1 - k_2)/3$. They are conjugate with the Jacobi coordinate $\mathbf{r}_{12}$ and $\frac{\sqrt{3}}{2}\boldsymbol{\rho}$. Indeed, in the center of mass frame $\sum_{i=1}^3 k_i \cdot \mathbf{r}_i = \mathbf{k}\cdot\mathbf{r}_{12} + \frac{\sqrt{3}}{2}\mathbf{K}\cdot\rho_3$. Using the fact that $\mathbf{K} = \mathbf{k}_3$, the function $\langle \mathbf{K}|A_\psi\rangle$ in the STM equation (2.13) and thus $D(K)$ in (2.14) are the Fourier transform of $\langle\boldsymbol{\rho}|A_\psi\rangle$ and from Eq.(2.50) one obtains

$$D(K) = \langle \mathbf{K}|A_\psi\rangle \propto \int d^3\rho \frac{F(\rho)}{\rho}\exp(i\sqrt{3}\mathbf{K}\cdot\boldsymbol{\rho}/2). \tag{2.51}$$

From Eq. (2.47) the homogeneous equation for $\phi(\alpha)$ is given by

$$\partial_\alpha^2\phi(\alpha) = -s^2\phi(\alpha). \tag{2.52}$$

Using the boundary condition $\phi(\pi/2) = 0$ deduced from Eq. (2.44), the solutions of Eq. (2.52) are of the form $\phi(\alpha) = \sin\left[s\left(\alpha - \frac{\pi}{2}\right)\right]$. Finally, injecting this last solution in Eq. (2.48) gives the same eigenequation for s as the one found by Danilov in Eq. (2.23). The differential equation verified by F and deduced from Eq. (2.47) corresponds to the two-dimensional radial equation of a fictive particle in a central inverse cube force:

$$\left(-\frac{d^2}{dR^2} - \frac{1}{R}\frac{d}{dR} + \frac{s^2}{R^2} + q^2\right)F(R) = 0. \tag{2.53}$$

An exhaustive study of this exotic quantum mechanical problem is done in Ref. [Mor57]. At large distance ($qR \gg 1$), the potential term in Eq. (2.53) is negligible and the solutions are of the form:

$$F(R) \underset{qR\gg 1}{=} \frac{A}{\sqrt{R}}\exp(-qR) + \frac{B}{\sqrt{R}}\exp(qR). \tag{2.54}$$

The normalizability of the solutions outside the potential radius imposes that the solutions of Eq. (2.53) converge toward zero at large distance *i.e.* $B = 0$ in Eq. (2.54). In the short distance limit ($R \to 0$), the term q^2 is negligible in Eq. (2.53). The two independent solutions in this region are of the form $F(R) = R^{\pm s}$ and depending on the sign of s^2 there are two types of behavior[3]:

$$s^2 > 0 \Longrightarrow F(R) \underset{R\to 0}{=} \mathcal{N}_{(+)}R^s + \mathcal{N}_{(-)}R^{-s} \tag{2.55}$$

$$s^2 < 0 \Longrightarrow F(R) \underset{R\to 0}{=} \mathcal{N}\sin\left[s_0\ln(qR) + \Delta\right]. \tag{2.56}$$

In Eq. (2.56) and in what follows, $s_0 = |s|$ and $s = is_0$. The solution of Eq. (2.53) which encapsulates the large distance behavior with $B = 0$ in Eq. (2.54) and the small radius asymptotic law in Eqs. (2.55,2.56) can be expressed in terms of a Bessel function K_s with

$$F(R) = K_s(qR). \tag{2.57}$$

[3]The case $s = 0$ where $F(R) \propto \ln(qR)$ at small hyper radius is included in the full solution of Eq. (2.57)

The general hyper radial solution of this three-body problem is a linear combination $F(R) = \sum_i c_i K_{s_i}(qR)$, where the s_i are the roots of Eq. (2.23). For $s_i^2 > 0$, the hyper radial potential is repulsive and is analogous to a centrifugal barrier while for the lowest hyper radial potential $-s_0^2/R^2$ one recovers the *so-called* fall to the center problem addressed in Ref. [Lan67] section 35. In the attractive case where $s = is_0$, Eq. (2.57) corresponds to the phase $\Delta = \Delta_0$ in Eq. (2.56) where

$$\Delta_0 = -s_0 \ln 2 - \arg \Gamma(1 + is_0) \sim 0.1281 \ldots \tag{2.58}$$

The matching of the small and large distance behavior does not lead to a quantization condition ans this basically corresponds to the pathology found for the isotropic and negative energy solutions of the STM equation. Coming back to a problem with a potential of finite range permits to realize that the solutions in Eq. (2.56,2.55) which have an exotic behavior at short distance have to coincide at least approximately with the actual solutions of Eq. (2.35) at some hyper radius R_0 very much larger than b [4] where also $qR_0 \ll 1$ in order to neglect the energy in the Schrödinger equation. In this regime the matching condition can be expressed in terms of the logarithmic derivative of the hyper radial wave function at a given value of the parameter $u = u_0 = qR_0$:

$$\left.\frac{dF}{Fdu}\right|_{u_0} = \cot \phi_0. \tag{2.59}$$

where ϕ_0 is a phase lying in the interval $[0, \pi]$ and which depends on the details of the actual pairwise potential but not on the energy of the states. In the case where $s^2 > 0$ the solutions are rapidly decreasing functions of R and can be neglected [5]. In the case where $s^2 < 0$, Eq. (2.59) provides the desired quantization condition on the binding wave number:

$$\cot(s_0 u_0 + \Delta_0) = \cot \phi_0 \tag{2.60}$$

which gives

$$q_n = \frac{\exp\left(\frac{\phi_0 - \Delta_0}{s_0}\right)}{R_0} \exp\left(\frac{-n\pi}{s_0}\right) \quad \text{where} \quad n \in \mathbb{Z} \tag{2.61}$$

Binding wave numbers in Eq. (2.60) have a physical meaning only for $q_n b \ll 1$ which is the case for n positive as a consequence of the hypothesis $R_0 \gg b$. The spectrum of the trimers at resonance ($|a| = \infty$) is then[6]:

$$E_n = -\frac{\hbar^2 \kappa^{\star\, 2}}{m} \exp\left(\frac{-2n\pi}{s_0}\right) \tag{2.62}$$

where the three-body parameter is

$$\kappa^\star = \frac{1}{R_0} \exp\left(\frac{\phi_0 - \Delta_0}{s_0}\right). \tag{2.63}$$

The three-body parameter is defined modulo a multiplicative factor $\lambda_0 = \exp(\pi/s_0)$, thus it is also possible to choose $\kappa^\star$ of the order of $1/b$ but in this case the quantum number n in Eq.(2.62) has to be sufficiently large. Hence one recovers the result of Minlos and Fadeev, however the reasoning made shows that the unitary spectrum is relevant only in the limit of vanishing binding energies. Eq. (2.62) is thus the asymptotic form of the actual spectrum of the three-body problem with finite range interparticle potentials at resonance ($|a| = \infty$). The previous discussion shows that the Efimov spectrum ends up for energies lower in absolute value than $\hbar^2/(mb^2)$. The matching condition of Efimov in Eq. (2.60) can be written in an form similar to the Danilov filtering condition in Eq. (2.27) by imposing the asymptotic phase shift in the short range limit $R \to 0$ of $F(R)$:

$$F(R) \underset{R \to 0}{\propto} \sin\left[s_0 \ln\left(\kappa^\star R\right) + \Delta_0\right]. \tag{2.64}$$

For large but finite values of the scattering length $|a| \gg b$ the zero range models of Danilov or Efimov are still relevant [Eq. (2.48) shows that the problem is separable in the variables ρ and α in the limit of small hyper radius $R \ll |a|$ moreover the contribution of the repulsive hyper spherical potentials with $s^2 > 0$ vanish in this limit so that Eq. (2.64) can be used for the hyper radial solution of the lowest branch $-s_0^2/R^2$]. However for a

[4] This condition is due to the zero-range approximation as discussed in the paragraph after Eq. (2.37).

[5] This reasoning is not true if $q \to 0$ for a hyper spherical potential branch $s^2 > 0$. This corresponds to the existence of an isolated shallow bound state (a 3-body resonance). Contrary to the case of the Efimov states such Borromean bound state is not universal as its appearance depends of the short range details of the pairwise potential [Wer08].

[6] The spectrum for an attractive $1/r^2$ potential is solved in the textbook of Morse and Feshbach [Mor57] by using a filtering technique analogous to the method of Danilov.

finite hyper radius the problem is no more separable and the resolution is thus involved [Fed93]. Nevertheless the general structure of the spectrum can be obtained without detailed calculations as follows. For negative values of the scattering length ($a < 0$), there is no shallow dimer and the trimers are Borromean states. In the limit of large hyper radius ($R \gg |a|$) the term $\chi_0(R, \pi/3)$ can be neglected in Eq. (2.48) and one recovers the WBP contact condition for an interacting pair while the third particle moves freely. Thus there is no more three-body attraction in this regime: the attractive potential in $1/R^2$ is cut off for ($R \gtrsim |a|$). The physical meaning of this behavior is clear: for interparticle distances much larger than $|a|$ the particles do not feel with each others because the two-body cross-section is proportional to a^2. Hence for a large and negative scattering length ($a < 0$):

(i) there is no accumulation point in the spectrum;

(ii) the order of magnitude of the hyper radius of the shallowest state is smaller or of the order of $|a|$;

(iii) thanks to the large value of the scaling factor λ_0 the structure and energy of an Efimov trimer (excepted the shallowest one) are very similar to the results given at unitarity;

(iv) analogously to the problem of a particle in a potential well, the spectrum crosses the three-particle continuum only for specific values of a.

For positive values of the scattering length $a > 0$, there exists a dimer branch which corresponds to the half-line $K = -a^{-1}$ ($K < 0$) in the (a^{-1}–K) plane where $K = \mathrm{sgn}(E)\sqrt{m|E|}/\hbar$. As we consider true *i.e.* stable trimers there is no three-body bound state above this half-line and obviously there is no accumulation point. The same reasoning than for the case $a < 0$ leads to the conclusion that the attractive potential $-s_0^2/R^2$ potential is cut off for large hyper radius $R > a$. The trimer state in the regime of large hyper radius and small hyper angle α corresponds to a particle-dimer bound state. In this regime, $\chi_0(R, \alpha) \sim \exp(-R\alpha/a)$ with a binding energy $E_{\mathrm{ad}} = -E - \frac{\hbar^2}{ma^2}$. For $\hbar^2/(ma^2)$ of the order of one of the possible eigenenergies of the unitary spectrum, one expects the existence of a crossing between the trimer spectrum and the dimer branch. To conclude, for a finite value of the scattering length, the binding wavenumber of the Efimov trimers lies approximately in the interval $[1/|a|, 1/b]$. Hence the number of trimers is finite and given by the approximate law

$$N \sim \frac{s_0}{\pi} \ln\left(\frac{|a|}{b}\right). \tag{2.65}$$

Another characteristics of the spectrum is its homothetic character which can be shown as follows. The only adimensional parameter in the low energy regime being qa, the phase shift Δ appearing in the limit of small hyper radius in Eq. (2.56) is an universal function of the variable $x = 1/(qa)$ and $\Delta(x)$ is such that $\Delta(0) = \Delta_0$. Using the matching condition in Eq. (2.59) the spectrum for a finite value of a provides:

$$E_n = -\frac{\hbar^2 {\kappa^\star}^2}{m} \exp\left(\frac{-2n\pi}{s_0}\right) e^{\frac{2[\Delta_0 - \Delta(x)]}{s_0}}. \tag{2.66}$$

For a given value of the quantum number n, Eq. (2.66) defines a branch of trimers in the (a^{-1}, K) plane. The previous discussion implies that each branch possesses two endpoints: one in the Borromean region at the boundary with the three-particle continuum and the other one on the dimer branch. Equation (2.66) shows that a given energy E_n on the branch n can be deduced from an energy $E_{n'}$ having the same value of x by a scaling factor $\lambda_0^{-2(n-n')}$. A constant value of the variable x corresponds to a straight line which crosses the origin of the Efimov plot. Consequently, the transformation of a branch n' to a branch n is a homothety of center at the origin of the plot and of ratio $\lambda_0^{-2(n-n')}$. This important property is displayed in Fig. (2.3).

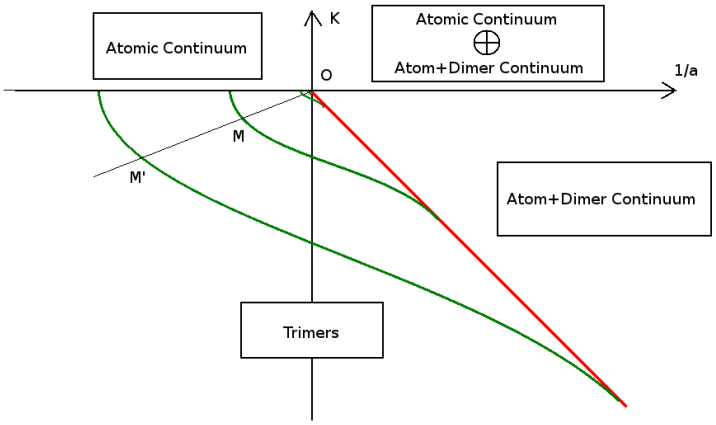

Figure 2.3: *Schematic representation of the Efimov plot in the plane* (a^{-1}, K) *where* $K = \mathrm{sign}(E) \times \sqrt{m|E|/\hbar^2}$. *Green solid line: trimer branch; Solid red line: dimer branch. Above the dimer branch, no trimer can exist and there is a continuum of dimer-atom states. In the Borromean region* $a < 0$, *there is no trimer above zero energy. Whatever the sign of the scattering length there is a continuum of atomic states above zero-energy. The two points* M *and* M' *which belong to the two successive Efimov branches are relied each other by a homothety of center* O *and scaling factor* λ_0.

This scaling symmetry implies that all the end points for $a < 0$ are related with each others by an integer power of the scaling factor λ_0 and idem for all the end points in the domain $a > 0$.

As a conclusion of this section, solving the three-boson problem in the configuration space helps to understand that:

- the Efimov effect is deeply linked to the 'fall to the center' problem;
- at unitarity, the scaling invariance of the contact condition implies the separability of the hyper radius and hyper angular variables. In this regime the attractive hyper radial potential has a $1/R^2$ tail which implies the existence of an infinite number of bound states at zero energy;
- at finite but still large values of $|a|$, the scaling invariance is almost verified for a large interval of the hyper radius $b \ll R \ll |a|$ and a finite number of Efimov states exists.

2.5 The full Efimov spectrum derived from the Skorniakov Ter-Martirosian equation

For a finite scattering length, the determination of the Efimov spectrum in the configuration space involves a coupling between the different hyper spherical harmonics. This problem is thus not simple to solve. It is then tempting to come back to the STM equation and to use the Danilov condition. However this issue is not also straightforward because the unitary spectrum is not bounded from below. A way to overcome this difficulty has been found by introducing a formal three-body force [Bed99]. This method is rather sophisticated and it is much more simple to use the subtractive regularization scheme introduced in Refs. [Pri10b, Pri11a]. The trick can be found by considering the shape of the function $k^2 D(k)$ of Eq. (2.25) which is plotted in Fig. (2.4). Eq. (2.25) shows that for increasing values of k starting from $k = 0$, the first zero of $D(k)$ is located at the momentum $k = \frac{2q}{\sqrt{3}} \sinh(\pi/s_0)$. By using, this property, it is possible to filter a set of solutions of Eq. (2.16) satisfying Eqs. (2.62) for sufficiently high quantum numbers (shallow states) and with a spectrum bounded from below. This is done by imposing a nodal condition on the eigenstates:

$$D(k_p^{\mathrm{reg}}) = 0, \tag{2.67}$$

where the node k_p^{reg} is chosen among the set:

$$k_p^{\mathrm{reg}} = \frac{\kappa^\star}{\sqrt{3}} e^{p\pi/s_0} \quad p \in \mathbb{Z}. \tag{2.68}$$

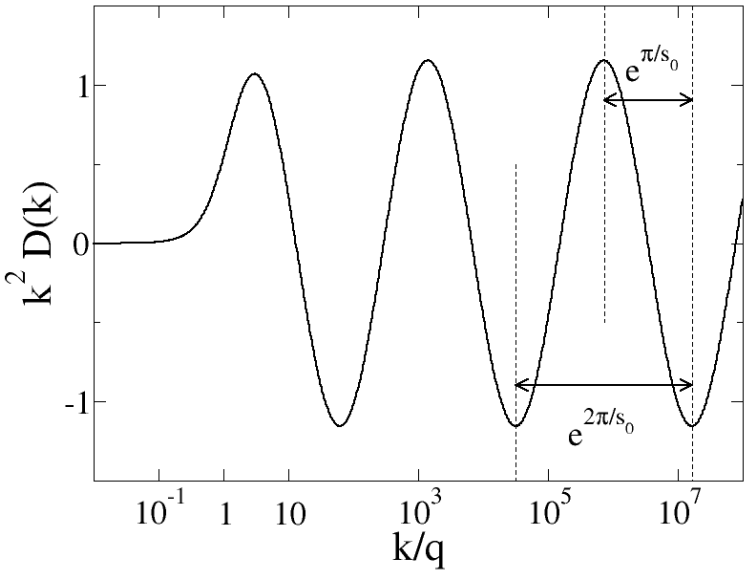

Figure 2.4: *Semi-log plot of the function* $k \longmapsto k^2 D(k)$ *where* $D(k)$ *is given in Eq.* (2.25).

The position of the node in Eq. (2.68) fixes the minimum energy of the spectrum. For example if one chooses the nodal condition for $p = 2$, using the fact that $\exp(\pi/s_0) \simeq 2\sinh(\pi/s_0)$, the minimum energy is almost equal to $-\hbar^2\kappa^{\star\,2}\exp(2\pi/s_0)/m$ [with a relative error $2\exp(-2\pi/s_0) \simeq 3.8\times10^{-3}$] and the spectrum at unitarity is asymptotically (*i.e.*, for large values of n) given by the unitary spectrum E_{n-1} in Eq. (2.62) with $n \in \mathbb{N}$. As noticed in section (2.4) for a finite scattering length a, the eigenfunctions $D(k)$ of Eq. (2.16) have the same high momentum behavior (for $k|a| \gg 1$) as the unitary solutions of Eq. (2.25). Hence, Eq. (2.67) can be also used as a filtering condition and allows to recover the Efimov spectrum at finite scattering length. In principle, the results of the Efimov-Danilov zero-range theory are recovered by imposing the nodal condition at an arbitrary large value $k_p^{\rm reg}$. To summarize this discussion, the nodal condition in Eq. (2.67) has two roles: first, it imposes the Danilov's asymptotic phase shift for states of sufficiently high quantum number and second, it imposes a minimum energy to the spectrum.

The nodal condition in Eq. (2.67) applied in Eq. (2.16) can be transformed into an integral condition:

$$0 = -\frac{2}{\pi}\int_0^\infty du\, D(u)\mathcal{K}_q(k_p^{\rm reg},u). \tag{2.69}$$

Subtracting Eq. (2.69) from Eq. (2.16) gives a regularized STM equation [Pri10b, Pri11a]:

$$\frac{D(k)}{f_W\left(i\sqrt{q^2+\frac{3k^2}{4}}\right)} = \frac{2}{\pi}\int_0^\infty du\,\left[\mathcal{K}_q(k,u)-\mathcal{K}_q(k_p^{\rm reg},u)\right]D(u), \tag{2.70}$$

which encapsulates the nodal condition. The Danilov-Efimov contact condition (2.62) is implemented *exactly* in the STM equation in the limit where the integer p tends to infinity in Eq. (2.70). For a realistic finite range force, the trimer spectrum coincides with the prediction given by the subtractive regularization scheme for high binding wave numbers such that $q_n b \ll 1$ and $q_n \ll k_p^{\rm reg}$. Numerical solutions of Eq. (2.70) are obtained by introducing an ultraviolet cut-off Q in the integral. One can verify that results are insensitive to the choice made on the cut-off for $Q \gg k_p^{\rm reg}$. For instance considering the unitary limit, taking the nodal condition at $k_1^{\rm reg}$ and an UV cut-off at $5\times10^2\times\kappa^\star$, one finds the relative error for the ground state equals to $3.8\times10^{-3} \simeq 2\exp(-2\pi/s_0)$ and for the first excited states ($n \leq 8$) one finds a relative error less than 10^{-4}. In practice, the value of the scaling factor $\exp(2\pi/s_0) \simeq 515$ is relatively large so that for the nodal condition at $k_2^{\rm reg}$, the spectrum is very close to the universal spectrum beginning from the second branch ($n \geq 1$) and for an inverse scattering length $1/|a|$ smaller or of the order of $\kappa^\star$.

In Fig. (2.5), the $n = 0$ Efimov branch obtained from the regularized STM equation (2.70) with the nodal condition at $k_2^{\rm reg}$ is plotted as a function of $(1/a)$. As in Ref. [Bra06], the end points for the branch labeled by

(n) (*i.e.* the branch $n = 0$ crosses $q_0 = \kappa^\star$ at unitarity) are denoted by $a_*^{(n)}$ at the atom-dimer continuum limit and by $a_-^{(n)}$ at the three-atom continuum limit. As a consequence of the choice of the nodal condition at $k_p^{\rm reg}$ for a finite p, results slightly differ from the zero-range model in Ref. [Bra06].

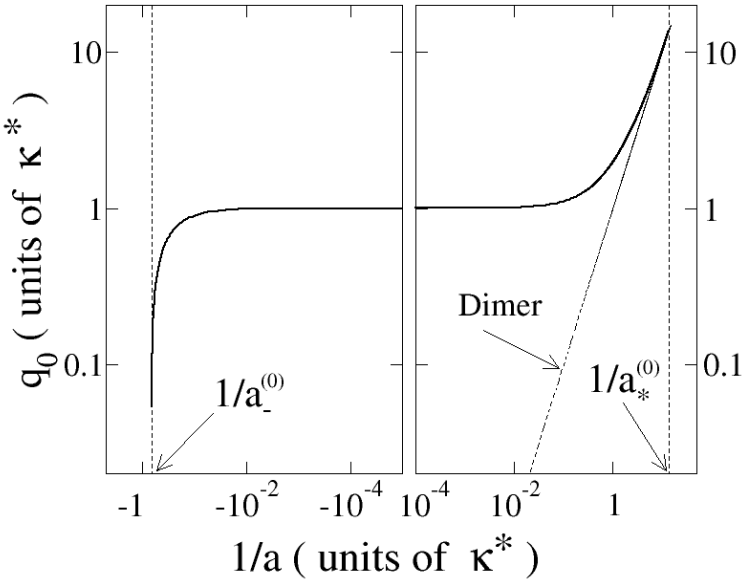

Figure 2.5: *Solid line: one branch of the trimer's spectrum obtained with the nodal condition at $k_2^{\rm reg}$. Oblique dashed line: Atom-dimer continuum limit. The values of the scattering length for the end points of the branch (vertical dashed lines) at $a_-^{(0)} \simeq -1.51/\kappa^\star$ and $a_*^{(0)} \simeq .0713/\kappa^\star$ are close to the results of the zero range model in Refs. [Bra06, Gog08] where $a_-^{(0)} \simeq -1.507/\kappa^\star$ and $a_*^{(0)} \simeq .0707/\kappa^\star$. The difference is due to the fact that the zero-range theory is recovered only for a nodal condition imposed at an arbitrarily large value $k_p^{\rm reg}$.*

2.6 Three-body recombination

In dipolar traps, atomic losses are essentially due to three-body recombination mechanism: an inelastic scattering of three ultra-cold atoms in the cloud which results in the creation of one two-body bound state (binding energy E_B) and one solitary atom. The precise measurement of atomic losses as a function of the scattering length give a signature for the existence of Efimov trimers and has been used in the historical experiments on the Efimov effect in ultracold gases. For an incoming state at almost zero energy, and an outcoming atom of momentum $\mathbf{K}$, the momentum-energy conservation rule gives:

$$-E_B + \frac{\hbar^2 K^2}{2m} + \frac{\hbar^2 K^2}{4m} = 0 \Longrightarrow \frac{\hbar^2 K^2}{2m} = \frac{2E_B}{3}. \tag{2.71}$$

Thus, depending on the value of E_B, the kinetic energy for the outcoming atom and bound state can be higher than the height of the trap potential and the particles can escape from the cloud. The rate of occurrence of the recombination process is equal to the rate of formation of dimers. It is defined for N atoms trapped in a cubic box of size L by

$$\frac{dN_{\rm dim}}{dt} = \alpha_{\rm rec} \frac{N(N-1)(N-2)}{L^6} \tag{2.72}$$

where $\alpha_{\rm rec}$ is the three-body recombination constant. For a given atomic density Eq. (2.72) provides an estimation of the lifetime of the atomic gas. The three-body recombination constant is thus an important characteristics

of the atomic gas. Assuming that the dimer and the atom flying apart escape from the trap, the atomic loss rate is $\frac{dN}{dt} = -3\frac{dN_{\rm dim}}{dt}$ if the gas is not condensed and $\frac{dN}{dt} = -\frac{1}{2}\frac{dN_{\rm dim}}{dt}$ if the gas is condensed [Kag85, Bra06]. Dimensional analysis provides the law $\alpha_{\rm rec} \propto \hbar a^4/m$ which implies a short lifetime for a bosonic gas near a Feshbach resonance. This is indeed what is observed since the first achievement of a magnetic Feshbach resonances [Ino98, Ste99]. However, this law does not take into account the existence of the three-body parameter which is a low energy scale for the three-body system. For a more precise determination of the three-body recombination rate, one has to distinguish between two qualitatively different processes depending whether the outcoming bound state is a Feshbach dimer or is a standard molecule *i.e.* a deep bound state.

Recombination into a shallow Feshbach dimer

In this case the scattering length is large and positive and this is the major decay channel in the gas. The Efimov-Danilov model describes the outcoming dimer and can be used without modification (the range of the interatomic forces is neglected). The three-body contact condition can be applied and an exact treatment can be performed. The analytical expression for the contribution to the recombination rate is [Mac06, Gog08, Hel10, Mor11b]:

$$\alpha_{\rm Fesh} = \frac{128\pi^2(4\pi - 3\sqrt{3})\sin^2\left[s_0\ln(\gamma_0 a\kappa^\star)\right]}{\sinh^2(\pi s_0) + \cos^2\left[s_0\ln(\gamma_0 a\kappa^\star)\right]}\frac{\hbar a^4}{m} \tag{2.73}$$

where $\gamma_0 = 3.1\ldots$. The oscillating part in the denominator (as a function of the scattering length) is negligible so that Eq. (2.73) is very well approximated by the expression found in Ref. [Bed00]: $\alpha_{\rm Fesh} \sim 67.1\frac{\hbar a^4}{m}\sin^2\left[s_0\ln(\gamma_0 a\kappa^\star)\right]$. Equation (2.73) exhibits a succession of zeros as a function of the scattering length with a log-periodic structure involving the scaling factor λ_0, *i.e.* the characteristics of Efimov effect.

Recombination into a deep bound-state

Deep dimers are not described by the zero-range model of Efimov-Danilov. Thus in order to evaluate these processes, Braaten and Hammer have enriched the zero-range model by introducing a second positive three-body parameter denoted by $\eta^\star$ and called the inelasticity parameter [Bra06, Bra07]. When three atoms are within the interior region of the potential *i.e.* in a volume of the order of $b^3 \equiv \mathcal{O}(R_{\rm vdW}^3)$ there is a given probability that they populate a state composed of deep molecule and an atom flying apart. The probability that three incoming atoms recombine in such process is $1-\exp(-4\eta^*)$ which can be taken as the definition of the inelasticity parameter. Now looking at the Efimov-Danilov filtering condition in Eq. (2.64), one can interpret the sinus as the superposition of a ingoing and outgoing waves from the contact of the three particles. Then, analogously to the introduction of the scattering phase-shift in Eq. (1.16), the inelasticity parameter can be incorporated in the three-body contact condition of Eq. (2.64) written in terms of the variable $u^\star = \ln(\kappa^\star R)$ with:

$$F(u) \underset{u^\star\to\infty}{\propto} e^{iu^\star s_0}e^{i\Delta_0 - 2\eta^\star} - e^{-iu^\star s_0}e^{-i\Delta_0}. \tag{2.74}$$

Formally, this amounts to replace the three-body parameter $\kappa^\star$ in Eq. (2.64) by a complex one as follows:

$$\kappa^\star \longrightarrow \kappa^\star\exp(i\eta^\star). \tag{2.75}$$

Using this method it is possible to derive analytical laws for the three-body losses due to the existence of deep molecular states and to compare with experimental data [Bra06, Bra07, Hel09, Hel10]. For example, the zero of the recombination rate in Eq. (2.73) transform into the more physical existence of local minima. Typical values of $\eta^\star$ in current experiments are of the order of 0.1.

2.7 Width of Efimov states

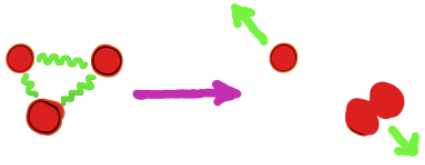

In ultra-cold gases, the actual Efimov states can also decay into one diatomic deep molecular state and one atom flying apart. Consequently, they are not true bound states but resonances characterized by an maximum at energy E_n, a width Γ_n and a quality factor E_n/Γ_n. Using the modified three-body contact condition in Eq. (2.74) one finds [Bra06]:

$$\frac{E_n}{\Gamma_n} = 2\cot\left(\frac{2\eta^\star}{s_0}\right). \tag{2.76}$$

2.8 Separable two-channel model: deviation from universality

2.8.1 Interest of a specific model for cold atoms

The most simple description of three resonant bosons is given by the zero-range Danilov-Efimov model which is characterized by only two parameters the scattering length and a three-body parameter. However this model gives no information about the value of the three-body parameter. At resonance, the results of Efimov are exact in the limit of vanishing energy while in practice only the deeper Efimov states can be observed (a consequence of the large value of the scaling factor λ_0). Hence, one can wonder what is the the value of the binding energies of the deep trimers [of the order of $\hbar^2/(mb^2)$]. Moreover, experiments are achieved for a finite detuning where even the dimer spectrum deviates from the universal law of Eq. (1.61). In order to analyze the experimental results one thus needs a model which takes into account off-resonance effects in Efimov physics in order to evaluate deviations from the universal laws. The two-channel model of Sec. (1.5.2) which encapsulates accurately the various regimes of magnetic Feshbach resonance (from broad to narrow) is relevant for such studies.

2.8.2 The modified STM equation

The three-boson problem formulated with the two-channel model of Sec. 1.5.2 has been solved in Ref. [Jon08] and more materials can be found also in Ref. [Pri11c]. In the center of mass frame, the general ansatz for a three-body eigenstate of the Hamiltonian in Eq. (1.68), is the coherent superposition of a tri-atomic state in the open channel and of an hybrid state made of one atom in the open channel and one molecule in the closed channel:

$$|\psi\rangle = \int \frac{d^3K d^3k}{(2\pi)^6} A_{\mathbf{K},\mathbf{k}}\, a^\dagger_{\frac{\mathbf{K}}{2}+\mathbf{k}} a^\dagger_{\frac{\mathbf{K}}{2}-\mathbf{k}} a^\dagger_{-\mathbf{K}}|0\rangle + \int \frac{dK}{(2\pi)^3}\beta_{\mathbf{K}} b^\dagger_{\mathbf{K}} a^\dagger_{-\mathbf{K}}|0\rangle. \tag{2.77}$$

In Eq. (2.77), $\beta_{\mathbf{K}}$ (respectively $A_{\mathbf{K},\mathbf{k}}$) represents after symmetrization the atom-molecule wavefunction (respectively the wave function for the three atoms in the open channel, where $\mathbf{K}$ and $\mathbf{k}$ are two Jacobi coordinates in momentum space). In the subsequent equations, without loss of generality $A_{\mathbf{K},\mathbf{k}}$ is considered to be an even function of $\mathbf{k}$. Similarly to what has been done for the two-body problem, the two coupled equations verified by $\beta_{\mathbf{K}}$ and $A_{\mathbf{K},\mathbf{k}}$ are obtained from the projection of the stationary Schrödinger equation at energy E [*i.e.* $(E-H)|\psi\rangle = 0$] onto firstly, the triatomic states and secondly, the atom-molecule states. A key point in this derivation is the introduction of a dressed atom-molecule wave function analogous to the one of Eq. (1.76):

$$\beta^{\rm eff}_{\mathbf{K}} = \frac{g_0\beta_{\mathbf{K}}}{2\Lambda^2}\left(E_{\rm col} - E_{\rm mol} + \frac{2\Lambda^2}{g_0}\right) \tag{2.78}$$

where $E_{\rm col} = E - \frac{3\hbar^2K^2}{4m}$ is the collisional (or relative) energy of an atomic pair of total momentum $\mathbf{K}$. In order to establish a close analogy with the zero-range model one can also introduce the amplitude:

$$\mathrm{D}^{\rm eff}_E(\mathbf{K}) = \frac{m\Lambda}{4\pi\hbar^2}\beta^{\rm eff}_{\mathbf{K}}. \tag{2.79}$$

Finally, the coupled equations for the amplitudes $\beta_{\mathbf{K}}$ and $A_{\mathbf{K},\mathbf{k}}$ lead to a single closed integral equation:

$$\int \frac{d^3k}{\pi^2}\frac{\mathrm{D}^{\rm eff}_E(\mathbf{k})\chi_b\left(\left|\frac{\mathbf{K}}{2}+\mathbf{k}\right|\right)\chi_b\left(\left|\mathbf{K}+\frac{\mathbf{k}}{2}\right|\right)}{k^2+K^2+\mathbf{k}\cdot\mathbf{K}-\frac{mE}{\hbar^2}-i0^+} = \frac{|\chi_b(k_{\rm rel})|^2\mathrm{D}^{\rm eff}_E(\mathbf{K})}{f_s(k_{\rm col})} + \int\frac{d^3k}{(2\pi)^3}\chi_b(k)\left(A^{(0)}_{\mathbf{K},\mathbf{k}} + 2A^{(0)}_{-\frac{\mathbf{K}}{2}+\mathbf{k},-\frac{3\mathbf{K}}{4}-\frac{\mathbf{k}}{2}}\right) \tag{2.80}$$

where $f_s(k)$ is the scattering amplitude in Eq. (1.79), $k_{\rm col}$ is the collisional momentum of Eq. (2.12) and $A^{(0)}_{\mathbf{K},\mathbf{k}}$ is a wavefunction at energy E for three free atoms in the open channel ($A^{(0)} \neq 0$ only if $E>0$). For a given three-body scattering process one has $\langle \mathbf{K}/2+\mathbf{k}, \mathbf{K}/2-\mathbf{k}, -\mathbf{K}|\psi^{(0)}\rangle = 3A^{(0)}_{\mathbf{K},\mathbf{k}}$

The similarity of Eq. (2.80) with the STM equation (2.13) is striking and the equivalence is found in the zero range limit where $b\to 0$, the scattering length a is kept fixed at a given value, $R^\star \to 0$ and $a_{\rm bg}\to 0$ (absence

of shape resonance). This similarity also exists for a finite value of b: at low-energy (*i.e.* $kb \ll 1$ and $bK \ll 1$) the kernel of the integral in (2.80) coincides with the one of the STM equation. In the 'high energy' limit ($k \to \infty$) the kernel plays itself the role of ultraviolet cutoff [via the function $\chi_b(k)$], and the Thomas collapse is avoided. At resonance, the trimer spectrum exhibits the discrete scale symmetry in Eq. (2.62) which is broken for energies of the order of $E_{\rm vdW}$.

As a conclusion of this section, Eq. (2.80) illustrates a remarkable feature of the separable two-channel model: the two-body physics is entirely encapsulated in the diagonal part of the integral equation (2.80) *via* the two-body scattering amplitude $f_s(k)$. This property remains true for the integral equation for the four-body problem [Mor11a].

2.9 The historical experiments on cesium

In the real world, it is never possible to reach a purely resonant regime where the scattering length is exactly infinite ($|a| = \infty$). However, the Efimov effect takes place also if the scattering length is sufficiently large (in absolute value) with respect to the potential radius. More precisely, the essential condition for the effect to occur is the existence of a large interval of momentum where the s wave two-body scattering amplitude can be well approximated by its unitary limit ($f_0(k) \sim -1/ik$). This condition is rather stringent as it means that $\left[\min\left(\frac{|a|}{R_{\rm vdW}}, \frac{|a|}{|r_e|}\right)\right]$ is of the order of few powers of the scaling factor λ_0. Eventually, the condition for achieving Efimov states are: (i) the diluteness of the medium in order to neglect many-body effects; (ii) a low temperature with respect to the low energy scale $\hbar^2/(ma^2)$; and (iii) the control of the interaction in order firstly to achieve the scale separation between the scattering length and the potential radius and secondly to explore the Efimov plot. The two first conditions are met in nuclear physics but not the third one. In current experiments on ultracold atoms the three conditions can be satisfied and especially the third one, thanks to the technique of magnetic Feshbach resonance which allows for a precise tuning of the scattering length.

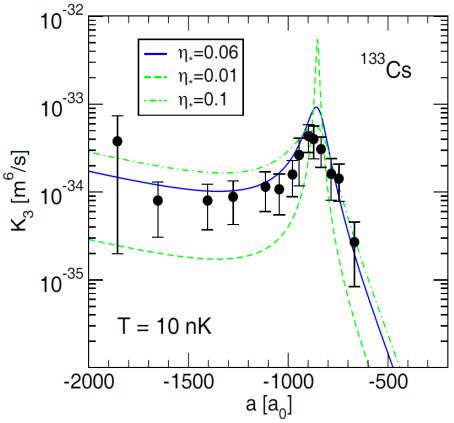

Figure 2.6: *Experimental data from Ref. [Kra06] fitted by using the zero-range model with the modified three-body contact condition in Eq. (2.74). This figure taken from Ref. [Bra06] shows a remarkable agreement between theory and experiments.*

The first observation of Efimov states has been achieved in a series of experiments at the university of Innsbruck [Kra06, Kno09]. In Ref. [Kra06], the measurement of the atomic loss rate in the Borromean region due to three-body recombination is reported in a gas of ^{133}Cs atoms for the broad resonance located near -12 G [7]. Figure (2.6) from Ref. [Bra07] displays the experimental findings fitted by using the zero-range model with the modified three-body contact condition in Eq. (2.74). Ref [Kno09] is linked to a second set of experiments where a gas composed of atoms and of shallow Feshbach dimers was prepared. A peak in the loss rate *i.e.* the signature of the crossing between the dimer branch and a trimer Efimov branch is reported. The zero-range model can again be successfully used for modeling the inelastic atom-dimer scattering process [Hel09]. In order to take into account finite range effects and more generally deviations from universal predictions, there has been also other theoretical studies of these experiments using more realistic one-channel [DIn09] and two-channel [Mas08, Lee07, Jon10] finite range models. An important issue concerns the measured ratio for the

[7] The characteristics of this resonance at the two-body level are given in tables (1.1,1.2) and in section (1.5.2)

end points of the Efimov branches $a_*^{(1)}/|a_-^{(0)}| \sim 0.5$ which is far from the prediction of the zero-range model $a_*^{(1)}/|a_-^{(0)}| = \lambda_0 a_*^{(0)}/|a_-^{(0)} = 1.06\ldots$.

In the subsequent lines, the results of the separable two-channel model are presented briefly. Equation (2.80) is solved with the parameter of the resonance in (1.1) and the short range parameter $b = R_{\rm vdW}$. The spectrum for the bound states obtained with this model is plotted as a function of the external magnetic field in Fig. (2.7). The same spectrum is also plotted in the (a^{-1}, K) plane in Fig. (2.8)

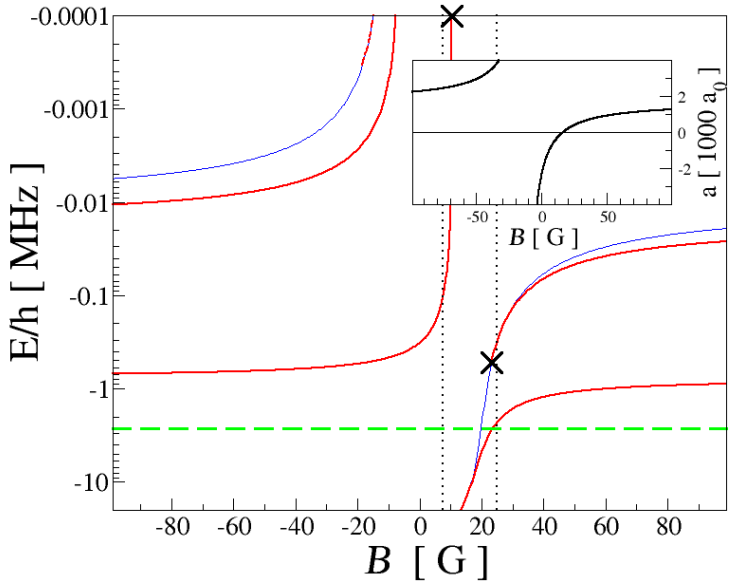

Figure 2.7: *Spectrum as a function of external magnetic field for low-energy two-and three-body bound states for cesium atoms in the vicinity of the resonance at* -12 *G. Red solid line: trimers, blue solid line: dimer, dashed green horizontal line: 'high energy' limit* $-\hbar^2/(mR_{\rm vdW}^2)$*; vertical dotted lines : position of the thresholds observed in experiments (respectively* 7.5 *G and* 25 *G); Crosses: thresholds calculated with the separable two-channel model (respectively,* 10.3 *G and* 23.2 *G). Inset: scattering length as a function of the magnetic field.*

The essential informations given by the model are as follows:

- there are two Efimov branches extending from the region $\mathcal{B} < 0$ to the region $\mathcal{B} > 0$. Each of these branches is continuous in the formal limit of arbitrarily large magnetic detunings ($|\mathcal{B}| = \infty$). Other Efimov branches are located in a narrow interval around the field $\mathcal{B}_0$ and are not visible in the figure (2.7);
- the threshold for the continuum of three atoms of the first branch of Efimov is a magnetic field of 10.3 G, which is quite close to the experimental value of 7.5 G in Ref. [Kra06];
- the crossing between an Efimov branch and dimer branch (which marks the border with the atom-dimer continuum) is marked by the existence of a peak in losses due to atom-dimer inelastic collisions. The experimental procedure in [Kno09] was to decrease the value of $\mathcal{B}$ from a high value and the peak was located at ~ 25 G. The theoretical value of 23.3 G is not far from the measured one. Furthermore, this peak corresponds to the threshold associated with the first excited Efimov branch;
- The peak in losses at the dimer-trimer crossing is observed experimentally at around 25 Gauss. For this magnetic field, the ratio between the scattering length and the effective range is relatively small ($a \sim 2|r_{\rm e}|$). This means that in this regime of detuning the two-body scattering amplitude is not well represented by the one of WBP model (1.28) for wave numbers of the order of (or above) $1/a$. Hence, the scale separation condition is not met at the observed dimer-trimer crossing explaining the large deviations with respect to the zero-range predictions.
- The ratio for the end points of the Efimov branches obtained from the two-channel model is $a_*^{(1)}/|a_-^{(0)}| \sim 0.69$. As the one measured in the experiments of Innsbruck, it exhibits also a large deviation from the prediction of the zero-range model.

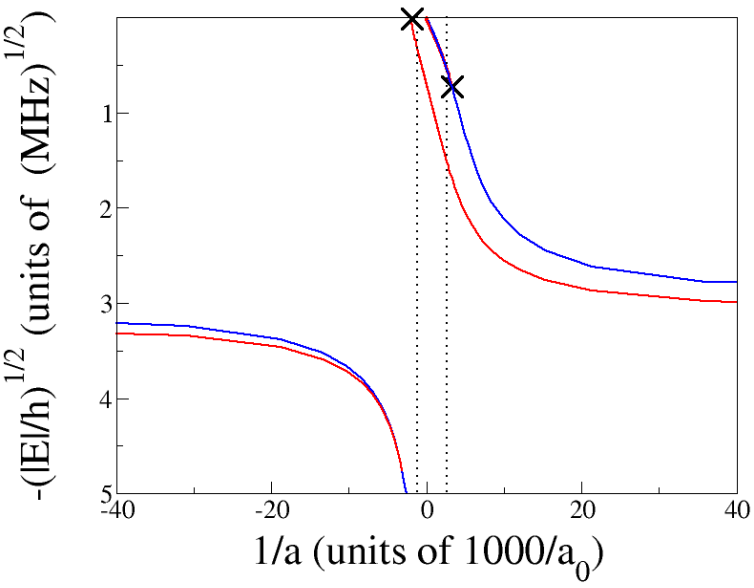

Figure 2.8: *Same spectrum as in Fig. (2.7) but displayed in the same coordinates as the Efimov plot of Fig. 2.3.*

Chapter 3

Theme and variations around Efimov physics

Contents

3.1 State of the art

The Efimov effect is not limited to the three identical bosons problem. For instance, it occurs also for two particles interacting with one impurity or in the case of three different fermions [Efi73, Bul75, Pet03, Bra07], or even in problems of mixed dimensions [Nis08, Nis09]. A general and nice introduction on Efimov physics is given in Ref. [Fer10]. Nevertheless, the domain is rapidly evolving and the following lines give a brief overview of the state of the art of this subject in ultracold atoms.

Since the first observation of an Efimov state several experiments have been achieved with other atomic species than cesium. A first set of experiments concerns the three-boson problem:

- Group at Firenze university: experiments using ^{39}K [Zac09]
- Group at Bar-Ilan University: experiments using ^{7}Li [Gro09, Gro11]
- Group at Rice university: experiments using ^{7}Li [Pol09]

In all these experiments atomic losses are used as a probe for the Efimov states. A maximum in the three-body loss rate provide the location of an end point of a trimer branch and a local minimum is relied on the log-periodic structure characteristics of the Efimov effect. Results in Refs. [Zac09, Gro09] are in accordance with the discrete scaling symmetry. However in Ref. [Pol09] while the data are in accordance with the predictions of the zero-range model at each side of the resonance, there is a large violation from the theoretical prediction on the ratio of the scattering lengths at the end points of a given branche. These results cannot be explained by using the separable two-channel model. In Ref. [Mac11] the authors have found a possible effect of the medium to explain these discrepancies. Another interesting recent issue in the three-boson problem concerns the surprising universality of the three-body parameter measured for few resonances in cesium by the group of

Innsbruck [Ber11]. This property confirmed by using a two-channel model very similar to the one introduced in these lectures [Nai11b] can be explained in terms of quantum reflection [Wan12].

Experiments on the three-spin-component fermionic gas using the three different Zeeman states of ^{6}Li have shown a specific structure in the three-body loss rate [Ott08, Huc09]. These results can be interpreted by the existence of Efimov states and other experiments have focused on this issue:

- Group of the university of Penn-State [Wil09]
- Group of the university of Heidelberg [Wen09, Lom10a, Lom10b]
- Group of the university of Tokyo [Nak10, Nak11]

Efimov states have been observed also for hetero-nuclear systems (with a ultra-cold gas composed of ^{41}K and ^{87}Rb atoms) in the group of Firenze [Bar09] where Efimov trimers correspond to KKRb and KRbRb molecules.

New and decisive experimental tools paving the way for tunable and precise measurements in few-body systems have been introduced recently. The first experiments on Efimov physics were based on atomic losses measurements which give indirect evidence for Efimov trimers. In contrast, it has been possible to explore more directly the three-body spectrum by spectroscopy using the photo-association mechanism. The technique was initially used for fermions [Lom10b, Nak11] and now it is also used in experiments on bosons [Mac12]. Another important step has been achieved recently thanks to the use of a micro-trap. With this technique it is possible to study a controllable number of atoms from one to ten [Ser11].

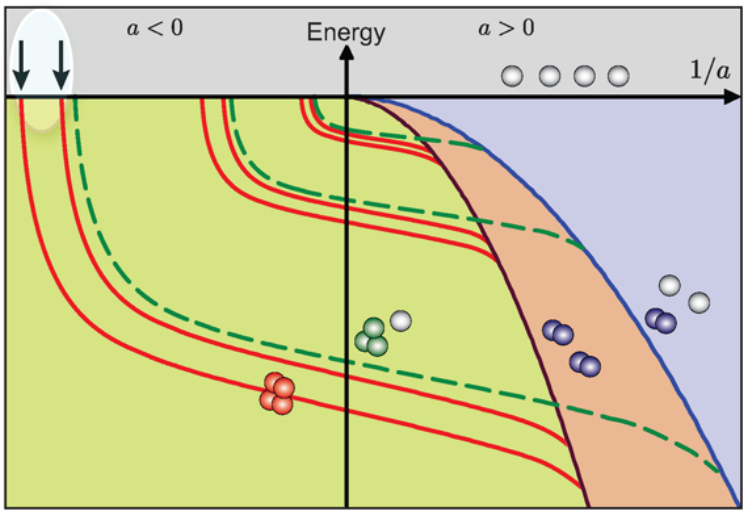

Figure 3.1: *Schematic plot of the spectrum of universal tetramers made of four identical bosons, predicted in Refs. [Ham07, Ste09]. The figure is taken from Ref. [Fer10]. Two tetramer branches (red solid lines) are associated with each trimer branch (green dashed lines).*

As shown in Ref. [Ama73] there is no four-bosons Efimov states. However the existence of universal four-bosons states tightly linked to the presence of a three-body Efimov trimers has been predicted in Ref. [Ham07]. A more detailed prediction of the four-body spectrum has been performed in Ref. [Ste09]. The figure (3.1) taken from Ref. [Fer10] provides a schematic picture of the actual spectrum. Two tetramer branches are associated with each trimer branch. The universal character of these states has not been demonstrated analytically. Nevertheless, numerical computations using finite range potentials provide strong evidences that their properties are only function of the characteristics of the Efimov trimers. However, the existence of a possible specific four-body scale has been conjectured in Ref. [Yam06]. A derivation of the spectrum from the zero-range Efimov-Danilov model should be decisive for answering this issue. Importantly, there are clear experimental evidences for these states in the Borromean region $a < 0$ [Fer09, Pol09]. Actually, as a consequence of the possible disintegration toward one atom and one Efimov trimer flying apart, the universal tetramers are resonances. In Refs. [Del10, Del11a, Del11b] the universal width of these states has been computed by using a refined numerical method which has also revealed an unexpected fine structure in the spectrum.

This short overview ends up with the prediction of a new class of universal three-body states in Ref. [Gue11]. In this numerical study, particles interact *via* a $1/r^2$ pairwise potential. An infinite number of trimers has been found in absence of two-body bound states. However, the spectrum is not the one of Efimov. Interestingly, the case of three fermions can be interpreted as resulting from the Born-approximation performed in a four-body problem where the three fermions interact resonantly with one light impurity *via* a zero-range force. Thus the predictions in Ref. [Gue11] have some links with the four-body Efimov states predicted in Ref. [Cas10]. However in Ref. [Cas10], a pure Efimov effect is predicted.

3.2 Two identical fermions interacting with one impurity: a tunable Efimov effect

The aim of this section is to show by means of a quite simple formalism how the Efimov effect can arise in others systems than three resonant bosons. For systems composed of three two-spin-component fermions, the attractive $1/R^2$ hyper spherical potential is not strong enough to counterbalance the Pauli repulsion. Nevertheless, the Efimov effect occurs for two identical heavy fermions of mass M interacting with one sufficiently light impurity of mass m. Assuming that the mass ratio between the heavy and the light particles is sufficiently high justifies the use of the Born-Oppenheimer approximation. As shown below this provides an intuitive picture of how the Efimov effect emerges: the $1/R^2$ interaction between the two heavy fermions is induced by the light particle.

The two identical fermions are labeled by the index $i = 1, 2$ and the index $i = 3$ is associated with the impurity. The coordinates of the three particles are denoted by $\mathbf{r}_i$. The interaction between the two identical fermions involves non zero partial waves and is thus neglected in the low energy limit and the stationary Schrödinger equation at energy E is:

$$\left[-\frac{\hbar^2}{2M}\left(\Delta_{\mathbf{r}_1}+\Delta_{\mathbf{r}_2}\right)-\frac{\hbar^2}{2m}\Delta_{\mathbf{r}_3}+V\left(\mathbf{r}_1-\mathbf{r}_3\right)+V\left(\mathbf{r}_2-\mathbf{r}_3\right)\right]\langle\mathbf{r}_1,\mathbf{r}_2,\mathbf{r}_3|\Psi\rangle=E\langle\mathbf{r}_1,\mathbf{r}_2,\mathbf{r}_3|\Psi\rangle \tag{3.1}$$

As a consequence of the inequality $M \gg m$, $\mathbf{r}_1$ and $\mathbf{r}_2$ can be considered as 'slow' variables in comparison to the 'fast' variable $\mathbf{r}_3$. The Born-Oppenheimer approximation is as follows. To begin with, the wave function is factorized into two parts

$$\langle\mathbf{r}_1,\mathbf{r}_2,\mathbf{r}_3|\Psi\rangle=\psi_{\text{slow}}(\mathbf{r}_1,\mathbf{r}_2)\psi_{\text{fast}}(\mathbf{r}_1,\mathbf{r}_2,\mathbf{r}_3). \tag{3.2}$$

Then, in a first step the one-body problem on the variable $\mathbf{r}_3$ is solved while the two point-like scattering centers are kept fixed at $\mathbf{r}_1$ and $\mathbf{r}_2$. This provides the eigenvalues associated with the 'eigenfunction' $\psi_{\text{fast}}(\mathbf{r}_1,\mathbf{r}_2,\mathbf{r}_3)$. In a second step, the two-body problem for the slow variables $\mathbf{r}_1$ and $\mathbf{r}_2$ is solved by using the eigenvalue obtained for ψ_{fast}. From Eq. (3.1), the eigenequation associated with the fast variables is:

$$\left[-\frac{\hbar^2}{2m}\Delta_{\mathbf{r}_3}+V\left(\mathbf{r}_1-\mathbf{r}_3\right)+V\left(\mathbf{r}_2-\mathbf{r}_3\right)\right]\psi_{\text{fast}}(\mathbf{r}_1,\mathbf{r}_2,\mathbf{r}_3)=\epsilon\psi_{\text{fast}}(\mathbf{r}_1,\mathbf{r}_2,\mathbf{r}_3). \tag{3.3}$$

Assuming that the pairwise interaction is resonant in the s wave, one replaces V by a source term as in Eq. (1.33) and uses the WBP contact condition. In the present case, one searches for the lowest energy solution and assume that the eigenvalue ϵ is negative with $\epsilon=-\frac{\hbar^2\kappa^2}{2m}$ and $\kappa>0$:

$$\frac{\hbar^2}{2m}\left[-\Delta_{\mathbf{r}_3}+\kappa^2\right]\psi_{\text{fast}}(\mathbf{r}_1,\mathbf{r}_2,\mathbf{r}_3)=-S^{1\leftrightharpoons3}\delta\left(\mathbf{r}_1-\mathbf{r}_3\right)-S^{2\leftrightharpoons3}\delta\left(\mathbf{r}_2-\mathbf{r}_3\right). \tag{3.4}$$

The general solution of Eq. (3.4) can be written in terms as of the Green's function at the negative energy ϵ:

$$\psi_{\text{fast}}(\mathbf{r}_1,\mathbf{r}_2,\mathbf{r}_3)=\frac{mS^{1\leftrightharpoons3}}{2\pi\hbar^2}\frac{e^{-\kappa|\mathbf{r}_1-\mathbf{r}_3|}}{|\mathbf{r}_1-\mathbf{r}_3|}+\frac{mS^{2\leftrightharpoons3}}{2\pi\hbar^2}\frac{e^{-\kappa|\mathbf{r}_2-\mathbf{r}_3|}}{|\mathbf{r}_2-\mathbf{r}_3|}. \tag{3.5}$$

The WBP contact condition at $\mathbf{r}_3=\mathbf{r}_1$ and $\mathbf{r}_3=\mathbf{r}_2$ provides a system of two equations

$$\begin{cases} S^{1\leftrightharpoons3}\left(\dfrac{1}{a}-\kappa\right)+S^{2\leftrightharpoons3}\dfrac{e^{-\kappa r}}{r}=0 \\ S^{1\leftrightharpoons3}\dfrac{e^{-\kappa r}}{r}+S^{2\leftrightharpoons3}\left(\dfrac{1}{a}-\kappa\right)=0 \end{cases} \tag{3.6}$$

where $\mathbf{r} = \mathbf{r}_{12}$ are the relative coordinates of the two heavy fermions. The only possible solution of Eq. (3.6) is such that $S^{1\rightleftharpoons 3} = S^{2\rightleftharpoons 3}$ and

$$a\kappa = 1 + \frac{a}{r}e^{-\kappa r}. \tag{3.7}$$

Thus κ is a function of the interparticle distance r. In what follows, the wavefunction for the two heavy fermions in the center of mass frame is denoted by $\psi_{\text{slow}}(\mathbf{r}_1, \mathbf{r}_2) = f(\mathbf{r})$. The eigenequation associated with the slow variables can then be written as

$$\left[-\frac{\hbar^2}{M}\Delta_{\mathbf{r}} - \epsilon(r)\right] f(\mathbf{r}) = E f(\mathbf{r}) \tag{3.8}$$

where the eigenenergy $\epsilon(r)$ of the wave function ψ_{fast} plays the role of a pairwise potential between the two heavy fermions. At unitarity where $|a| = \infty$ in the zero range model the solution of Eq. (3.7) is $\kappa = x_0/r$ where $x_0 \sim 0.56714\ldots$ is the solution of the transcendental equation $x_0 = \exp(-x_0)$. One thus recovers the attractive $1/r^2$ potential characteristics of the Efimov effect. The regime of positive scattering length where there is a shallow dimer state composed of one fermion and the impurity is another regime of interest. In this case, the large distance behavior ($r \gg a$) of the solution of Eq. (3.7) is

$$\kappa \sim \frac{1}{a} + \frac{\exp(-r/a)}{r} \quad \text{and} \quad \epsilon(r) \sim -\frac{\hbar^2}{2m}\left(\frac{1}{a^2} + \frac{\exp(-r/a)}{ar}\right). \tag{3.9}$$

One thus recovers a Yukawa potential: the light particle plays the role of an intermediate massive boson.

Using the rotational symmetry, the general solution of Eq. (3.8) can be expanded in terms of the Legendre polynomials as

$$f(\mathbf{r}) = \sum_{l=0}^{\infty} \frac{F_l(r)}{\sqrt{r}} P_l(\hat{\mathbf{e}}_{\mathbf{r}} \cdot \hat{\mathbf{e}}_z). \tag{3.10}$$

Furthermore, using the fact that the wave function $\psi_{\text{fast}}(\mathbf{r}_1, \mathbf{r}_2, \mathbf{r}_3)$ is symmetric under the exchange of the coordinates $\mathbf{r}_1$ and $\mathbf{r}_2$, the spin-statistic theorem imposes that $\psi_{\text{slow}}(\mathbf{r})$ is an odd function. Consequently, the sum in Eq. (3.10) concerns only odd values of the azimuthal quantum number l. At unitarity, $|a| = \infty$ and the radial equation in the partial wave l can be written in the form

$$\frac{\hbar^2}{M}\left(-\partial_r^2 - \frac{1}{r}\partial_r + \frac{s_l^2}{r^2}\right) F_l(r) = E F_l(r) \quad \text{where} \quad s_l^2 = \left[\left(l + \frac{1}{2}\right)^2 - \frac{M}{2m}x_0^2\right]. \tag{3.11}$$

The expression of the coupling constant s_l^2 reveals two opposite trends. First, for growing values of l the effective interaction between the two heavy particles becomes more and more repulsive: a consequence of the kinetic barrier. Second, the more the value of the mass ratio $\frac{m}{M}$ is small the more the interaction is attractive: the role of 'intermediate boson' played by the impurity is enhanced. The Efimov effect appears when the smallest value of s_l^2 is smaller than zero. This occurs in the p wave *i.e.* for $l = 1$ and for mass ratios M/m greater than the critical value $M/m = 13.99\ldots$. This threshold is an approximate value which is consistent with the hypothesis $M \gg m$. This system has been studied in an exact treatments in Refs. [Efi73, Bul75, Pet03] and the critical value 13.6 is relatively near the one obtained in the Born-Oppenheimer approximation.

This example is particularly interesting as the very existence of the Efimov effect depends on the value of the mass ratio. As it will be shown further, this characteristics is an essential ingredient for the four-body Efimov effect.

3.3 Efimov effect for N particles

3.3.1 Conditions for finding a pure N-body Efimov effect

We are now ready for having a general definition of the Efimov effect applying for an arbitrary number of particles $N \geq 3$ and whatever the statistics of the particles. As explained in chapter 2, the three-body Efimov effect is linked to the separability in the hyper angular and the hyper radial coordinates which follows from the scaling invariance of the WBP contact condition at unitarity. We thus stick to the unitarity limit assuming that the pairwise interaction can be described at the two-body level by the WBP zero-range model and follow the formalism of Ref. [Wer06a, Wer06b, Wer08]. However for $N > 3$, the unitarity condition is not sufficient for ensuring separability: one needs also that no M-body bound state *i.e.* Efimov states exist for $M < N$. If

this condition is not satisfied, the Efimov-Danilov contact condition must be applied at the M-body level and breaks the separability in the N-body problem. This last condition is rather stringent, for example it precludes the existence of a pure N-body Efimov effect for identical bosons. Nevertheless as is shown in this section, the general formalism for the Efimov effect is quite simple to set up ... but unfortunately not easy to solve.

3.3.2 Jacobi variables

The particles are labeled by the index i, their coordinates are denoted by $\mathbf{r}_i$ and their mass m_i. The Jacobi variables privilege a given pair of interacting particles. These coordinates has been proven to be very useful in solving the three-body problem in the configuration space. In what follows, the Jacobi variable are introduced for an arbitrary number of particles. The idea is to construct iteratively a set of three-dimensional vectors by defining at the step n the relative particle formed by the particle n and the relative particle of the step $n-1$. For this purpose, one introduces first the mass and center of mass of the first j particles:

$$M_j = \sum_{i=1}^{j} m_i \qquad ; \qquad \mathbf{C}_j = \frac{1}{M_j} \sum_{i=1}^{j} m_i \mathbf{r}_i. \tag{3.12}$$

The center of mass of the system is denoted $\mathbf{C} = \mathbf{C}_N$. The reduced mass and the coordinates for the relative particle formed by the j^{th} particle and the set composed of the first $j-1$ particles is

$$\mu_j = \frac{m_{j+1} M_j}{M_{j+1}} \qquad ; \qquad \boldsymbol{\eta}_j = \sqrt{\frac{\mu_j}{m_R}} \left(\mathbf{r}_{j+1} - \mathbf{C}_j\right) \quad \text{where} \quad 1 \leq j \leq N-1, \tag{3.13}$$

where m_R is an arbitrary mass of reference. Beginning the iteration from a given pair, for instance the pair (12), the $N-1$ vectors $\{\boldsymbol{\eta}_1, \boldsymbol{\eta}_2 \ldots \boldsymbol{\eta}_{N-1}\}$ form a possible set of Jacobi coordinates [1]. Then one introduces the $N-1$-dimensional hyper radius vector

$$\mathbf{R} = \left(\boldsymbol{\eta}_1, \boldsymbol{\eta}_2, \ldots \boldsymbol{\eta}_{N-1}\right), \tag{3.14}$$

and the hyper radius defined by $R = \sqrt{\sum_{i=1}^{N-1} \eta_i^2}$. The $N-1$-dimensional vector $\left(\frac{\boldsymbol{\eta}_1}{R}, \frac{\boldsymbol{\eta}_2}{R}, \ldots \frac{\boldsymbol{\eta}_{N-1}}{R}\right)$ is unitary and can be thus parameterized by using a set of $3N-4$ independent angles denoted by $\Omega_{\mathbf{R}}$. This set of angles $\Omega_{\mathbf{R}}$ is composed of $2N-2$ spatial angles associated with the unit vectors $\boldsymbol{\eta}_i/\eta_i$ and of $N-2$ hyper angles α_i defined by:

$$\begin{cases} \eta_1 = R \sin\alpha_1 \\ \eta_2 = R \cos\alpha_1 \sin\alpha_2 \\ \eta_3 = R \cos\alpha_1 \cos\alpha_2 \sin\alpha_3 \\ \vdots \\ \eta_{N-1} = R \cos\alpha_1 \cos\alpha_2 \ldots \cos\alpha_{N-2} \end{cases} . \tag{3.15}$$

Consequently, in configuration space the system of particles is described by a set of $3N$ degrees of freedom which can be expressed in terms of the coordinates $(\mathbf{C}, R, \Omega_{\mathbf{R}})$. The kinetic operator of the N-body system is

$$T = \sum_{i=1}^{N} \frac{-\hbar^2}{2m_i} \Delta_{\mathbf{r}_i}. \tag{3.16}$$

By using the relation

$$\frac{1}{M_{j-1}} \Delta_{C_{j-1}} + \frac{1}{m_j} \Delta_{r_j} = \frac{1}{M_j} \Delta_{C_j} + \frac{1}{m_R} \Delta_{\boldsymbol{\eta}_{j-1}}, \tag{3.17}$$

the kinetic operator in the center of mass framecan be expressed in terms of the hyper radius vector $\mathbf{R}$ as

$$T = \frac{-\hbar^2}{2m_R} \Delta_{\mathbf{R}} \tag{3.18}$$

Then, it can be decomposed as sum of two bits: an operator T_R acting only on the hyper radius R and an operator $\frac{T_{\Omega_{\mathbf{R}}}}{R^2}$ acting on the angles:

$$T = T_R + \frac{T_{\Omega_{\mathbf{R}}}}{R^2}. \tag{3.19}$$

[1] A system of Jacobi coordinates beginning from another pair can be deduced from the initial one by applying a hyper rotation.

The expression of T_R can be obtained from the Green-Ostrogradski theorem applied on a test function h which depends only on the hyper radius R:

$$\int_{\mathcal{B}_\epsilon} d^{3N-3}R\, \Delta_{\mathbf{R}} h(R) = \int_{\partial\mathcal{B}_\epsilon} d^{3N-4}R\, (\hat{\mathbf{n}}\cdot\boldsymbol{\nabla})\, h(R) \tag{3.20}$$

$\mathcal{B}_\epsilon$ is a $3N-3$ dimensional ball of radius ϵ, $\partial\mathcal{B}_\epsilon$ is the boundary of $\mathcal{B}_\epsilon$: a $3N-4$ dimensional sphere of radius ϵ, $\hat{\mathbf{n}}$ is the outward pointing unit normal vector of $\partial\mathcal{B}_\epsilon$ and $\boldsymbol{\nabla}$ is the $3N-3$-dimensional nabla operator. Integration over the hyper angle can be performed at the left and right hand side of Eq. (3.20) and after a derivation with respect to ϵ one is left with:

$$\Delta_{\mathbf{R}} h(R) = \frac{1}{R^{3N-4}}\partial_R \left[R^{3N-4}\partial_R h(R)\right] = \left(\partial_R^2 + \frac{3N-4}{R}\partial_R\right) h(R). \tag{3.21}$$

The kinetic operator is thus:

$$T = -\frac{\hbar^2}{2m_R}\left(\partial_R^2 + \frac{3N-4}{R}\partial_R\right) - \frac{\hbar^2}{2m_R}\frac{T_{\Omega_{\mathbf{R}}}}{R^2}. \tag{3.22}$$

3.3.3 General equations and filtering condition

At unitarity, assuming that no Efimov effect exists for less than N particles, the interactions are modeled solely by using the WBP contact condition for each interacting pair (ij). Considering for instance the contact between particles 1 and 2, this means that there exists a function A_Ψ such that in the limit of vanishing interparticle distance r_{12} or equivalently of η_1, one has

$$\langle \mathbf{R}|\psi\rangle \underset{\eta_1\to 0}{=} -\sqrt{\frac{\mu_1}{m_R}}\frac{\langle \boldsymbol{\eta}_2, \boldsymbol{\eta}_3, \dots \boldsymbol{\eta}_{N-1}|A_\psi\rangle}{\eta_1} + \mathcal{O}(\eta_1). \tag{3.23}$$

where the limit is taken while the coordinates $\boldsymbol{\eta}_2, \boldsymbol{\eta}_3, \dots \boldsymbol{\eta}_{N-1}$ are kept fixed. Importantly, for $N \geq 3$, the limit $r_{ij} \to 0$ can be expressed as the limit of a vanishing hyper angle. For example, the contact condition associated with the pair (12) is achieved for vanishing values of the relative distance $\eta_1 = R\sin\alpha_1$ which corresponds to the limit $\alpha_1 \to 0$. It turns out that the WBP contact condition is then invariant in the scale transformation $\mathbf{r}_i \to \lambda\mathbf{r}_i$ and $A_\Psi \to \lambda A_\Psi$. Furthermore, almost everywhere that is excepted for $\mathbf{r}_i = \mathbf{r}_j$ where (ij) is a pair of interacting particles, the Hamiltonian is equal to the kinetic operator T. There is thus separability in the hyper angle and the hyper radius coordinates. Hence any eigenstate can be written as a product:

$$\langle \mathbf{R}|\psi\rangle = h(R)\phi(\Omega_{\mathbf{R}}). \tag{3.24}$$

where the hyper angular function $\phi(\Omega_{\mathbf{R}})$ is an eigenstate of the laplacian on the unit sphere:

$$T_{\Omega_{\mathbf{R}}}\phi(\Omega_{\mathbf{R}}) = -\theta\phi(\Omega_{\mathbf{R}}) \tag{3.25}$$

The eigenequation on the hyper angular part Eq. (3.25) has to be solved by taking into account the contact conditions for each interacting pairs. For instance for the pair (12) it reads $\lim_{\alpha\to 0}\partial_\alpha\alpha\phi(\Omega_{\mathbf{R}}) = 0$. This set of boundary conditions leads to a discrete set of eigenvalues θ and for each eigenvalue their exists a hyper radial equation:

$$\frac{\hbar^2}{2m_R}\left[-\left(\frac{d^2}{dR^2} + \frac{3N-4}{R}\frac{d}{dR}\right) + \frac{\theta}{R^2}\right] h(R) = Eh(R). \tag{3.26}$$

As done by Efimov in the three-boson problem, it is relevant to write the hyper radial equation in terms of the two-dimensional laplacian. This is indeed possible by introducing the function

$$F(R) = R^{\frac{3N-5}{2}} \times h(R) \tag{3.27}$$

so that Eq. (3.26) transforms into

$$\frac{\hbar^2}{2m_R}\left[-\left(\partial_R^2 + \frac{1}{R}\partial_R\right) + \frac{s^2}{R^2}\right] F(R) = EF(R) \quad \text{where} \quad s^2 = \frac{(3N-5)^2}{4} + \theta. \tag{3.28}$$

If *all* the eigenvalues s are positive, there is no Efimov effect and no bound states. In this regime, Eq. (3.26) shows that the system is characterized by a continuous scale symmetry where a state of energy E can be deduced

from a state of energy E/λ^2 by the change $\mathbf{r}_i \to \lambda \mathbf{r}_i$. Efimov effect occurs if one of the eigenvalue s^2 is negative with $s = \pm iS$ and $S > 0$. With the choice $m_R = \frac{m}{2}$ and the formal substitution $S = s_0$, the filtering or N-body contact condition which makes the model self-adjoint has exactly the same form as the Efimov-Danilov one in Eq. (2.64). The resulting spectrum at unitarity is thus given by Eq. (2.62). As happens in the three-boson problem, the Danilov-Efimov contact condition breaks the continuous scale symmetry which turns out to be only a discrete scaling symmetry characterized by the scaling factor $\lambda = \exp(\pi/S)$. Notice that at zero energy ($E = 0$), Eq. (3.28) is invariant in a scale transformation and the two independent solutions are simply

$$F(R) = R^{\pm s}. \tag{3.29}$$

The general definition of the N-body Efimov effect is quite simple as the phenomenon is linked to the behavior of the hyper radial part of the wave function which is basically the same as in the three-body problem. However the problem is highly non trivial because of the hyper-angular eigenvalue problem which is constrained by the WBP contact conditions.

3.4 N identical particles interacting with one impurity

In section 3.2 it was shown that the system composed of two identical fermions of mass M in resonant interaction with an impurity of mass m can exhibit a three-body Efimov effect depending on the value of the mass ratio between the two species. Let us denote by $x_{\rm crit}(2)$ the exact critical ratio (not the one obtained in the Born-Oppenheimer approximation). For $M/m < x_{\rm crit}(2)$ there is no three-body Efimov effect and one can then wonder if in this regime of mass ratio, an $N+1$-body Efimov effect exists for a system composed of N identical identical fermions interacting with one impurity. This section focuses on this particular system.

3.4.1 Integral equation

Deriving the general integral equation for N identical particles of mass M in a s wave resonant interaction with one impurity of mass m is another occasion to illustrate the formalism of section 1.3.2. In what follows, the mass ratio between the two species is denoted by x:

$$x = \frac{M}{m}. \tag{3.30}$$

To be a little bit more general than is needed, the identical particles can be either bosons or fermions. Neglecting the interaction between identical fermions in the s wave partial wave follows from the Pauli principle. However for identical bosons this assumption means that this pairwise interaction is non resonant. Thus the actual interatomic forces of the hetero-nuclear interacting pairs are in the vicinity of a s wave resonance while interaction for pairs of identical bosons is neglected. The particles are labeled by an integer i in the interval $[1, N]$ and the impurity is labeled by the integer $N+1$. For conciseness, we introduce the number η such that

$$\eta = \begin{cases} 1 & \text{if the identical particles are bosons} \\ -1 & \text{if the identical particles are fermions} \end{cases}. \tag{3.31}$$

The pairwise interaction between a particle i and the impurity is replaced by a zero-range source term of amplitude $S_\Psi^{i \leftrightharpoons N+1}$. Thus, there are N source terms associated with the interacting pairs $\{i, N+1\}$ ($i = 1 \dots N$). In the center of mass frame the wave function Ψ factorizes as

$$\langle \mathbf{k}_1, \dots \mathbf{k}_{N+1} | \Psi \rangle = \delta \left(\sum_{i=1}^{N+1} \mathbf{k}_i \right) \langle \mathbf{k}_1, \dots \mathbf{k}_{N+1} | \psi \rangle. \tag{3.32}$$

Each source amplitude is a function of $N-1$ independent wavevectors. Moreover using the exchange symmetry, the source amplitudes can be deduced from only one of them. For the pair $\{1, N+1\}$ of reduced mass $\mu = \frac{mM}{m+M}$ the source amplitude is written as

$$\langle \mathbf{k}_1 + \mathbf{k}_{N+1}, \mathbf{k}_2, \mathbf{k}_3, \dots \mathbf{k}_N | S_\Psi^{1 \leftrightharpoons N+1} \rangle = \delta \left(\sum_{i=1}^{N+1} \mathbf{k}_i \right) \frac{2\pi\hbar^2}{\mu} \langle \mathbf{k}_2, \dots \mathbf{k}_N | A_\psi \rangle. \tag{3.33}$$

For instance, using this notation the source amplitude for the pair $\{3, N+1\}$ is equal to $\eta\langle \mathbf{k}_2, \mathbf{k}_1, \mathbf{k}_4 \dots \mathbf{k}_N | A_\psi\rangle$. In the zero-range limit $\epsilon \to 0$, the stationary Schrödinger equation for a state Ψ at energy E provides the expression:

$$\langle \mathbf{k}_1, \dots \mathbf{k}_{N+1}|\psi\rangle = \langle \mathbf{k}_1, \dots \mathbf{k}_{N+1}|\psi^{(0)}\rangle - \frac{2\pi\hbar^2}{\mu} \times \frac{\langle \mathbf{k}_2, \dots \mathbf{k}_N|A_\psi\rangle + \eta\langle \mathbf{k}_1, \mathbf{k}_3, \dots \mathbf{k}_N|A_\psi\rangle + \eta\langle \mathbf{k}_2, \mathbf{k}_1, \mathbf{k}_4, \dots \mathbf{k}_N|A_\psi\rangle + \dots + \eta\langle \mathbf{k}_2, \dots \mathbf{k}_{N-1}, \mathbf{k}_1|A_\psi\rangle}{\frac{\hbar^2}{2M}\sum_{i=1}^N k_i^2 + \frac{\hbar^2 k_{N+1}^2}{2m} - E - i0^+}, \quad (3.34)$$

where $\sum_{i=1}^{N+1} \mathbf{k}_i = 0$. In Eq. (3.34), $|\psi^{(0)}\rangle$ is non zero for a positive energy E and is a regular solution of the free Schrödinger equation satisfying the desired asymptotic condition of a given process. As in the case of the three-boson problem, the desired integral equation on the function $\langle \mathbf{k}_2, \dots \mathbf{k}_N|A_\Psi\rangle$ is deduced directly from the WBP contact condition (2.2) expressed in the momentum representation as in (1.53). For the pair $\{1, N+1\}$, this provides:

$$\int \frac{d^3k_{1,N+1}}{(2\pi)^3}\left(\langle \mathbf{k}_1, \dots \mathbf{k}_{N+1}|\psi\rangle + \frac{4\pi\langle \mathbf{k}_2, \dots \mathbf{k}_N|A_\psi\rangle}{k_{1,N+1}^2 + \Lambda^2}\right) = -\frac{\langle \mathbf{k}_2, \dots \mathbf{k}_N|A_\psi\rangle}{f_W(i\Lambda)}, \quad (3.35)$$

where Λ is an arbitrary positive real number and the relative wavevector for the pair is

$$\mathbf{k}_{1,N+1} = \frac{m\mathbf{k}_1 - M\mathbf{k}_{N+1}}{m+M}. \quad (3.36)$$

Following the same reasoning as done for the three-boson problem, the collisional energy $E_{\rm col}$ is defined similarly to Eq. (2.11) by a rewriting of the kinetic term in the denominator of Eq. (3.34) with

$$\frac{\hbar^2}{2M}\sum_{i=1}^N k_i^2 + \frac{\hbar^2 k_{N+1}^2}{2m} - E \equiv \frac{\hbar^2 k_{1,N+1}^2}{2\mu} - E_{\rm col}. \quad (3.37)$$

Then, from the identity

$$\frac{k_1^2}{M} + \frac{k_{N+1}^2}{m} = \frac{(\mathbf{k}_1 + \mathbf{k}_{N+1})^2}{M+m} + \frac{k_{1,N+1}^2}{\mu} \quad (3.38)$$

one finds

$$E_{\rm col} = E - \frac{\hbar^2}{2(M+m)}(\mathbf{k}_1 + \mathbf{k}_{N+1})^2 - \frac{\hbar^2}{2M}\sum_{i=2}^N k_i^2. \quad (3.39)$$

Finally, using the fact that $\sum_{i=1}^N \mathbf{k}_i = \mathbf{0}$, the collisional energy can be written as

$$E_{\rm col} = E - \frac{\hbar^2}{2(m+M)}\left(\sum_{i=2}^N \mathbf{k}_i\right)^2 - \frac{\hbar^2}{2M}\sum_{i=2}^N k_i^2. \quad (3.40)$$

The collisional wavenumber is defined by

$$\frac{\hbar^2}{2\mu}(k_{\rm col})^2 = E_{\rm col} \quad (3.41)$$

with $k_{\rm col} > 0$ for a positive collisional energy $E_{\rm col} > 0$ and $k_{\rm col} = iq_{\rm col}$ where $q_{\rm col} > 0$ otherwise, so that:

$$q_{\rm col} = \left(\frac{1+2x}{(1+x)^2}\sum_{i=2}^N k_i^2 + \frac{2x}{(1+x)^2}\sum_{2\le i<j\le N} \mathbf{k}_i\cdot\mathbf{k}_j - \frac{2\mu E}{\hbar^2}\right)^{\frac{1}{2}}. \quad (3.42)$$

In the domain where the collisional energy is negative and for the choice $\Lambda = q_{\rm col}$ the terms involving $\langle \mathbf{k}_2, \dots \mathbf{k}_N|A_\psi\rangle$ in the integration in the left hand side of Eq. (3.35) simplifies with each others. Using the identity $d^3k_{1,N+1} = d^3k_1$ [2] the integral equation is

$$\int \frac{d^3k_1}{2\pi^2}\frac{\langle \mathbf{k}_1, \mathbf{k}_3, \dots \mathbf{k}_N|A_\psi\rangle + \langle \mathbf{k}_2, \mathbf{k}_1, \mathbf{k}_4, \dots \mathbf{k}_N|A_\psi\rangle + \dots \langle \mathbf{k}_2, \dots \mathbf{k}_{N-1}, \mathbf{k}_1|A_\psi\rangle}{\sum_{i=1}^N k_i^2 + \frac{2x}{1+x}\sum_{1\le i<j\le N} \mathbf{k}_i\cdot\mathbf{k}_j - \frac{2\mu E}{\hbar^2}} = \eta\frac{\langle \mathbf{k}_2, \dots \mathbf{k}_N|A_\psi\rangle}{f_W(iq_{\rm col})}. \quad (3.43)$$

[2] The wavevector $\mathbf{k}_1 + \mathbf{k}_{N+1}$ is kept fixed in the contact condition.

For a state of positive energy, the integral equation is obtained from Eq. (3.43) by adding the term $\int \frac{d^3k_1}{(2\pi)^3}\langle \mathbf{k}_1,\dots \mathbf{k}_{N+1}|\psi^{(0)}\rangle$ in the left hand side of the equation and by making the substitution $E \to E + i0^+$.

This section ends up by considering the limit of zero energy ($E \to 0^-$) in the unitarity limit $f_{\rm W}(iq_{\rm col}) = 1/q_{\rm col}$. This regime is interesting for searching an hypothetical Efimov effect as Eq. (3.43) is invariant in a scale transformation. This property already present in the general formalism in configuration space [see section 3.3.3] allows to simplify calculations because $\langle \mathbf{k}_2, \mathbf{k}_3, \dots \mathbf{k}_N|A_\psi\rangle$ can be searched as the product of a power law on the hyper wavenumber $K_{\widehat{1}} = \sqrt{k_2^2 + k_3^2 + k_4^2 + \dots + k_N^2}$ with a function of the generalized angles $(\frac{\mathbf{k}_2}{K_{\widehat{1}}}, \frac{\mathbf{k}_3}{K_{\widehat{1}}}, \dots \frac{\mathbf{k}_N}{K_{\widehat{1}}})$. Furthermore, the exponent of this power law can be deduced from the one of the function $F(R)$ in Eq. (3.29). For this purpose, we introduce the shorthand notation for the hyper wave vectors:

$$\mathbf{K}_{\widehat{1}} = (\mathbf{k}_2, \mathbf{k}_3, \dots \mathbf{k}_N) \quad , \quad \mathbf{R}_{\widehat{1}} = (\boldsymbol{\eta}_2, \boldsymbol{\eta}_3, \dots \boldsymbol{\eta}_N) \tag{3.44}$$

and for the hyper angles

$$\mathbf{\Omega}_{R_{\widehat{1}}} = (\frac{\boldsymbol{\eta}_2}{R_{\widehat{1}}}, \frac{\boldsymbol{\eta}_3}{R_{\widehat{1}}}, \dots \frac{\boldsymbol{\eta}_N}{R_{\widehat{1}}}) \quad , \quad \mathbf{\Omega}_{R_{\widehat{1}}} = (\frac{\mathbf{k}_2}{K_{\widehat{1}}}, \frac{\mathbf{k}_3}{K_{\widehat{1}}}, \dots \frac{\mathbf{k}_N}{K_{\widehat{1}}}). \tag{3.45}$$

We consider the Jacobi variables associated with the pair $(1, N+1)$ making also the natural choice $m_R = \mu$:

$$\eta_1 = R\sin\alpha_1 = |\mathbf{r}_1 - \mathbf{r}_{N+1}|\,. \tag{3.46}$$

For $N > 1$, the WBP contact condition in the configuration space reads:

$$\langle \mathbf{R}|\psi\rangle \underset{\alpha_1\to 0}{=} -\frac{\langle \mathbf{R}_{\widehat{1}}|A_\psi\rangle}{R\alpha_1} + \mathcal{O}(R\alpha_1) \tag{3.47}$$

From Eqs. (3.24,3.27,3.47), one finds[3]:

$$\langle \mathbf{R}_{\widehat{1}}|A_\psi\rangle = -F(R)R^{-\frac{3N}{2}+2}\lim_{\alpha_1\to 0}\alpha_1\phi(\Omega_{\mathbf{R}}). \tag{3.48}$$

Thus

$$\langle \mathbf{K}_{\widehat{1}}|A_\psi\rangle = -\int dRd\Omega_{\mathbf{R}_{\widehat{1}}}\left\{F(R)R^{\frac{3N}{2}-2}\lim_{\alpha_1\to 0}[\alpha_1\phi(\Omega_{\mathbf{R}})]\exp(-i\mathbf{K}_{\widehat{1}}\cdot\mathbf{R}_{\widehat{1}})\right\} \tag{3.49}$$

and using the fact that $F(R) = R^{\pm s}$ one obtains

$$\langle \mathbf{K}_{\widehat{1}}|A_\psi\rangle = -K_{\widehat{1}}^{\pm s-\frac{3N}{2}+1} \times \int dud\Omega_{\mathbf{R}_{\widehat{1}}}\left\{u^{\pm s+\frac{3N}{2}-2}\lim_{\alpha_1\to 0}[\alpha_1\phi(\Omega_{\mathbf{R}})]\exp(-iu\Omega_{\mathbf{K}_{\widehat{1}}}\cdot\Omega_{\mathbf{R}_{\widehat{1}}})\right\}. \tag{3.50}$$

The threshold for an Efimov effect corresponds to the case where $s = 0$.

3.4.2 Exact critical mass ratio for two fermions interacting with one impurity

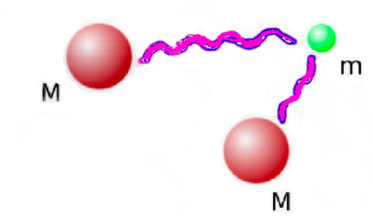

As a first application of the formalism of section 3.4.1 let us come back to the problem of two identical fermions interacting with one impurity. This problem was solved in the Born-Oppenheimer approximation in section (3.2). Now using the general integral equation (3.43) in the particular case where $N = 2$ it is possible to solve this problem exactly. The threshold for the Efimov effect is found by considering the states of zero energy at the unitary limit ($|a| = \infty$) and searching for the mass ratio such that the exponent s in (3.50) is zero. The collisional energy and the scattering amplitude are given by:

$$q_{\rm col} = \frac{\sqrt{(1+2x)}}{1+x}k_2 \qquad \text{and} \qquad f_W(iq_{\rm col}) = \frac{1}{q_{\rm col}}. \tag{3.51}$$

[3] One has to take into account the fact that the formalism in section 3.3.3 is for N particles, while we consider in this section $N+1$ particles.

Performing the substitution $\mathbf{k}_2 \to \mathbf{k}$ and $\mathbf{k}_1 \to \mathbf{u}$, the integral equation is

$$\eta \frac{\sqrt{(1+2x)}}{1+x} k \langle \mathbf{k}|A_\psi\rangle = \int \frac{d^3u}{2\pi^2} \frac{\langle \mathbf{u}|A_\psi\rangle}{u^2+k^2+\frac{2x}{1+x}\mathbf{k}\cdot\mathbf{u}}. \tag{3.52}$$

The rotational invariance of the kernel in Eq. (3.52) allows to fix an arbitrary direction $\hat{e}_\mathbf{q}$ and to expand the source amplitude $\langle \mathbf{k}|A_\psi\rangle$ in terms of partial waves as:

$$\langle \mathbf{k}|A_\psi\rangle = \sum_{l=0}^{\infty} P_l(\hat{e}_\mathbf{k}\cdot\hat{e}_\mathbf{q}) D_l(k). \tag{3.53}$$

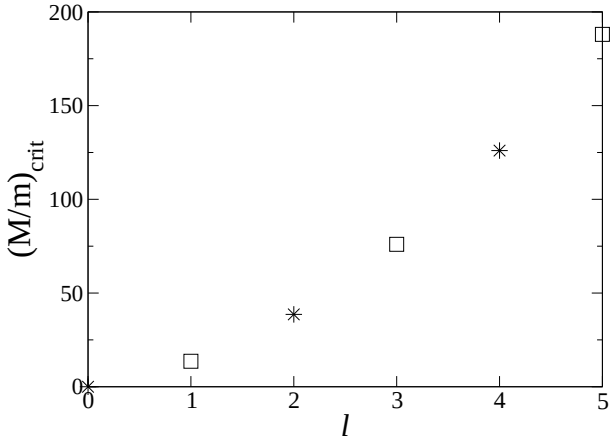

Figure 3.2: *Critical mass ratio* $\left(\frac{M}{m}\right)_l^{\text{crit}}$ *for the threshold of appearance of an Efimov spectrum in each partial wave* l *of Eq. (3.54). The Efimov effect occurs in each even partial wave for a mass ratio* $M/m \geq \left(\frac{M}{m}\right)_l^{\text{crit}}$ *and for even (respectively odd) values of* l *in the case of two bosons (respectively fermions) interacting with one impurity. The figure is taken from Ref. [Pri11a].*

The angular integration can be performed and each component $D_l(k)$ verifies the integral equation

$$\eta x \frac{\sqrt{1+2x}}{(1+x)^2}(-1)^l k^2 D_l(k) = \int_0^\infty du \, \frac{u D_l(u)}{\pi} Q_l\left(\frac{(u^2+k^2)(1+x)}{2xku}\right), \tag{3.54}$$

where Q_l is a Legendre function of the second kind [4]. Equation (3.54) is invariant in a scale transformation and its solutions can thus be searched as power laws deduced from Eq. (3.50) where for $N=2$ the angular factor reduces to the function of the spatial angle:

$$D_l(k) = k^{\pm s-2}. \tag{3.55}$$

The Efimov effect occurs for $s^2 < 0$. As in the three-boson case the integration in Eq. (3.54) can be performed analytically for each value of l [Pri11a, Cas11]. The solutions of Eq. (3.54) for even (respectively odd) values of l corresponds to the case where the identical particles are bosons where ($\eta = 1$) (respectively fermions where $\eta = -1$). For $l = 0$ *i.e.* in the bosonic case, the Efimov effect occurs even for negligible values of M (formally for $M \to 0$). For $l = 1$, the threshold for the mass ratio $x = \frac{M}{m}$ is equal to [Bul75, Pet03]:

$$x_{\text{crit}}(N=2) = 13.607\ldots \tag{3.56}$$

which is a value quite close to the one obtained in the Born Oppenheimer approximation. For increasing values of l the threshold for the Efimov effect correspond to increasing values of the mass ratio [Efi73]. The critical values of the mass ratio of the Efimov threshold in the l wave [denoted $\left(\frac{M}{m}\right)_l^{\text{crit}}$] are plotted in Fig. (3.2).

[4] Using the definition $Q_0(x) = \frac{1}{2}\ln\left(\frac{x+1}{x-1}\right)$, one recovers the STM equation for three bosons ($\eta = 1$) in the wave $l = 0$ by multiplying the right hand side of Eq. (3.54) by a factor 2.

At finite energy and/or large values of the scattering length the function D_l have the same behavior as the zero energy solution in the unitary regime. Thus in the Efimovian regime and for large values of k, $D_l(k)$ is a linear combination of the two elementary solutions $k^{-2\pm i|s|}$ ($s \in \mathbb{R}$). As in the three-boson case, the problem is made self-adjoint by imposing the Efimov-Danilov condition.

3.4.3 Efimov effect for three identical fermions interacting with one impurity

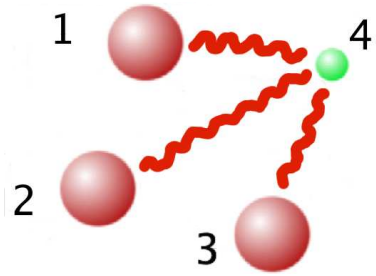

This section is an introduction to the work of Ref. [Cas10]. As noticed in section 3.3.3 if there exists a three-body Efimov effect there is no four-body Efimov states. Thus in our quest for a four-body Efimov effect, we can eliminate systems where there is more than one boson. That is why in this section we consider three identical fermions in interaction with one impurity and we search for an Efimov effect for a mass ratio $x = m/M < x_{\text{crit}}(2) = 13.607\ldots$. We denote by $x_{\text{crit}}(3)$ the critical mass ratio for the threshold of appearance of the four-body effect. To find this mass ratio, we restrict our study to the unitary limit and for sake of simplicity we consider only the eigenstates in the limit of zero energy.

Integral equation

The integral equation is found from Eq. (3.43) as:

$$\int \frac{d^3k_1}{2\pi^2} \frac{\langle \mathbf{k}_1, \mathbf{k}_3 | A_\psi \rangle + \langle \mathbf{k}_2, \mathbf{k}_1 | A_\psi \rangle}{\sum_{i=1}^3 k_i^2 + \frac{2x}{1+x} \sum\limits_{1\le i<j\le 3} \mathbf{k}_i \cdot \mathbf{k}_j} + \left[\frac{1+2x}{(1+x)^2}(k_1^2 + k_2^2) + \frac{2x\mathbf{k}_1 \cdot \mathbf{k}_2}{(1+x)^2} \right]^{1/2} \langle \mathbf{k}_2, \mathbf{k}_3 | A_\psi \rangle = 0 \tag{3.57}$$

Symmetry considerations

The translational invariance has been already taken into account by considering the problem in its center of mass frame

1. **Statistics**: the fermionic statistics impose the anti symmetry of the source amplitude

$$\langle \mathbf{k}_1, \mathbf{k}_2 | A_\psi \rangle = -\langle \mathbf{k}_2, \mathbf{k}_1 | A_\psi \rangle. \tag{3.58}$$

2. **Isotropy and parity**: the integral kernel in Eq. (3.57) is isotropic and invariant in an inversion of the coordinates $\mathbf{k} \to -\mathbf{k}$. It is thus possible to reduce the problem into sectors of defined values of the angular momentum and of the parity. This simplifies the problem as an angular integration in Eq. (3.57) can be performed analytically. For the sectors $l = 0$ and $l = 1$ we can use a reasoning 'à la Landau':

   - In the isotropic sector ($l = 0$): the only way to form scalars from $\mathbf{k}_1$ and $\mathbf{k}_2$ is to use k_1, k_2 and $\mathbf{k}_1 \cdot \mathbf{k}_2$. The ansatz (necessarily of even parity) is thus of the form:

$$\langle \mathbf{k}_1, \mathbf{k}_2 | A_\psi \rangle = f^{(0)}(k_1, k_2, \mathbf{k}_1 \cdot \mathbf{k}_2) \tag{3.59}$$

     and the exchange symmetry in Eq. (3.58) imposes $f^{(0)}(k_1, k_2, \mathbf{k}_1 \cdot \mathbf{k}_2) = -f^{(0)}(k_2, k_1, \mathbf{k}_1 \cdot \mathbf{k}_2)$.

   - In the p wave sector ($l = 1$): the p wave spherical harmonics behaves as the projection of vectors in rotations (see the footnote 13 of section 1.5.3). The three possible vectors available are $\mathbf{k}_1, \mathbf{k}_2$ and $\mathbf{k}_1 \wedge \mathbf{k}_2$. Choosing the quantification axis along $\hat{\mathbf{e}}_z$ gives three basic components $\hat{\mathbf{e}}_z \cdot \mathbf{k}_1, \hat{\mathbf{e}}_z \cdot \mathbf{k}_2$ and $\hat{\mathbf{e}}_z \cdot (\mathbf{k}_1 \wedge \mathbf{k}_2)$. These three components behaves differently in a parity transformation: while $\hat{\mathbf{e}}_z \cdot \mathbf{k}_1$ and $\hat{\mathbf{e}}_z \cdot \mathbf{k}_2$ are in the odd sector, $\hat{\mathbf{e}}_z \cdot (\mathbf{k}_1 \wedge \mathbf{k}_2)$ is in the even sector. Thus a first possible ansatz is

$$\langle \mathbf{k}_1, \mathbf{k}_2 | A_\psi \rangle = \hat{\mathbf{e}}_z \cdot (\mathbf{k}_1 \wedge \mathbf{k}_2) f^{(1)}_{(+)}(k_1, k_2, \mathbf{k}_1 \cdot \mathbf{k}_2). \tag{3.60}$$

which is also compatible with Eq. (3.58) if $f^{(1)}_{(+)}$ is symmetric in the exchange of $\mathbf{k}_1$ and $\mathbf{k}_2$:

$$f^{(1)}_{(+)}(k_2, k_1, \mathbf{k}_1 \cdot \mathbf{k}_2) = f^{(1)}_{(+)}(k_1, k_2, \mathbf{k}_1 \cdot \mathbf{k}_2). \tag{3.61}$$

The second possible ansatz is in the odd sector and to be compatible with (3.58), the only possibility is to antisymmetrize the product $(\hat{\mathbf{e}}_z \cdot \mathbf{k}_1) f^{(1)}_{(-)}(k_1, k_2, \mathbf{k}_1 \cdot \mathbf{k}_2)$:

$$\langle \mathbf{k}_1, \mathbf{k}_2 | A_\psi \rangle = (\hat{\mathbf{e}}_z \cdot \mathbf{k}_1) f^{(1)}_{(-)}(k_1, k_2, \mathbf{k}_1 \cdot \mathbf{k}_2) - (\hat{\mathbf{e}}_z \cdot \mathbf{k}_2) f^{(1)}_{(-)}(k_2, k_1, \mathbf{k}_1 \cdot \mathbf{k}_2) \tag{3.62}$$

and $f^{(1)}_{(-)}$ has no particular exchange symmetry.

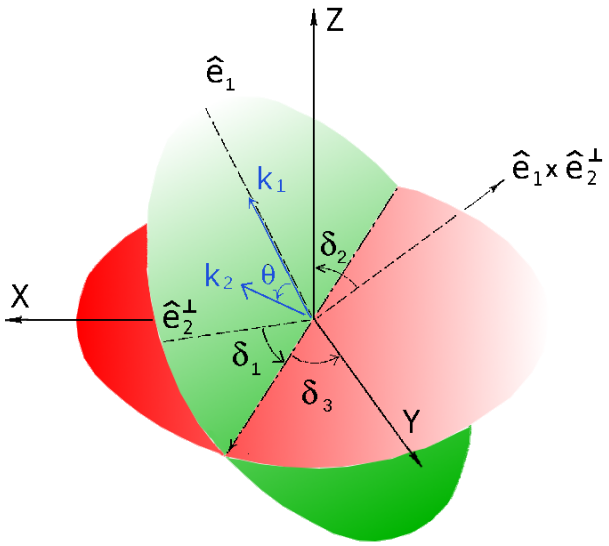

Figure 3.3: *Sketch of the rotation which is used to express* $\langle \mathbf{k}_1, \mathbf{k}_2 | A_\psi \rangle$ *in terms of functions of three variables only. From the two given vectors* $\mathbf{k}_1$ *and* $\mathbf{k}_2$ *one can form an orthonormal basis* $\hat{\mathbf{e}}_1, \hat{\mathbf{e}}_2^\perp, \hat{\mathbf{e}}_1 \wedge \hat{\mathbf{e}}_2^\perp$. *The rotation is parameterized by the Euler's angles* δ_1, δ_2 *and* δ_3.

In the general case, the more efficient way to find the general ansatz in each symmetry sector is to use the group theory [Mor11a]. In the sector $l = 1$, $\langle \mathbf{k}_1, \mathbf{k}_2 | A_\psi \rangle$ is the component of a vector or of a pseudo-vector along the quantization axis $\hat{\mathbf{e}}_z$. For a higher momentum, $\langle \mathbf{k}_1, \mathbf{k}_2 | A_\psi \rangle$ has a spinorial character and as a consequence of the rotational invariance, one can consider without loss of generality that it corresponds to the $m = 0$ component of a spinor of rank l. The behavior of this object under a rotation is well known (see [Chai98]-chapter 6). In order to take advantage of the rotational symmetry, the idea is to express $\langle \mathbf{k}_1, \mathbf{k}_2 | A_\psi \rangle$ where $\mathbf{k}_1$ and $\mathbf{k}_2$ are two vectors of any direction, as a function of its rotated image in the plane (Oxy) where $\mathbf{k}_1{}'$ is along a given axis say (Ox). For this purpose, we introduce the basis

$$\hat{\mathbf{e}}_1 = \frac{\mathbf{k}_1}{k_1} \quad ; \quad \hat{\mathbf{e}}_2^\perp = \frac{1}{\sin\theta}\left(\frac{\mathbf{k}_2}{k_2} - \cos\theta \frac{\mathbf{k}_1}{k_1}\right) \quad ; \quad \hat{\mathbf{e}}_1 \wedge \hat{\mathbf{e}}_2^\perp = \frac{\mathbf{k}_1 \wedge \mathbf{k}_2}{|\mathbf{k}_1 \wedge \mathbf{k}_2|}. \tag{3.63}$$

where $\theta \in [0, \pi]$ denotes the angle between the vectors $\mathbf{k}_1$ and $\mathbf{k}_2$. The desired rotation is such that the basis $\hat{\mathbf{e}}_1, \hat{\mathbf{e}}_2^\perp, \hat{\mathbf{e}}_1 \wedge \hat{\mathbf{e}}_2^\perp$ is transformed in the basis $\hat{\mathbf{e}}_x, \hat{\mathbf{e}}_y, \hat{\mathbf{e}}_z$. The corresponding (active) rotation $\mathcal{R}$ is expressed in terms of the Euler's angles $(\delta_1, \delta_2, \delta_3)$ with the product of three elementary rotations $\mathcal{R} = \mathcal{R}_z(\delta_1)\mathcal{R}_y(\delta_2)\mathcal{R}_z(\delta_3)$. The rotation is represented in Fig. (3.3). From this last figure the Euler's angles $\delta_1 \in [0, 2\pi]$ and $\delta_2 \in [0, \pi]$ verify:

$$\cos\delta_2 = \hat{\mathbf{e}}_z \cdot \hat{\mathbf{e}}_1 \wedge \hat{\mathbf{e}}_2^\perp \quad ; \quad \sin\delta_2 \cos\delta_1 = \hat{\mathbf{e}}_1 \cdot \hat{\mathbf{e}}_z \quad ; \quad \sin\delta_2 \sin\delta_1 = \hat{\mathbf{e}}_2^\perp \cdot \hat{\mathbf{e}}_z, \tag{3.64}$$

while the expression of $\delta_3 \in [0, 2\pi]$ is not useful in what follows. By construction, the components of the rotated spinor on the plane (Oxy) denoted by $f^{(l)}_m(k_1, k_2, \theta)$ depend only on three coordinates, and one

has (see Eq. 6.3.25 of Ref. [Chai98] considered for $m = 0$):

$$\langle \mathbf{k}_1, \mathbf{k}_2 | A_\psi \rangle = \sqrt{\frac{4\pi}{2l+1}} \sum_{l,m} Y^*_{lm}(\delta_2, \delta_1) f^{(l)}_m(k_1, k_2, \theta), \tag{3.65}$$

As a consequence of the parity symmetry in the integral equation (3.57), for a given value of l there is a decoupling between the set of functions $f^{(l)}_m$ which are of even parity (*i.e.* m is even) and the one which are of odd parity (*i.e.* m is odd). The exchange symmetry imposes also a constraint on the $f^{(l)}_m$. From Fig. (3.3) the exchange $\mathbf{k}_2 \leftrightarrow \mathbf{k}_1$ corresponds to the transformation $\delta_1 \to \theta - \delta_1$ and $\delta_2 \to \pi - \delta_2$. From the property $Y_{lm}(\pi - \delta_2, \theta - \delta_1) = (-1)^l e^{im\theta} Y_{l,-m}(\delta_2, \delta_1)$, one finds from the Fermi statistics:

$$f^{(l)}_m(k_2, k_1, \theta) = (-1)^{l+1} e^{im\theta} f^{(l)}_{-m}(k_1, k_2, \theta). \tag{3.66}$$

3. **Scaling invariance**: as discussed in sections 3.3.3 and 3.4 the scale invariance of the solution follows from the fact that we consider zero energy states at unitarity. Equation (3.50) specialized to the case $N = 3$ gives

$$\langle \lambda \mathbf{k}_1, \lambda \mathbf{k}_2 | A_\psi \rangle = \lambda^{-\frac{7}{2} \pm s} \langle \mathbf{k}_1, \mathbf{k}_2 | A_\psi \rangle. \tag{3.67}$$

Importantly, in each symmetry sector of given momentum and parity, the ansatz $\langle \mathbf{k}_1, \mathbf{k}_2 | A_\psi \rangle$ can be factorized in the product of a power law on the hyper wavenumber $k = (k_1^2 + k_2^2)^{s - \frac{7}{2}}$ and of a function of two variables: k_1/k_2 and θ.

4-body Efimov effect

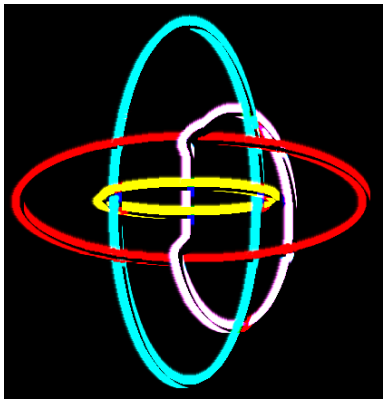

Figure 3.4: *Generalization of the Borromean rings to the case of four rings. If one rings is left out all the other rings are free.*

From the symmetry considerations, the problem is reduced to the finding in each symmetry sector of a set of function depending only on two coordinates: k_1/k_2 and θ. The integral operator in the left hand side of Eq. (3.57) depends on the two independent variables s and $x = M/m$. Thus all the eigenvalues λ_n of this operator are also functions of these two variables. The infinite set of exponents $\{s\}$ solutions of the problem is found by searching the zeros of the eigenvalues λ_n. In absence of Efimov effect, all the values s^2 are positive. Setting $s = 0$ in the integral equation, the Efimov threshold is obtained by studying the minimal eigenvalue denoted by λ_0 as a function of the mass ratio $x = M/m$. The threshold is found when λ_0 crosses zero. A mass ratio at the threshold which must be less than $x_{\rm crit}(2) = 13.606\ldots$ is obtained numerically for $l \leq 6$ only in the even sector $l = 1$ at $x_{\rm crit}(3) = 13.384\ldots$ Hence there exists a four-body Efimov effect in the narrow interval

$$13.384 < \frac{M}{m} < 13.607. \tag{3.68}$$

In a systematic study of the Mendeleev's table including long lived isotopes, one finds three possible pair of species (fermion-impurity) for achieving this prediction:

- ^{41}Ca-^{3}He* with $M/m \simeq 13.58$

- ^{149}Sm-^{11}B with $M/m \simeq 13.53$
- ^{95}Mo-^{7}B with $M/m \simeq 13.53$

These species have never been cooled down toward ultra-low temperatures and this represents a challenging issue ! Another possibility is to use less exotic species as ^{3}He*-^{40}K ($M/m \simeq 13.25$) with one of the species trapped in an optical lattice in order to tune the mass ratio.

In the interval of mass ratio where the Efimov effect occurs the exponent s is imaginary $s = iS$ and can be also calculated numerically. The result is given in Fig. (3.5). As already pointed out, the minimal eigenvalue of the integral operator in the left hand side of Eq. (3.57) *i.e.* λ_0 is a function of the two independent variables x and s. The behavior of λ_0 in the vicinity of $s = iS = 0$ and for $x > x_{\rm crit}(3)$ is of the form: $\lambda_0(x,S) = \lambda_0(x,0) + \left(\frac{d^2\lambda_0}{dS^2}\right)_{(x,0)} \frac{S^2}{2} + \mathcal{O}(S^4)$, where the symmetry $S \leftrightarrow -S$ has been used. On the other hand, in the vicinity of the critical mass ratio $\lambda_0(x,0)$ can be expanded as $\lambda_0(x,0) = \left(\frac{d\lambda_0}{dx}\right)_{(x_{\rm crit},0)} [x - x_{\rm crit}(3)] + \ldots$. The solution of the integral equation associated with this branch of eigenvalue is found for $\lambda_0(x,S) = 0$ which implies

$$|s| = |S| \propto [x - x_{\rm crit}(3)]^{1/2} \tag{3.69}$$

This behavior is indeed verified in the numerical computations as shown in Fig. (3.5).

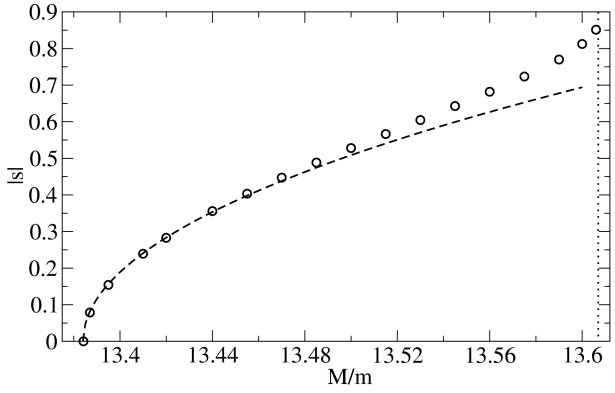

Figure 3.5: *Modulus of the purely imaginary Efimov exponent $s = iS$ in the even sector $l = 1$ plotted as a function of the mass ratio $x = M/m$. The dashed line results from a linear fit of $|s|^2$ as a function of x in a vicinity of the critical value $x_{\rm crit}(3)$, $|s|^2 \simeq 2.23 \times [x - x_{\rm crit}(3)]$. The vertical dotted line indicates the critical value $x_{\rm crit}(2)$ for two fermions interacting with one impurity. The figure is taken from Ref. [Cas10].*

3.5 Three identical fermions

the unitary limit exists also for a p wave resonance in the regime of large and negative scattering volume. Thus, one might guess that an Efimov effect is also possible for three identical fermions interacting through a pairwise short range potential in a regime of p wave scattering resonance. We use the parameterization of the scattering amplitude in Eq. (1.30) where α is the effective range parameter and $\mathcal{V}_{\rm s}$ is the scattering volume. In section 1.4.1, it was shown that the unitary limit $f_1(k) \sim i/k$ is reached only in presence of a quasi bound state *i.e.* when $\mathcal{V}_{\rm s}$ is large and negative but only in a narrow interval of momentum. Moreover at resonance, the unitary limit cannot be reached as a consequence of the radius-range inequality. Thus in a system composed of three identical fermions in resonant p wave interaction, the eigenequation for the stationary states cannot exhibit any regime where a scale invariance occurs. This prevents separability and as a major consequence an Efimov effect is not possible in such a system.

However as shown in Ref. [Jon08], some interesting results can be found for three resonant identical fermions by using the two-channel model of section 1.5.3. They are summarized in the following paragraphs:

Atom-dimer scattering- For a large and positive value of the scattering volume, a shallow dimer of wavenumber $q_B \sim 1/\sqrt{\alpha \mathcal{V}_{\rm s}}$ exists. If one excludes the possible regimes where a three-body resonance occurs, the atom-dimer scattering is dominated by the s wave and the scattering length is of the order of the potential radius.

Consequently, the elastic collision rate is of the same order of magnitude than the loss rate. This shows the difficulty to obtained a thermodynamical equilibrium in a many-body system for identical and resonant fermions. Nevertheless, in the p wave scattering channel, the atom-dimer scattering volume ($\mathcal{V}_{\rm s}^{\rm at-dim}$) follows an universal law:

$$\mathcal{V}_{\rm s}^{\rm at-dim} \sim -\frac{8}{3}\mathcal{V}_{\rm s}. \tag{3.70}$$

Bound states: In the regime of 'broad' resonance where $\alpha b \sim 1$, the model predicts two Borromean bound states. These states have not an Efimovian character and have not a universal character. The thresholds of their appearance correspond to isolated three-body resonances.

Three-body recombination: In the degenerate Bose gas, the three-body recombination constant can be defined from the relation [Kag85]:

$$\frac{dN_{\rm dim}}{dt} = \alpha_{\rm rec} \int d^3r \langle \Psi^\dagger(\mathbf{r})\Psi^\dagger(\mathbf{r})\Psi^\dagger(\mathbf{r})\Psi(\mathbf{r})\Psi(\mathbf{r})\Psi(\mathbf{r})\rangle, \tag{3.71}$$

where the field operator $\Psi^\dagger(\mathbf{r})$ creates an atom at the point $\mathbf{r}$ and the mean value is performed on the many-body state *i.e.* approximately a Hartree state. Implicitly, the spatial scale where the recombination mechanism occurs is given by the potential range and is supposed to be much more smaller than the typical lengths involved in the many-body state (de Broglie length, healing length and interparticle distance). For a two-spin components Fermi gas the definition in Eq. (3.71) is no longer relevant as it vanishes because of the Pauli principle (two identical fermions cannot be at the same point). Physically, the recombination process occurs when three atoms are inside a sphere of radius $b = \mathcal{O}(R_{\rm vdW})$ and Eq. (3.71) is a zero-range approximation for the recombination process. For the two-spin components Fermi gas, one thus can consider an average where derivative of the atomic field take into account the non-local character of the process. At the first order, one can define the recombination rate from the average $\langle \partial_\alpha \Psi_\uparrow^\dagger(\mathbf{r})\Psi_\uparrow^\dagger(\mathbf{r})\Psi_\downarrow^\dagger(\mathbf{r})\Psi_\downarrow(\mathbf{r})\Psi_\uparrow(\mathbf{r})\partial_\alpha\Psi_\uparrow(\mathbf{r})\rangle$. This explains the factor k_F^2 (where k_F is the Fermi wavenumber) in the recombination rate (see for example Eq. (11) in Ref. [Pet03]). Following the same reasoning for a gas of identical fermions, the recombination constant can be defined as [Jon08]:

$$\frac{dN_{\rm dim}}{dt} = \mathcal{K}_{\rm rec} \sum_{\substack{(\alpha,\beta)\in\{(x,y),\\(x,z),(y,z)\}}} \int d^3r \langle \partial_\alpha\Psi^\dagger(\mathbf{r})\partial_\beta\Psi^\dagger(\mathbf{r})\Psi^\dagger(\mathbf{r})\Psi(\mathbf{r})\partial_\beta\Psi(\mathbf{r})\partial_\alpha\Psi(\mathbf{r})\rangle. \tag{3.72}$$

The average over the Slater determinant provides a loss rate proportional to k_F^4 and allows to define the three-body recombination constant $\mathcal{K}_{\rm rec}$ as:

$$\frac{dN_{\rm dim}}{dt} = \frac{3k_F^4}{25}\mathcal{K}_{\rm rec} n^2 N. \tag{3.73}$$

For a recombination toward a shallow dimer (*i.e.* in the regime $\mathcal{V}_{\rm s} \gg R_{\rm vdW}$) the definition in (3.73) is valid only if k_F is much smaller than the dimer wavenumber $q_B \sim 1/\sqrt{\alpha\mathcal{V}_{\rm s}}$. For a recombination toward a deep bound state Eq. (3.73) is always valid as $k_F R_{\rm vdW} \ll 1$ follows from the diluteness of the gas. In absence of a three-body resonance, the two-channel model provides the two following results:

- the recombination constant for atomic losses into Feshbach dimers follows an universal law:

$$\mathcal{K}_{\rm rec}^{\rm Fesh} = \frac{\hbar}{m}(48\pi)^2\left(\frac{\mathcal{V}_{\rm s}^5}{3\alpha}\right)^{\frac{1}{2}}. \tag{3.74}$$

  This law cannot be obtained by use of dimensional analysis and shows again the importance of the effective range parameter;

- the recombination constant for atomic losses into deep dimers follows the approximate law:

$$\mathcal{K}_{\rm rec}^{\rm deep} \propto \frac{\hbar}{m} b^3 \mathcal{V}_{\rm s}^2 \alpha \tag{3.75}$$

  where $b \equiv \mathcal{O}(R_{\rm vdW})$.

In the vicinity of the resonance, the ratio $\mathcal{K}_{\rm rec}^{\rm Fesh}/\mathcal{K}_{\rm rec}^{\rm deep}$ is large. Thus the rate of formation of shallow dimers dominates the rate for the deep dimers. Unfortunately the atom-dimer and dimer-dimer inelastic collisions precludes the existence of a thermodynamical equilibrium in the system.

Bibliography

[Ama73] R.D. Amado and F. C. Greenwood, Phys. Rev. D **7**, 2517 (1973). 43

[Bar09] G. Barontini, C. Weber, F. Rabatti, J. Catani, G. Thalhammer, M. Inguscio, and F. Minardi, Phys. Rev. Lett. **103**, 043201 (2009). 43

[Bed99] P.F. Bedaque, H.-W. Hammer, and U. van Kolck, Phys. Rev. Lett. **82**, 18 (1999). 34

[Bed00] P.F. Bedaque, Eric Braaten, and H.-W. Hammer, Phys. Rev. Lett. **85**, 908 (2000). 37

[Ber11] M. Berninger, A. Zenesini, B. Huang, W. Harm, H.-C. Nägerl, F. Ferlaino, R. Grimm, P. S. Julienne, J. M. Hutson Phys. Rev. Lett. **107**, 120401 (2011). 43

[Bet35] H. Bethe and R. Peierls, Proc. R. Soc. London, Ser. **A 148**, 146 (1935). 9

[Bla52] J.M. Blatt and V.F. Weisskopf, *"Theoretical Nuclear Physics"*, Wiley, New York (1952). 4

[Bra02] Eric Braaten, H.-W. Hammer, and Thomas Mehen, Phys. Rev. Lett. **88**, 040401 (2002).

[Bra06] E. Braaten and H.-W. Hammer, Phys. Rept. **428**, 259 (2006). 35, 36, 37, 38, 39

[Bra07] E. Braaten, H.-W. Hammer, Ann. Phys. **322**, 120 (2007). 37, 39, 42

[Bul75] A. Bulgac and V. Efimov, Sov. Jour. Nucl. Phys. **22**, 296 (1975). 42, 45, 51

[Cas04] Yvan Castin, Comptes Rendus Physique **5**, 407 (2004). 29

[Cas10] Y. Castin, C. Mora, L. Pricoupenko, Phys. Rev. Lett. **105**, 223201 (2010). 44, 52, 55

[Cas11] Y. Castin and E. Tignone, Phys. Rev. A **84**, 062704 (2011). 51

[CCT] C. Cohen-Tannoudji, *"Cours du Collège de France"* (1998-99); *"Atom-atom interactions in ultracold gases"*, Institut Henri Poincaré, Paris, 25 Avril 2007 4, 10

[Chai98] M. Chaichian and R. Hagedorn, in '*Symmetries in Quantum Mechanics*' IOP publshing (Bristol and Philadelphia - 1998) 53, 54

[Chi10] C. Chin, R. Grimm, P. Julienne, and E. Tiesinga, Rev. Mod. Phys. **82**, 1225 (2010). 4, 16

[Dal98] J. Dalibard, Proceedings of the International School of Physics "Enrico Fermi", Course CXL: *"Bose-Einstein condensation in gases"*, Varenna 1998, M. Inguscio, S. Stringari, C. Wieman edts. 4, 5

[Del10] A. Deltuva, Phys. Rev. A **82**, 040701(R) (2010). 43

[Del11a] A. Deltuva Eur. Phys. Lett. **95**, 43002 (2011). 43

[Del11b] A. Deltuva, Phys. Rev. A **84**, 022703 (2011). 43

[Dan61] G. Danilov, Sov. Phys. JETP **13**, 349 (1961). 26, 28

[Der07] C. D'Errico, M. Zaccanti, M. Fattori, G. Roati, M. Inguscio, G. Modugno, A. Simoni, New Jour. Phys. **9**, 223 (2007). 20

[DIn09] J.P. D'Incao, Chris H. Greene and B.D. Esry, J. Phys. B: At. Mol. Opt. Phys. **42**, 044016 (2009). 39

[Fad61] L. D. Faddeev, Sov. Phys. JETP **12**, 1014 (1961). 29

[Fed93] D.V. Fedorov and A.S. Jensen, Phys. Rev. Lett. **71**, 4103 (1993). 33

[Efi70] V. Efimov, Phys. Lett. B **33**, 563 (1970). 29

[Efi71] V. Efimov, Sov. J. Nucl. Phys. **12**, 589 (1971). 29

[Efi73] V. Efimov, Nucl. Phys. A, **210** 157 (1973). 42, 45, 51

[Fer09] F. Ferlaino, S. Knoop, M. Berninger, W. Harm, J. P. D'Incao, H.-C. Nägerl, R. Grimm, Phys. Rev. Lett. **102**, 140401 (2009). 43

[Fer10] F. Ferlaino and R. Grimm, Physics **3**, 9 (2010). 42, 43

[Fes58] H. Feshbach, Ann. Phys. (N. Y.) **5**, 357 (1958); *ibid.* **19**, 287 (1962).

[Gao98] B. Gao, Phys. Rev. A **58**, 4222 (1998). 5, 8

[Gog08] A.O. Gogolin, C. Mora, R. Egger, Phys. Rev. Lett. **100**, 140404 (2008). 27, 36, 37

[Gon99] D. E. González *et al*, Phys. Rev. Lett. **83**, 3788 (1999). 9

[Gri93] G.F. Gribakin and V.V. Flambaum, Phys. Rev. A **48**, 546 (1993). 5

[Gro09] Noam Gross, Zav Shotan, Servaas Kokkelmans, and Lev Khaykovich, Phys. Rev. Lett. **103**, 163202 (2009). 42

[Gro11] N. Gross , Z. Shotan , O. Machtey , S. Kokkelmans and L. Khaykovich, Comp. Rend. Phys. **12**, 4 (2011). 42

[Gue11] Nicolais Guevara, Yujun Wang, B. D. Esry, *arXiv:1110.0476*. 44

[Ham07] H.-W. Hammer, L. Platter, Eur. Phys. J. A **32**, 113 (2007). 43

[Hel09] K. Helfrich and H.-W. Hammer, Eur. Phys. Lett. **86**, 53003 (2009). 37, 39

[Hel10] K. Helfrich, H.-W. Hammer, D. S. Petrov, Phys. Rev. A **81**, 042715 (2010). 37

[Huc09] J. H. Huckans, J. R. Williams, E. L. Hazlett, R. W. Stites, K. M. O'Hara, Phys. Rev. Lett. **102** 165302 (2009). 43

[Ino98] S. Inouye, M.R. Andrews, J. Stenger, H.-J. Miesner, D.M. Stamper-Kurn, and W. Ketterle, Nature (London) **392**, 151 (1998). 37

[Jon08] M. Jona-Lasinio, L. Pricoupenko and Y. Castin, Phys. Rev. A **77**, 043611 (2008). 16, 17, 21, 22, 38, 55, 56

[Jon10] M. Jona-Lasinio, L. Pricoupenko, Phys. Rev. Lett. **104**, 023201 (2010). 16, 17, 39

[Kag85] Yu. Kagan, B. V. Svistunov, and G. V. Shlyapnikov, JETP Lett. **42**, 209 (1985). 37, 56

[Kno09] S. Knoop, F. Ferlaino, M. Mark, M. Berninger, H. Schoebel, H.-C. Naegerl, R. Grimm, Nature Physics **5**, 227 (2009). 39, 40

[Koh06] Thorsten Köhler, Krzysztof Góral, and Paul S. Julienne, Rev. Mod. Phys. **78**, 1311 (2006). 4, 16

[Kra06] T. Kraemer, M. Mark, P. Waldburger, J. G. Danzl, C. Chin, B. Engeser, A. D. Lange, K. Pilch, A. Jaakkola, H.-C. Nägerl and R. Grimm, Nature **440**, 315 (2006). 39, 40

[Lee07] M. Lee, T. Köhler and P. Julienne, Phys. Rev. A **76**, 012720 (2007). 16, 39

[Lan67] L. Landau et E. Lifchitz, Tome III *"Mécanique Quantique"*, Editions MIR Moscou (1967). 4, 12, 19, 22, 32

[Lom10a] T. Lompe, T. B. Ottenstein, F. Serwane, K. Viering, A. N. Wenz, G. Zürn, S. Jochim, Phys. Rev. Lett. **105**, 103201 (2010). 43

[Lom10b] Thomas Lompe, Timo B. Ottenstein, Friedhelm Serwane, Andre N. Wenz, Gerhard Zürn, Selim Jochim, Science **330**, 940 (2010). 43

[Mac06] J. H. Macek, S. Yu Ovchinnikov, G. Gasaneo, Phys. Rev. A **73**, 032704 (2006). 37

[Mac11] O. Machtey, D.A. Kessler, L. Khaykovich, *arXiv:1111.5503*. 42

[Mac12] O. Machtey, Z. Shotan, N. Gross, L. Khaykovich *arXiv:1201.2396*. 43

[Mar94] M. Marinescu, H.R. Sadeghpour and A. Dalgarno, Phys. Rev. A **49**, 982 (1994). 5

[Mar07] M. Mark, F. Ferlaino, S. Knoop, J. G. Danzl, T. Kraemer, C. Chin, H.-C. Nägerl, and R. Grimm, Phys. Rev. A **76**, 042514 (2007). 21, 22

[Mas08] P. Massignan, and H.T.C. Stoof, Phys. Rev. A **78**, 030701(R) (2008). 39

[Maz06] I. Mazumdar, A. R. P. Rau, and V. S. Bhasin, Phys. Rev. Lett. **97**, 062503 (2006).

[Mes61] A. Messiah, "*Quantum Mechanics*", North Holland, Amsterdam (1961). 4

[Min62] R. Minlos and L. Faddeev, Sov. Phys. JETP **14**, 1315 (1962). 26, 28, 29

[Moe95] A. J. Moerdijk, B. J. Verhaar, and A. Axelsson, Phys. Rev. A **51**, 4852 (1995). 14, 15

[Mor57] P.M. Morse and H. Feshbach, "*Methods of theoretical physics*" Mc Graw-Hill (New York, 1953); pages 1665-1667. 31, 32

[Mor11a] C. Mora, Y. Castin, L. Pricoupenko, C. R. Physique **12**, 71 (2011). 16, 17, 39, 53

[Mor11b] Christophe Mora, Alexander O. Gogolin, Reinhold Egger, C. R. Physique 12, 27 (2011). 37

[Mot65] N.F. Mott and M.S. Massey, in "*The Theory of Atomic Collisions*", Oxford at the Clarendon press (1965). 4

[Nai11b] P. Naidon, E. Hiyama, M. Ueda, *arXiv:1109.5807*. 43

[Nak10] S. Nakajima, M. Horikoshi, T. Mukaiyama, P. Naidon, M. Ueda, Phys. Rev. Lett. **105**, 023201 (2010). 43

[Nak11] S. Nakajima, M. Horikoshi, T. Mukaiyama, P. Naidon, M. Ueda, Phys. Rev. Lett. **106**, 143201 (2011). 43

[Nis08] Y. Nishida and S. Tan, Phys. Rev. Lett. **101**, 170401 (2008). 42

[Nis09] Y. Nishida and S. Tan, Phys. Rev. A **79**, 060701(R) (2009). 42

[Ols01] M. Olshanii and L. Pricoupenko, Phys. Rev. Lett. **88**, 010402 (2001). 11

[Ott08] T. B. Ottenstein, T. Lompe, M. Kohnen, A. N. Wenz, S. Jochim, Phys. Rev. Lett. **101**, 203202 (2008). 43

[Pet03] D. S. Petrov, Phys. Rev. A **67**, 010703(R) (2003). 42, 45, 51, 56

[Pet04a] D. S. Petrov, C. Salomon, and G. V. Shlyapnikov, Phys. Rev. Lett. **93**, 090404 (2004).

[Pet04b] D.S. Petrov, Phys. Rev. Lett. **93**, 143201 (2004). 15, 20

[Pol09] Scott E. Pollack, Daniel Dries, Randall G. Hulet, Science **326**, 1683 (2009). 42, 43

[Pri04b] L. Pricoupenko, Phys. Rev. A **70**, 013601 (2004). 11

[Pri06a] L. Pricoupenko, Phys. Rev. A **73**, 012701 (2006). 12

[Pri06b] L. Pricoupenko, Phys. Rev. Lett. **96**, 050401 (2006). 12

[Pri08] L. Pricoupenko, Phys. Rev. Lett. **100**, 170404 (2008). 10

[Pri10a] L. Pricoupenko, P. Pedri, Phys. Rev. A **82**, 033625 (2010). 10

[Pri10b] L. Pricoupenko, Phys. Rev. A **82**, 043633 (2010). 34, 35

[Pri11a] L. Pricoupenko, Phys. Rev. A **83**, 062711 (2011). 10, 12, 17, 34, 35, 51

[Pri11b] L. Pricoupenko, Phys. Rev. A **84**, 053602 (2011). 11, 17

[Pri11c] L. Pricoupenko, M Jona Lasinio, Phys. Rev. A **84**, 062712 (2011). 20, 38

[Ser11] F. Serwane, G. Zürn, T. Lompe, T. B. Ottenstein, A. N. Wenz, S. Jochim Science **332**, 6027 (2011). 43

[Sko57] G.V. Skorniakov and K.A. Ter-Martirosian, Sov. Phys. JETP **4**, 648 (1957). 26

[Ste99] J. Stenger, S. Inouye, M. R. Andrews, H.-J. Miesner, D. M. Stamper-Kurn, and W. Ketterle, Phys. Rev. Lett. **82**, 2422 (1999). 37

[Ste09] Javier von Stecher, Jose P. D'Incao, Chris H. Greene, Nature Physics **5**, 417 (2009). 43

[Tay72] John R. Taylor, "*Scattering theory*", Wiley, New York (1972). 4, 6

[Tho35] L. H. Thomas, Phys. Rev. **47**, 903 (1935). 28

[Tic04] C. Ticknor, C. A. Regal, D. S. Jin, and J. L. Bohn, Phys. Rev. A **69**, 042712 (2004). 12, 22

[Wan12] Jia Wang, J. P. D'Incao, B. D. Esry, Chris H. Greene, *arXiv:1201.1176*. 43

[Wei99] J. Weiner, V.S. Bagnato, S. Zilio, P.S. Julienne, Rev. Mod. phys. **71**, 1 (1999). 4

[Wen09] A. N. Wenz, T. Lompe, T. B. Ottenstein, F. Serwane, G. Zürn, and S. Jochim, Phys. Rev. A **80**, 040702(R) (2009). 43

[Wer06a] Félix Werner, Yvan Castin, Phys. Rev. Lett. **97**, 150401 (2006). 45

[Wer06b] Félix Werner, Yvan Castin, Phys. Rev. A **74**, 053604 (2006). 45

[Wer08] Félix Werner, in *Atomes froids piégés en interaction résonnante: gaz unitaire et problème à trois corps*, PhD thesis (2008). 32, 45

[Wer09] F. Werner, L. Tarruell, and Y. Castin, Eur. Phys. J. B **68**, 401 (2009). 16, 17

[Wil09] J. R. Williams, E. L. Hazlett, J. H. Huckans, R. W. Stites, Y. Zhang, and K. M. O'Hara, Phys. Rev. Lett. **103**, 130404 (2009). 43

[Wig33] E. Wigner, Zeits. f. Physik **83**, 253 (1933). 9

[Yam06] M. T. Yamashita, Lauro Tomio, A. Delfino and T. Frederico, Europhys. Lett. **75**, 555 (2006). 43

[Zac09] M. Zaccanti, B. Deissler, C. D'Errico, M. Fattori, M. Jona-Lasinio, S. Müller, G. Roati, M. Inguscio, G. Modugno, Nature Phys. **5**, 586 (2009). 42